N° d'ordre : 4517

THÈSE

PRÉSENTÉE A

L'UNIVERSITÉ BORDEAUX 1

ÉCOLE DOCTORALE DES SCIENCES CHEMIQUES

Carolina GARCIA DARRAS

POUR OBTENIR LE GRADE DE

DOCTEUR

SPÉCIALITÉ : PHYSICO-CHEMIE DE LA MATIÈRE CONDENSÉE

CONCEPTION ET DÉVELOPPEMENT D'UN MICROCALORIMÈTRE POUR L'ETUDE DE L'OXYDATION D'UNE HUILE VEGETALE

Directeur de recherche : Mme Maud CANSELL
Co-directeurs de recherche : M Christophe PRADERE et M Jean TOUTAIN

Soutenue le 10 mai 2012

Devant la commission formée de :

Rapporteurs	M. FUDYM, Olivier	Professeur, École des Mines, Albi
	M. MERCADIER, Jaques	Professeur, ENSGTI, Pau
Examinateurs	M. LEAL CALDERON, Fernando	Professeur, Université de Bordeaux, IPB
	M. ROJAS, Juan	Responsable R&D Technologie et Procédés, Groupe LDC, Sablé sur Sarthe
Directeur de thèse	Mme CANSELL, Maud	Professeur, Université de Bordeaux, IPB
Co-encadrant de thèse	M. PRADERE, Christophe	Chargé de Recherche, CNRS, Bordeaux
	M. TOUTAIN, Jean	Maître de Conférences, Université de Bordeaux, IPB

Order number: 4517

THESIS

PRESENTED AT

UNIVERSITY BORDEAUX 1

DOCTORAL SCHOOL OF CHEMICAL SCIENCES

By **Carolina GARCIA DARRAS**

TO OBTAIN THE DEGREE OF

DOCTOR

SPECIALITY: PHYSICAL-CHEMISTRY OF CONDENSED MATTER

CONCEPTION AND DEVELOPMENT OF A CALORIMETRIC THERMAL ANALYSIS DEVICE FOR THE STUDY OF VEGETAL OIL OXIDATION

Director: Mrs. Maud CANSELL
Co-Directors: Mr. Christophe PRADERE and Mr. Jean TOUTAIN

Defended on: 10th of May 2012

In front of a jury composed of:

Rapporteurs	M. FUDYM, Olivier	Professeur, École des Mines, Albi
	M. MERCADIER, Jaques	Professeur, ENSGTI, Pau
Examiners	M. LEAL CALDERON, Fernando	Professeur, Université de Bordeaux, IPB
	M. ROJAS, Juan	Responsable R&D Technologie et Procédés, Groupe LDC, Sablé sur Sarthe
Director	Mme CANSELL, Maud	Professeur, Université de Bordeaux, IPB
Co-Director	M. PRADERE, Christophe	Chargé de Recherche, CNRS, Bordeaux
	M. TOUTAIN, Jean	Maître de Conférences, Université de Bordeaux, IPB

Thesis developed at:

Institut de Mécanique et d'Ingénierie de Bordeaux **I2M** , Département TRansferts Ecoulements FLuides Energétique **TREFLE,** UMR 5295 CNRS-ENSAM-Paristech, Esplanade des Arts et Métiers, 33405 Talence, France

Tel: +33(0)556 845 400

Fax: +33(0)556 845 436

Web: http : // www.trefle.u-bordeaux1.fr

Laboratoire Chimie et Biologie des Membranes et des Nanoobjets **CBMN**, CNRS, UMR 5248, Université de Bordeaux, IPB, Allée Geoffroy Saint Hilaire, 33600 Pessac, France

Tel: +33(0)540 006 819

Fax: +33(0)556 370 336

Web: http : // www.cbmn.u-bordeaux.fr

Thesis funded by:

Erasmus Mundus External Cooperation Windows **EM ECM Lot 17** (34 months scholarship from February 2009)

Web: http : // eacea.ec.europa.eu

To my husband, Andrea

Acknowledment

Acknowledment

I would like to express my sincere gratitude to my thesis Director Prof. Maud Cansell for welcoming in her lab and helping me to develop this experience abroad, also for her supervision and the guidance during my work.

My sincere thanks also goes to my Co-Directors Christophe Predere and Jean Toutain for their contribution in my project and for challenges me every day introducing me in the Thermal Analysis, a whole new world for me. Beside, a special mention to Alain Sommier for his help in the experimentation part and for the advices about Food Science and Technology, thanks to all of you to make me a better scientist.

Furthermore, I would like to thank the members of my reading committee Prof. Olivier Fudym, Prof. Jacques Mercadier, Prof Fernando Leal Calderon and Mr. Juan Rojas, your remarks and contribution were greatly appreciated.

I gratefully acknowledge the financial support of the Erasmus External Cooperation Windows Programme particularly in the award of a 34 months scholarship to support this research work.

My colleagues and close friends thanks for all your support and valuable advices that helped me throughout the duration of my work.

Finally, this thesis is dedicated to you, beside my colleague and friend, also my beloved husband, Dr. Andrea Cappella my infinite gratitude for your love, daily support and encouragement and for always believes in me no matter what, *Te amo*.

TABLE OF CONTENTS

LIST OF TABLES

LIST OF FIGURES

LIST OF SYMBOLS

Notation

a Thermal diffusivity ($m^2.s^{-1}$)

a Geometry factor (m)

C_p Heat capacity ($J.kg^{-1}.K^{-1}$)

Ea Activation energy ($J.mol^{-1}$)

Q_M Measured heat flux (W)

P Delivered power (W)

U_M Measured voltage (V)

R Universal gas constant ($J.K^{-1}.mol^{-1}$)

T Temperature (K)

α Calibration coefficient ($W.V^{-1}$)

β Heating rate ($K.min^{-1}$)

ρ Density ($kg.m^{-3}$)

λ Thermal conductivity ($W.m^{-1}.K^{-1}$)

τ Time (s)

Abbreviations

Ab Absorbance

CD Conjugated diene

DHA Docosahexaenoic acid

DIL Dilatometry

DMA Dynamic mechanical analysis

DSC Differential scanning calorimetry

DTA Differential thermal analysis

EGA Evolved gas analysis

EPA Eicosapentaenoic acid

ESR Electron spin resonance

FTIR Fourier transform infrared spectroscopy

GC Gas chromatography

GUI Graphical user interface

HPLC High-performance liquid chromatography

ICTAC International confederation of thermal analysis and calorimetry

Ln α-Linolenic acid

Lo Linoleic acid

LOOH Hydroperodixe

MA Malonaldehyde

MP Melting point

NMR Nuclear magnetic resonance

O Oleic acid

OSI Oil stability index

para-AnV Anisidine value

P Palmitic acid

PC Phosphatidylcholine

PI Peroxide index

PL Phospholipid

PUFA Polyunsaturated fatty acid

PV Peroxide value

SLPC 1-stearoyl-2-linoleoyl-*sn*-glycero-3-phosphocholine

SOPC 1-stearoyl-2-oleoyl-*sn*-glycero-3-phosphocholine

SOS 1,3-stearoyl-2-oleoyl-glycerol

TAG Triacylglycerol

TBA Thiobarbituric acid

TGA Thermogravimetry analysis

TMA Thermomecanical analysis

UV ultraviolet

Index

$_{imp}$ imposed

$_{M}$ measured

$_{max}$ maximum

s sample

r reference

General Context

Dietary lipids, naturally occurring in raw food materials or added during food processing, play an important role in food nutrition, texture and flavor. Meanwhile, the non-controlled **lipid oxidation** process is one of the most important technological problem in the food industry because oxidation spoils the structure and, as a consequence, the functional and chemical properties of polyunsaturated fatty acids (PUFA) which are part of the triacylglycerols (TAG) in fats and oils. Thus, lipid oxidation represents one of the major causes of food quality degradation.

Lipid oxidation has been extensively studied by **food scientists**, during the last 70 years, to investigate the mechanisms involved and to identify the products formed. Autoxidation is the most common process leading to oxidative deterioration. It is defined as the spontaneous reaction of atmospheric oxygen with lipids. More precisely, lipid oxidation can occur by either di-radical triplet oxygen or non-radical singlet oxygen. It leads to numerous oxidation products, like free radicals, peroxides, hydroperoxides, aldehydes, ketones, epoxides, oxiacids, hydrocarbons, and even polymers when high temperatures are involved. Several factors influence the oxidation reactions such as the chemical composition (especially the fatty acid present in the triacylglycerols), the physical state of the oil (bulk oil/emulsion) and the storage conditions. In this latter case, it is known that lipids are susceptible to oxidative processes in the presence of catalytic systems such as light, heat, enzymes, metals, metalloproteins, and microorganisms. Thus, beyond the knowledge of the lipid oxidation mechanisms, it is worth controlling the storage conditions that influence the production (both in terms of nature and amount) of the oxidized species.

For **manufacturers**, handling lipid oxidation during storage or lipid processing is a great challenge. Indeed, it leads to the development, in edible oils and fat-containing foods, of various off-flavors and off-odors mainly due to the production of aldehydes and ketones, which render these foods less acceptable. In addition, oxidative reactions can decrease the nutritional quality of food by reducing the amount of available PUFA. Finally, some oxidation products, like free radicals or epoxides are potentially toxic. On the other hand, under certain conditions, a limited degree of lipid oxidation is sometimes desirable, as in aged cheeses and

some fried foods. One can easily understand that, because of these nutritional and sensory parameters, managing lipid oxidation is a great economic and technological concern to the food industry.

In this context, it appears of peculiar importance to have at our disposal a simple, adaptable and convenient method of characterization of lipid oxidation. Numerous methods are available to give a quantitative or qualitative picture of the extent of lipid oxidation. Some are very simple in their concept and use like chemical tests dealing with the standardized determination of index. These methods request the use of organic solvents and are often time-consuming. On the other hand, the characterization of specific oxidation compounds requires more sophisticated methods often needing specific instrumentation. Among the available methods, thermo-analytical methods have been developed based on the release energy in the form of heat of exothermic oxidation reaction. These techniques are interesting because they do not use organic solvents, the principle of heat measurement is quite simple and they can be correlated to other chemical tests. However, the experimental apparatus is quite expensive and the samples are confined in a cell that does not allow parameters such as the amount of oxygen, the presence of light to be varied. Moreover, the apparatus often lacks of sensibility. Finally, samples have to be studied one by one.

The purpose of this PhD project is thus to design a **micro-calorimeter for lipid oxidation** measurement, sensible, adaptable and able to follow simultaneously several samples. This project requires pooling of resources of different partners: the laboratory Chemistry and Biology of Membranes and Nanoobjects (CBMN, UMR CNRS 5248) for its knowledge in lipid chemistry and chemical characterisation of oil oxidation and the Institute of Mechanics and Engineering of Bordeaux (I2M, UMR CNRS, 5295) for its skill in thermal metrology and numerical modelling of the thermal systems.

The first chapter of this thesis focuses only on lipid autoxidation and reviews the chemistry of triplet and singlet oxygen, the chemical mechanisms involved in lipid oxidation and the formation of the oxidation compounds. It also presents in details the thermo-analytical approach used in the literature to characterize lipid oxidation. In the second chapter, the oil characteristics are presented as well as

the different methods used to follow lipid oxidation by chemical methods. Chapter 3 deals with a presentation of the micro-calorimeter designed in the laboratory and the different validations used to ensure reliable heat measurements. In chapter 4, the various results obtained with both the chemical tests and the micro-calorimeter are presented and discussed. Correlation between chemical analysis and reaction enthalpy obtained by microcalorimetry is tested. A kinetic modelling of the oxidation reactions is proposed. The last chapter deals with general conclusions and perspectives that can be given to this work.

CHAPTER 1

GENERAL INTRODUCTION

1.1 PRESENTATION OF LIPID OXIDATION

Numerous books report data on lipid oxidation (Frankel, 2005; Schaich, 2005; Wassef, 1996). From a general point of view, lipids can be oxidized by both enzymatic and non enzymatic mechanisms. In this latter case, lipid oxidation is recognized as a free radical chain reaction, where the free radicals generated react with the O_2 to form peroxyl free radicals that in turn can react with another fatty acid. The process continues indefinitely until no hydrogen source is available or the radical is intercepted. In addition, the oxidation of fatty acids may occur either directly or indirectly through the action of enzyme systems (microsomal enzymes, peroxidases, and dioxygenases, such as lipoxygenase or cyclooxygenase). The enzymatic reactions are not discussed in this chapter. We will only focus on autoxidation that implies molecular oxygen and photosensitized oxidation involving singlet oxygen. Thermal oxidation that occurs above 120°C will not be described either in this chapter.

The direct reaction of a lipid molecule with a molecule of oxygen is highly improbable because the activation energy for the reaction of normal oxygen with double bounds is very high (in the range of 146-273 $kJ.mol^{-1}$). This accounts for the fact that the ground state oxygen is in a triplet state ($^3O_2$) (two free electrons in separate orbitals have same spin direction), whereas the C=C double bond of the fatty acid is in a singlet state (no unpaired electrons, paired electrons are in the same orbital and have opposite spin) (Figure 1).

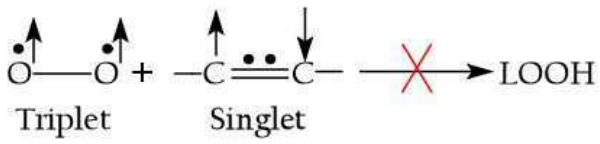

Figure 1: Schematic representation of the reaction of oxygen in a triplet state and a double bond in a single state

To overcome this spin restriction, initiators are required to activate oxygen such as metals or light. This reaction leads to an oxygen molecule in the more reactive state, i.e. in a singlet form ($^1O_2$). Singlet oxygen is an electrophilic substance reacting with electron-rich olefinic systems, but also producing allylic hydroperoxides.

1.1.1 AUTOXIDATION

Autoxidation can be defined as the reaction of triplet oxygen (•O-O•) with unsaturated fatty acid chains at allylic or bisallylic centers (Figure 2).

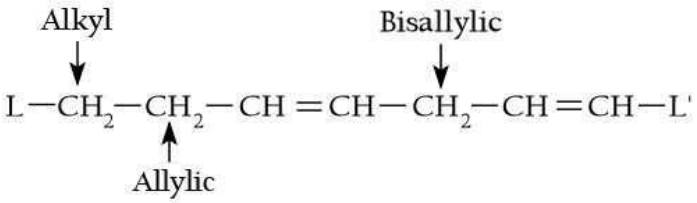

Figure 2: Possible abstraction of hydrogen from allylic and bisallylic C–H bonds of unsaturated fatty acids

Lipid oxidation proceeds via a complex, free radical chain reaction that is classically described by three stages: initiation, propagation, and termination. A general scheme summarizing the overall picture of lipid autoxidation is given in (Figure 3).

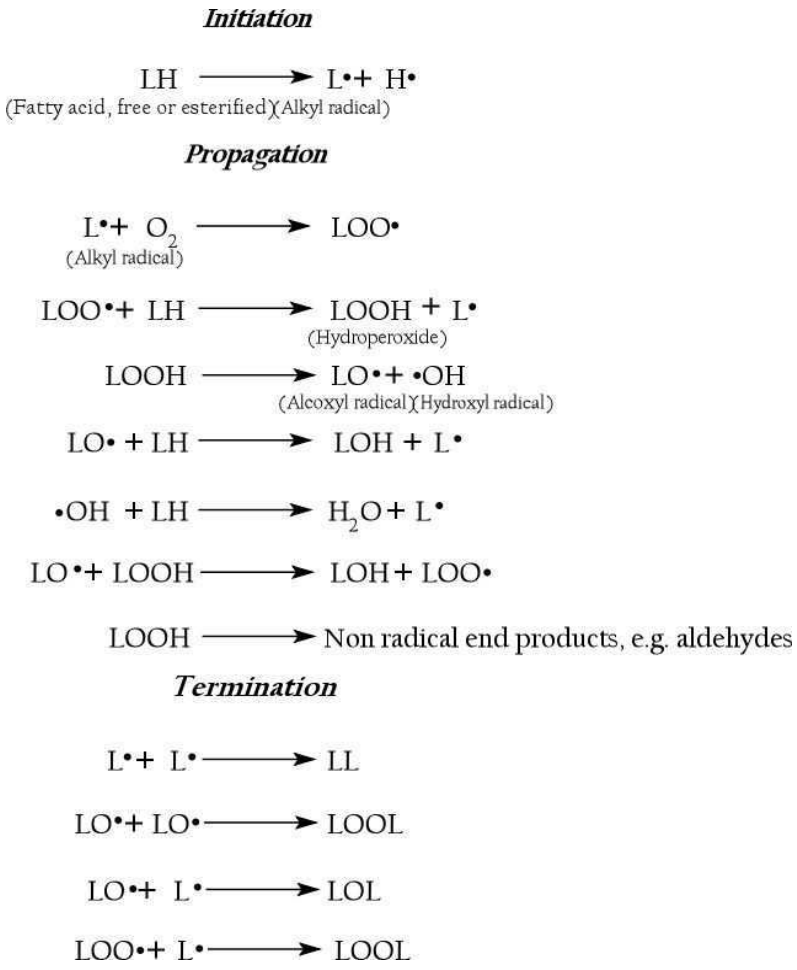

Figure 3: General mechanism of lipid oxidation

1.1.1.1 Initiation

The initiation reaction involves the abstraction of a hydrogen atom from a methylene (CH_2) group adjacent to a double bond in an unsaturated molecule (allylic and bisallylic groups). This generates a fatty acid radical (alkyl radical, L●).

$$LH \longrightarrow L\bullet + H\bullet$$

The dissociation energy of hydrogen in various olefinic compounds is given in Table 1.

Table 1:Bond energies of hydrogens at various positions in acyl chains (bold font): sites of preferential hydrogen abstraction (Schaich, 2005)

	E (KJ.mol^{-1})
H-CH=CH_2	431
H-CH_2-CH=CH_2	356
L-**H**CH-CH=CH-CH_2-CH_3	322
L-CH=CH-HC**H**-CH=CH-	272

Other mechanisms involving pre-formed hydroperoxides (LOOH) are proposed to produce the resonance-stabilized radicals:

Metal-catalysed decomposition

$$LOOH + M^{2+} \longrightarrow LO^{\bullet} + OH^{-} + M^{3+} \text{ (reducing metals)}$$

$$LOOH + M^{3+} \longrightarrow LOO^{\bullet} + H^{+} + M^{2+} \text{ (oxidizing metals)}$$

Formation of hydroperoxide by photooxidation

$$LOOH + h\nu \longrightarrow LOO^{\bullet} + H^{\bullet}$$

Thermal or UV ($h\nu$) dissociation of hydroperoxides

$$LOOH \longrightarrow LO^{\bullet} + {}^{\bullet}OH$$

Exposure to light in the presence of a sensitizer such as a ketone

$$LCOL + h\nu \longrightarrow LCO^{\bullet} + L^{\bullet}$$

1.1.1.2 Propagation

Propagation reactions proceed directly and entirely by hydrogen abstraction. It includes numerous reactions, some of them being presented in Figure 4 and Table 2.

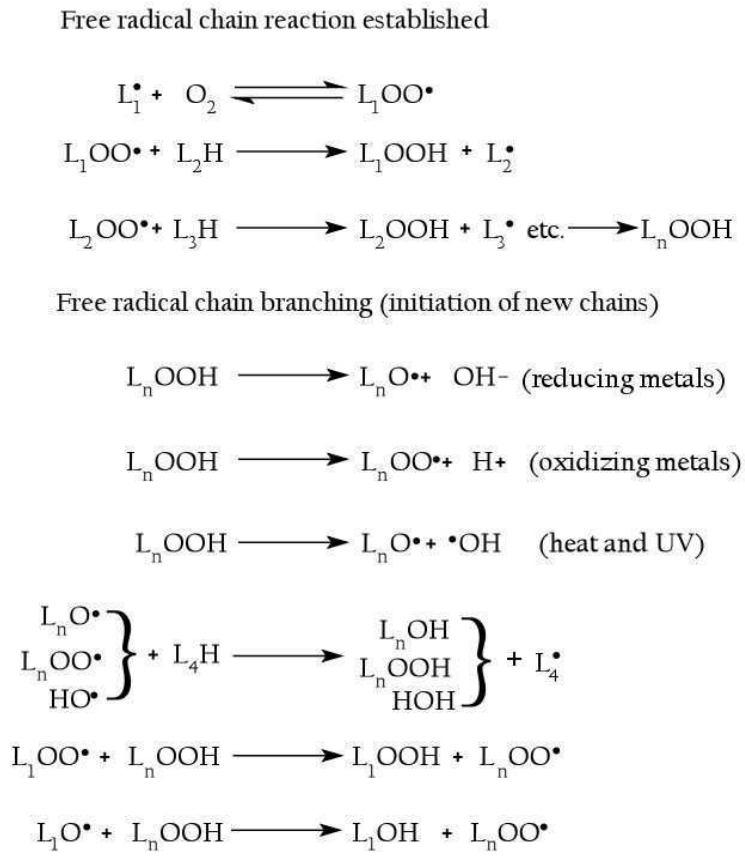

Figure 4: Main products formed upon the propagation reactions of lipid oxidation

Table 2: Main reactions implied in the propagation step of lipid oxidation (Schaich, 2005)

Chain Propagation by	Reactions implied	Consequences
Peroxyl radicals (LOO•)	Atom or group transfer (H-abstraction)	Chain propagation
	Rearrangement/cyclization	Chain propagation
	Addition of LOO• to double bonds (→ crosslinks)	Chain propagation
	Disproportionation (radical self-recombination) of LOO• peroxyl	Branching
	β-scission	Isomerization
	Recombination	Termination of radical chains
	Electron transfer (LOO• + e- →LOO-)	Termination of radical chains
Alkoxyl radicals (LO•)	Hydrogen abstraction	Chain propagation
	Rearrangements/cyclization	Chain propagation
	Addition	Termination of radical chains
	β-scission	Mixture of carbonyl products and free radicals production

The alkyl radical (L•) is extremely reactive and can combine with molecular oxygen to produce a peroxyl radical (LOO•). The newly formed peroxyl radical can, in turn, abstract hydrogen from an adjacent unsaturated fatty acid and generate the corresponding hydroperoxide (LOOH) and a new alkyl radical L•. The new group L• reacts with oxygen, and the sequence of reactions just described is repeated. Due to resonance stabilization of the L• species, the reaction sequence is usually accompanied by a shift in position of the double bonds, resulting in the formation of isomeric hydroperoxides that often contain conjugated diene groups (atypical of unoxidized, natural acylglycerols) (Figure 5).

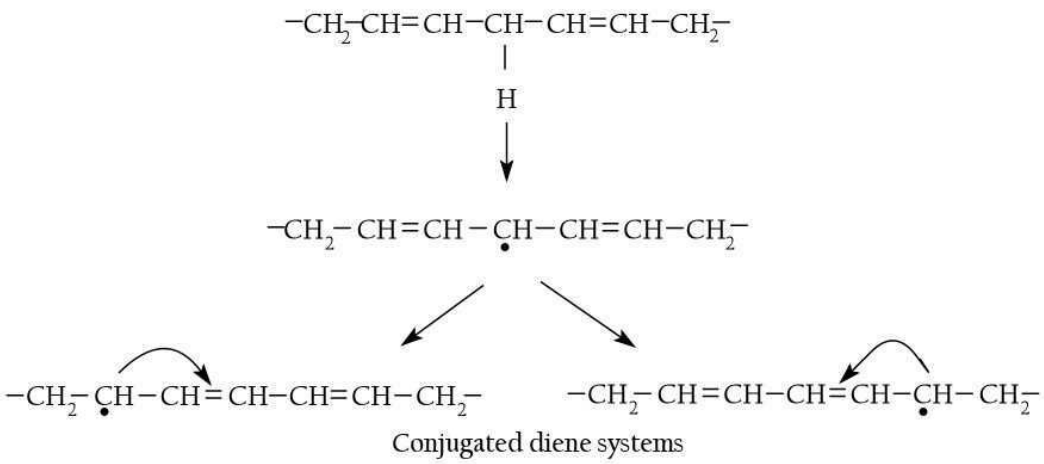

Figure 5: Conjugated diene hydroperoxide formation

Alternatively, the hydroperoxides can degrade to produce an alkoxyl radical (LO•) and a hydroxyl radical (•OH), both of which are extremely reactive and can propagate the chain reaction by reacting with further LH molecules. Indeed, the activation energy for cleaving between oxygen and oxygen of L–O–O–H is 770 $kJ.mol^{-1}$, whereas the cleavage between the oxygen and hydrogen of L–O–O–H is 1578 $kJ.mol^{-1}$.

Moreover, carbon-carbon bond cleavage on either side of the alkoxyl group can occur in decomposition of the hydroperoxides. In general, cleavage on the acid

side (i.e., the carboxyl or ester side) results in formation of an aldehyde and an acid (or ester), while scission on the hydrocarbon (or methyl) side produces a hydrocarbon and an oxoacid (or oxoester). If, however, a vinylic radical results from such cleavage, an aldehydic functional group is formed. The hemolytic β-scission is an important free-radical reaction that produces volatile compounds in edible oils during oxidation.

Hydrogen abstraction by LOO• is very slow and selective, abstracting only hydrogens with low bond energy (e.g., doubly allylic -CH_2-, thiols, phenols). Consequently, alternative reactions can compete with H abstraction such as addition, cyclization, and scission reactions (Figure 6).

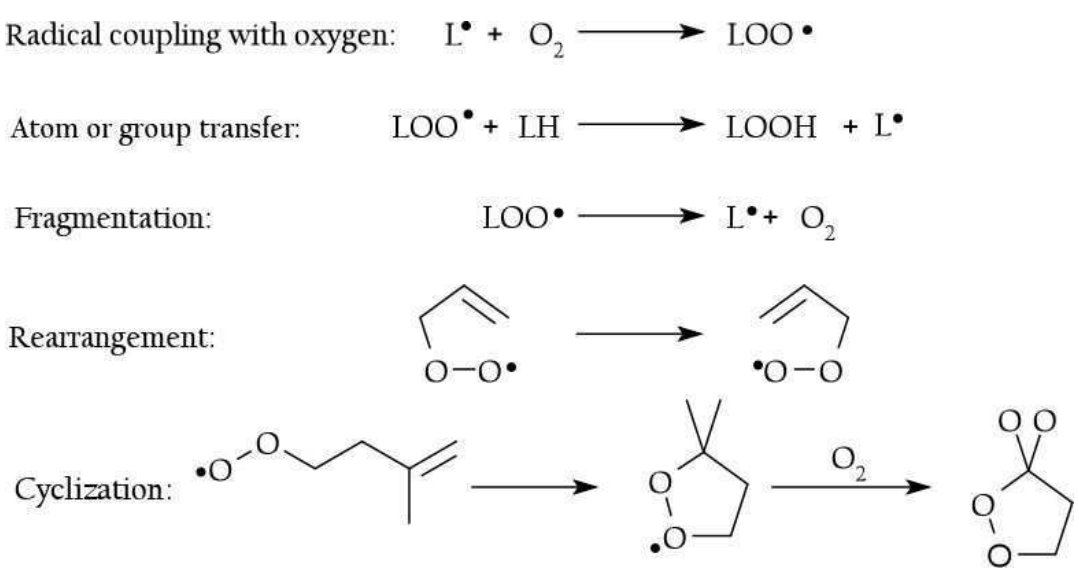

Figure 6: Alternative reactions to hydrogen abstraction

Thus, each fatty acid radical produces a set of initial breakdown products that are typical of the specific hydroperoxide and depend on the position of the peroxide group in the parent molecule. The decomposition products can themselves undergo further oxidation and decomposition, thus contributing to a large and varied free-radical pool. It should also be mentioned that hydroperoxides begin to decompose as soon as they are formed. In the first stages of autoxidation, their rate

of formation exceeds their rate of decomposition. The reverse takes place at later stages.

1.1.1.3 TERMINATION

Termination corresponds to reactions in which free radicals terminate to form nonradical products.

Figure 7 presents the different major mechanisms that are implied in this step.

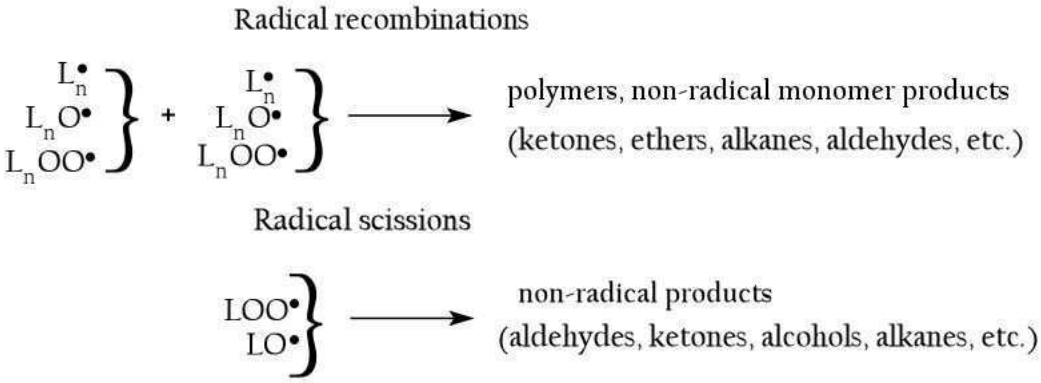

Figure 7: Main products formed upon the propagation reactions of lipid oxidation

Secondary peroxyl radical recombine rapidly to form a variety of products, including aldehydes, alcohols, ketones, acids esters, or short-chain hydrocarbons. The number of variations possible for radical recombination is nearly limitless, and this accounts, in part, for the broad range of oxidation products detected in lipid oxidation. Nonetheless, recombinations are promoted by chemical and physical factors such as oxygen concentration (cf. § 1.2.3) and temperature (cf. § 1.2.4).

1.1.2 PHOTOOXIDATION

As mentioned previously (cf. § 1.1.1), oxidation of unsaturated fatty acids can occur through a self-catalytic free-radical mechanism (autoxidation) that accounts for the chain reaction of hydroperoxide formation and decomposition. However, because it is unlikely that initiation occurs by direct attack of oxygen in its most stable form (triplet state) on double bonds of fatty acids, the singlet oxygen ($^1O_2$) is believed to be implied in the initiation step. Singlet-state oxygen is more electrophilic than triplet state oxygen. It can thus react rapidly (1500 times faster than $^3O_2$) with C=C bonds. The resulting hydroperoxides can then cleave to initiate a conventional, free-radical chain reaction.

Photosensitization in foods is probably the most important way to produce singlet oxygen. Several substances are commonly found in fat-containing foods that can act as photosensitizers to produce $^1O_2$. They include synthetic colorants and natural pigments, such as chlorophyll, pheophytin, and hematoporphyrin (the pigment portion of haemoglobin), riboflavin, myoglobin, aromatic amino acids, and any molecules with carbonyls or an extended conjugated double bond system. These molecules are able to collect the low level quantum energy of visible light (› 400 nm) that lacks the energy to produce radicals directly and to convert it to chemical energy.

Sensitizers (Sens) exist in two excited states: by absorption of light, the singlet (^{1}Sens) is converted to the triplet state (^{3}Sens), which has a longer life-time and initiates photosensitized oxidation. Figure 8 presents the chemical mechanism for the formation of singlet oxygen in the presence of sensitizer, light, and triplet oxygen in foods. The ^{3}Sen* reacts with $^3O_2$ to form $^1O_2$ and ^{1}Sen. ^{1}Sen may begin the cycle again to generate singlet oxygen. Sensitizers may generate 103–105 molecules of singlet oxygen before becoming inactive.

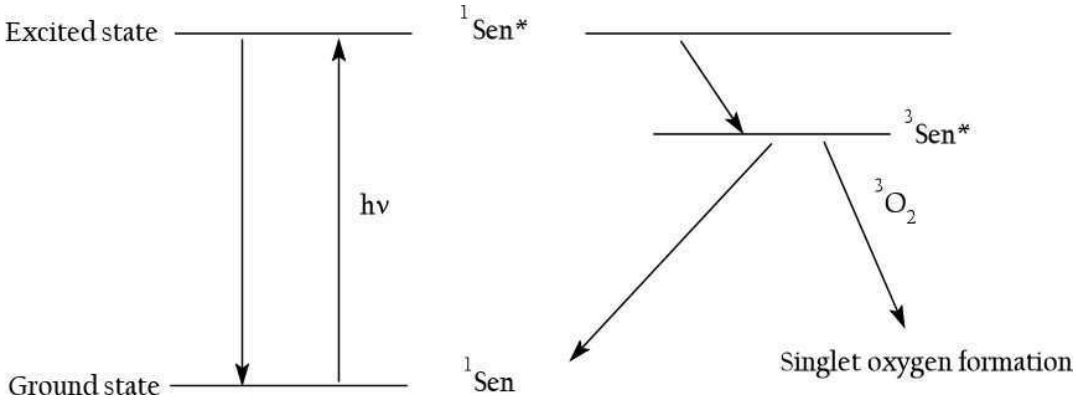

Figure 8: Effect of light on sensitizer state (Akoh & Min, 2002) ^{1}Sen: ground state singlet sensitizer; ^{1}Sen: excited sensitizer by light energy absorption; ^{3}Sen*: excited triplet state molecule*

Figure 9 shows the two pathways proposed for hydroperoxide formation from sensitizers. Type I and Type II reactions will enhance oxidation by the formation of reactive radical compound species and the production of singlet oxygen, respectively. More precisely, in the Type I pathway, excited triplet sensitizer (^{3}Sen*) may react directly with a compound (LH) to form intermediates (free radicals or free radical ions) that in turn react with ground-state (triplet) oxygen to yield hydroperoxides. In the Type II pathway, triplet oxygen is presumably the species that reacts with ^{3}Sen* to form singlet oxygen and singlet sensitizer that react further with unsaturated lipids.

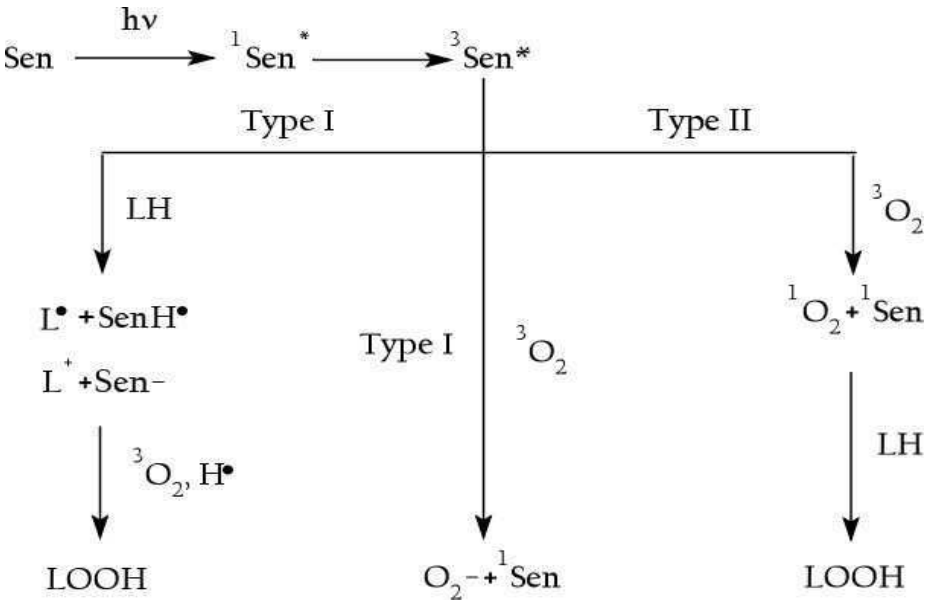

Figure 9: Types I and II pathways for hydroperoxide production by photooxidation

The competition between compounds and triplet oxygen for the excited triplet sensitizer determines whether the reaction pathway is Type I or Type II. Photosensitized oxidation may change the types of pathway during the course of the reaction as the concentration of compounds and oxygen changes. In aqueous lipid biphasic systems, the longer half-life of singlet oxygen in the lipid phase favors Type II pathway.

In conclusion, lipid oxidation is an autocatalytic reaction, i.e. once started, the reaction is self-propagating and self-accelerating. Moreover, it produces multiple intermediates and products that change with reaction conditions and time. Because product analysis and studies of mechanisms have become more sophisticated, a new overall reaction scheme for lipid oxidation has been proposed to replace the classic chain reaction into the three main stages initially described (Figure 10). On the whole, these features present distinct challenges in measuring and controlling lipid oxidation, and are part of the reason why lipid oxidation is a major problem in storage stability of foods.

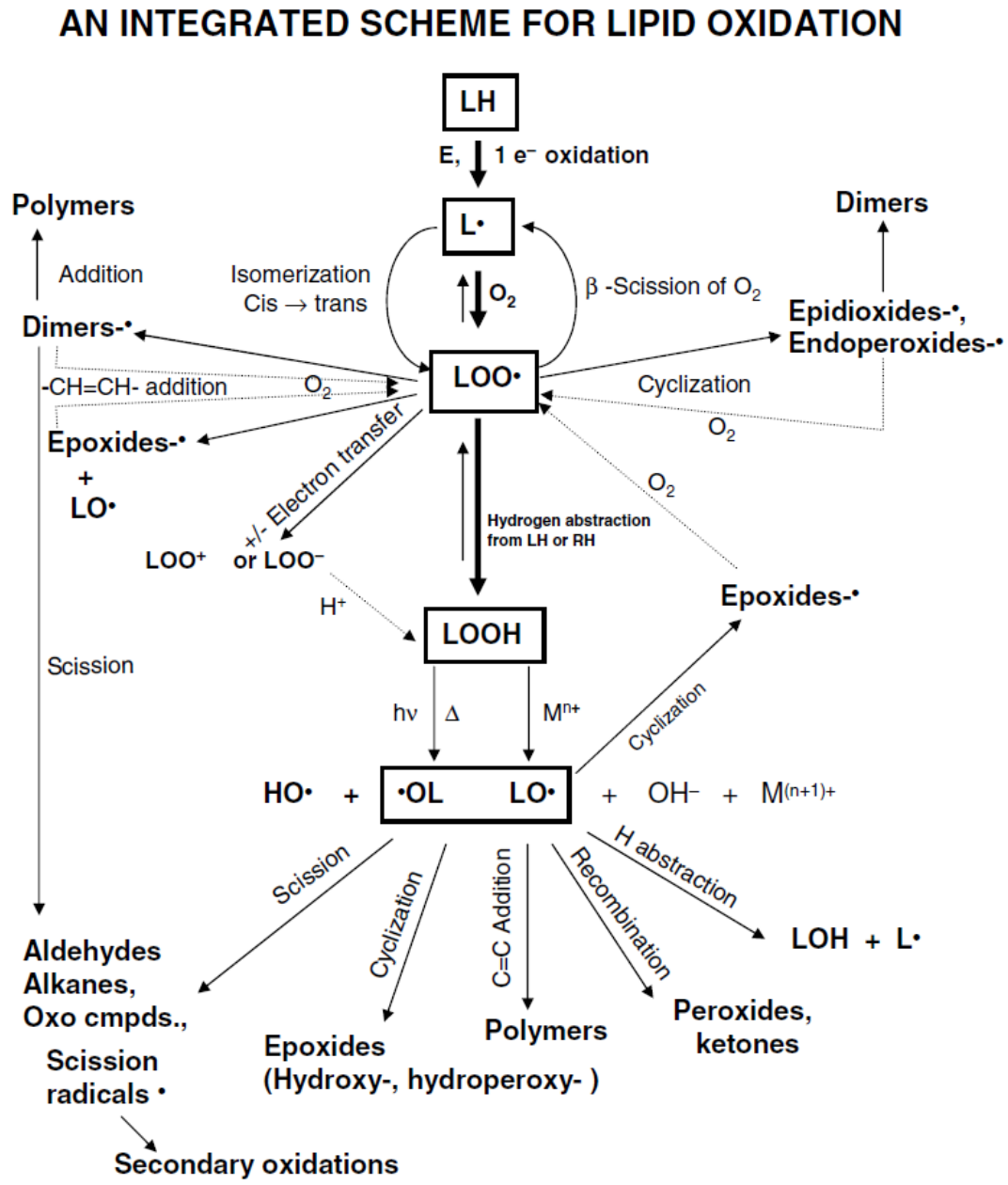

Figure 10: Integrated scheme for lipid oxidation accounting for multiple reaction pathways competing with the classic hydrogen abstraction (Schaich, 2005). Dotted lines indicate paths for oxygen addition to secondary radicals formed in cyclic and addition product

1.2 FACTORS INFLUENCING THE RATE OF LIPID OXIDATION IN OILS AND FATS

1.2.1 FATTY ACID TYPE

Triacylglycerols (Figure 11) represent more than 95% of the lipids in oils and fats. TAG are constituted of three fatty acids esterified to a glycerol molecule. The type of fatty acids and their positions on the glycerol backbone are key factors in the oxidative behaviour of the oil (Colakoglu, 2007).

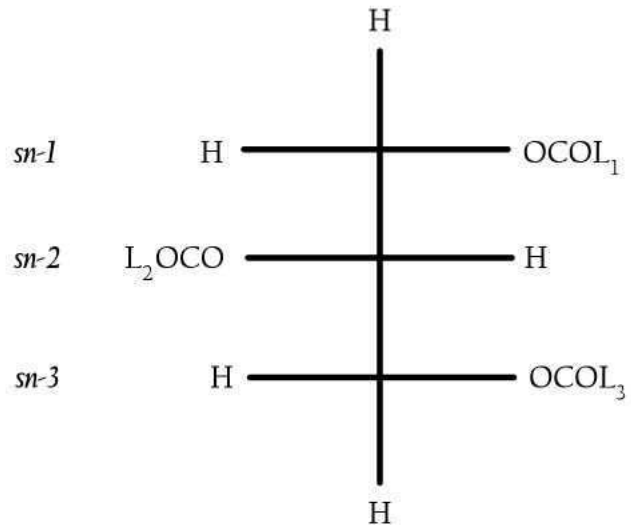

Figure 11: Triacylglycerol and the fatty acid positions in the glycerol frame

1.2.1.1 NUMBER AND POSITION OF THE FATTY ACID DOUBLE BONDS

The number of bisallylic bonds present in the fatty esters determines the oxidation rate of the oil. Thus, the oxidability of oleic acid (O, 18:1), linoleic acid (Lo, 18:2), α-linolenic acid (Ln, 18:3), arachidonic acid (20:4), eicosapentaenoic acid (EPA, 20:5) and docosahexaenoic acid (DHA, 22:6) increases with the number of unsaturations (Frankel, 1980). Because Lo reacts 40 times faster than oleic acid high-oleic oils have improved oxidative stability compared with the original oils (Kamal-Eldin, 2006). Using synthetic TAG with long chain PUFA in presence of a radical initiator, highly unsaturated TAG with three moles of EPA are slightly less unstable than TAG with three moles of DHA as shown by the oxidative rates,

estimated from oxygen consumed: 1.21 ± 0.04 and 1.28 ± 0.07 ml O_2.mmol^{-1} of fatty acid.h^{-1} of for tri-EPA and tri-DHA, respectively (Endo et al, 1997).

Oxidative stability can be evaluated either by data obtained on initial oil samples or under heating conditions. For example, different blends of two polyunsaturated oils, palm oil olein and olive oil are characterized regarding their initial content in primary (peroxide value) and secondary (anisidine value) oxidation products (Naghshineh et al, 2010). Increasing the proportion of olive oil in the blends increases the contents in oleic acid (18:1) (from 43% to 75%) and decreases the linolenic acid proportion (18:3) (from 11% to 7%). Both the peroxide and anisidine values increase with the olive oil content suggesting that the chemical stability of the blends decreases with increasing the proportion of monounsaturated fatty acid. This may result from the high content of saturated fatty acids in palm oil olein (more than 40% in palmitic acid (P 16:0)).

In the case of oxidation tests, it is reported that the resistance of purified oils from different soybean germplasms to oxidation at 60°C, measured as peroxide value, correlated positively with the average number of double bonds (R = 0.81), Ln (R = 0.85), and Lo (R = 0.63), and negatively with oleic acid (R = 0.76) (Kamal-Eldin, 2006). As a consequence, oils with high PUFA contents are more sensitive to oxidation than those with low PUFA contents. For example, soybean oil (24% O and 51% Lo) exhibits a lower stability against thermal oxidation (6 h, 180°C) than olive oil (71% O and 10% Lo) as measured by peroxide value (Lee et al, 2007). Another study dealing with the thermal stability of edible vegetable oils (determined by the temperature of the beginning of the decomposition) shows the following stability order corn›rice›soybean›olive›rapeseed›sunflower (Santos et al, 2004). In this case, the comparison does neither make differences between Lo and Ln contents among the PUFA nor take into account the presence of natural antioxidants.

Another example concerns fish oil. Oils extracted from menhaden, bonita and sardine rich in EPA (20.1, 7.4 and 24.7%, respectively) and DHA (12.3, 30.1 and 14.6%, respectively) are much more susceptible to oxidation than unsaturated vegetable oils (soybean and canola oils) containing linolenic acid (6.6 and 10.8%,

respectively) as measured by the production of volatile compounds (propanal and hexanal) as secondary oxidation products at 100°C (Frankel, 1993).

1.2.1.2 Location of the fatty acid on the glycerol backbone

Besides the degree of unsaturation of the TAG, the position of the fatty acids on the glycerol moiety may affect their oxidability. Numerous studies report that unsaturated fatty acids located at the sn-2-position are more stable than fatty acids at the sn-1- or 3-positions of TAG. These studies deal with either native oils or chemically synthetized TAG.

The case of structured TAG containing only one unsaturated fatty acid either in internal position or in external position is reported (Neff & El-Agaimy, 1996). Two different synthetical TAG with linoleic acid (18:2) and palmitic acid, (16:0) in different positions (PLoP, PPLo) are oxidized at 60°C, for 144 h, in dark. The oxidative state is evaluated by the presence of primary oxidation products. PLoP is slightly more sensitive to oxidation than PPLo (peroxide values of 12.6 and 10.4 $mEq.kg^{-1}$, at 144 h, respectively). Another example reports the use of synthetic TAG containing DHA (D) at the internal position in combination with palmitic acid or oleic acid. When subjected to accelerated auto-oxidation (at 40 or 50°C inside a dark oven), DHA at the sn-2 position (PDP and ODO) is oxidized more slowly compared with the sn-1(3) position (PPD and OOD), as evidenced by the lower generation of both primary and secondary oxidation products (Wijesundera et al, 2008).

For structured TAG containing several unsaturated fatty acids in a single TAG molecule, the oxidative stability is compared (Neff & El-Agaimy, 1996). Dilinoleic-monosaturated acids containing TAG (PLoLo and LoPLo) oxidize more and much faster than the monolinoleic-disaturated fatty acids TAG (PLoP, PPLo) due to the higher unsaturated degree of the former. Moreover, PLoLo oxidize faster than LoPLo (peroxide values of 135.5 and 57.8 $mEq.kg^{-1}$, at 144 h, respectively). This suggests that the position of Lo adjacent to another linoleic acid (PLoLo) has a lower stability than LoPLo with Lo separated by a saturated fatty acid. Conversely, the oxidation of trilinolenin autoxidized at 40°C does not show any

difference between the formation of monohydroperoxide either in the 1(3)- or 2-triacylglycerol position (Neff et al., 1990; Frankel et al, 1990).

When natural and enzymatically interesterified fish oils (sardine, cod liver, skipjack) are compared, it appears that interesterification leads to more stable oils towards autooxidation at 40°C (Kimoto et al., 1994). Knowing that interesterification is associated to a redistribution of fatty acids on the glycerol backbone (and a decrease of the PUFA located at the sn-2 position), it may be assumed that EPA and DHA are more evenly distributed in interesterified oils. It is worth noting that in the case of minke whale oil containing less EPA and DHA than the previous fish oils, oxidative stability was reduced after interesterification although interesterified oil was richer in PUFA at the internal position than the native oil (Kimoto et al., 1994). This controversial result may account for different content in antioxidant compounds.

In the case of vegetable oils, the study of the oxidative stability of natural and genetically modified canola oils at 60°C in the dark shows that the less stable oils correspond to that containing increased amount of linoleic acid and decreased amount in oleic acid on the triacylglycerol carbon 2 (Neff et al., 1997). Conversely, other works report no effect of glycerol position of constituent fatty acids on the oxidative stability of structured TAG (Neff et al., 1997).

In conclusion, results about the influence on oxidation of the position of fatty acid in the glycerol structure of TAG are sometimes confusing. This may be due the lack of standardized, sensitive experimental designs and oxidative stability tests as well as the lack of accurate knowledge of the antioxidant composition.

1.2.2 Lipid type

1.2.2.1 Free fatty acids versus triacylglycerols

Esterification of fatty acids improves their oxidative stability. For example, at 70°C, oleic acid presents an induction time of 39 h while more than 90 h is measured for triolein (cf § 1.3.1 for the definition of the induction time) (Knothe & Dunn, 2003).

1.2.2.2 Phospholipids versus triacylglycerols

To accurately compare TAG and phospholipid (PL) species in terms of their stability to oxidative treatment, fatty acids should be esterified at the same position of the glycerol backbone. This is actually the case in the study of Le Grandois et al, (2010). It is demonstrated that phosphatidylcholine (PC) species containing oleic acid or linoleic acid in internal position is more stable than the corresponding TAG species to heat-induced oxidation (at 150°C and 125°C over 2 h of oxidation time). For example, the induction time measured at 150°C is 45 min for 1-stearoyl-2-oleoyl-*sn*-glycero-3-phosphocholine (SOPC) versus 15 min for 1,3-stearoyl-2-oleoyl-glycerol (SOS). A similar behaviour is found for the di-unsaturated species compared at 125°C (SLPC, 1-stearoyl-2-linoleoyl-*sn*-glycero-3-phosphocholine and SLS, 1,3-stearoyl-2-linoleoyl-glycerol). The best oxidative stability for PC species compared with the corresponding TAG species may account for the presence of a polar head group that affects the oxidation kinetics of the glycerol-based lipids. Similar results are obtained with TAG and PL enriched in DHA (Song et al, 1997) with the same constituent fatty acids, stored at 25°C in dark. After 10 weeks of storage, the oxygen uptake of the PL enriched in DHA is 7 times lower than the corresponding TAG. Additionally, the content of DHA in TAG drastically decreased (from 10.7 to 0.3 mol%) compared with its amount in PL (from 10.7 versus 9.6 mol%). The PL could act as chelating agent, since a reductive conversion of lipid hydroperoxide to the corresponding hydroxyl compound by the polar head group is observed with unesterified choline and ethanolamine.

Several other postulates have been proposed to understand the antioxidant properties of PL (King et al., 1992):

- Synergism between PL and tocopherol present in the vegetable oil

- Chelation of pro-oxidant metals by phosphate groups

- Formation of Maillard-type products between PL and oxidation products

- Action as an oxygen barrier between oil/air interfaces

However, all PL do not exhibit similar antoxidant ability (King et al., 1992).

1.2.3 OXYGEN CONCENTRATION

Oxygen is a requirement for oxidative deterioration of lipids. Oxygen has a greater solubility in non-polar than in polar solvents, and hence is more soluble in oil than in water. Oxygen content either in headspace concentration or dissolved in the product is a very important factor because it influences the oxidation rate and, in turns, the oxidation reactions towards specific pathways leading to different oxidation products (Andersson & Lingnert, 1998a, 1998b, 1999; Choe & Min, 2006; Velasco & Dobarganes, 2002). From a general point of view, three cases can be distinguished (Labuza, 1971):

-at high oxygen partial pressures, i.e; when oxygen is not limiting, the oxidation rate depends on the substrate concentration or, in other words, the propagation step (Figure 3) is so rapid that all of the free radicals are in the form of peroxyl radical, independently of the oxygen concentration.

-at intermediate partial pressures, an increased influence of oxygen partial pressure occurs.

-at low oxygen partial pressures, when the oxygen is limiting, if the initiation rate is constant (Figure 3) and the amount of substrate is high, the substrate concentration does not change substantially and the oxidation rate is independent of substrate concentration and directly dependent of oxygen partial pressures.

For example, a study compares rapeseed oil oxidation stored in air, or with 1.1%, 0.17% and 0.04% oxygen in the head space (Andersson & Lingnert, 1998b). It is worth noting that to maximize the surface area of the oil and thereby minimize the effect of oxygen diffusion, the oil (2.5 ml) is applied to dental cotton wool rolls. For a storage at 40°C, during 35 days, in darkness, oxygen consumption in the headspace is low unless a prooxidant metal is added. This study points out that the effect of oxygen in promoting lipid oxidation is better detected when the change in oxygen concentration is low. Hexanal amount doubles when the oxygen concentration is raised from 0.04% to 0.17%. However, the increase of oxygen to 21% only doubles the hexanal increase.

The surface area/volume ratio or in other words, the area interface between lipid phase and air can also influence the dependence of oxygen concentration on the oxidation rate. When the ratio of volume to surface increases, oxidation rate decreases. This negative change in oxidation rate is directly related to reduced oxygen partial pressure (Labuza, 1971).

A study compares the effect of the storage container size (or sample size) in the oxygen accessibility of canola and cottonseed oils at room temperature and in accelerated storage conditions (60-65°C) (Malcolmson et al., 1994). Three storage sample sizes were studied: 75 mL (68 g) in a 100-mL beaker, 150 mL in a 240-mL jar and 250 mL in a 500-mL beaker. Headspace varied from one fourth to one-half of the sample volume. In all cases, the samples are covered or stoppered loosely during storage. Significant variations in terms of flavour intensity (related to secondary product formation) are observed among the samples.

In conclusion, comparing different experiments of lipid oxidation requires the knowledge of the exact storage conditions because they can be performed at different oxygen levels.

1.2.4 TEMPERATURE

According to Frankel (1984), the rate of oxidation is exponentially related to temperature, that means that the shelf life of a food lipid decreases logarithmically with increasing temperature. Thus, the oxidation rate of fatty acids can be described by the Arrhenius Equation:

$$K = Ae^{-Ea/RT} \quad (1)$$

where A is a pre-exponential factor related to the geometry of the reaction medium, e is a constant, *Ea* is the activation energy ($J.mol^{-1}$), R is the universal gas constant ($8.314\ J.K^{-1}.mol^{-1}$), and *T* is the absolute temperature (in Kelvin).

Different oxidation products are formed as a function of temperature (Velasco & Dobarganes, 2002). At low or moderate temperatures, hydroperoxides are mainly formed so that the formation of secondary oxidation products such as volatile compounds only becomes significant after the end of the induction period. At high temperatures, hydroperoxides are practically absent above 150°C indicating that their rate of decomposition becomes higher than that of their formation and polymeric compounds are formed since the very early stages of heating.

Many other works (Hess & Ohare, 1947; Kamal-Eldin et al., 2003; Sathivel et al., 2008; Simon & Kolman, 2001; Tan et al., 2001) show the dependence of lipid oxidation on temperature.

For example, the temperature effect on linseed oil oxidation is studied at constant conditions of air flow and agitation (Hess & Ohare, 1947). Temperature affects both the induction period and the peroxide value as shown in Figure 12.

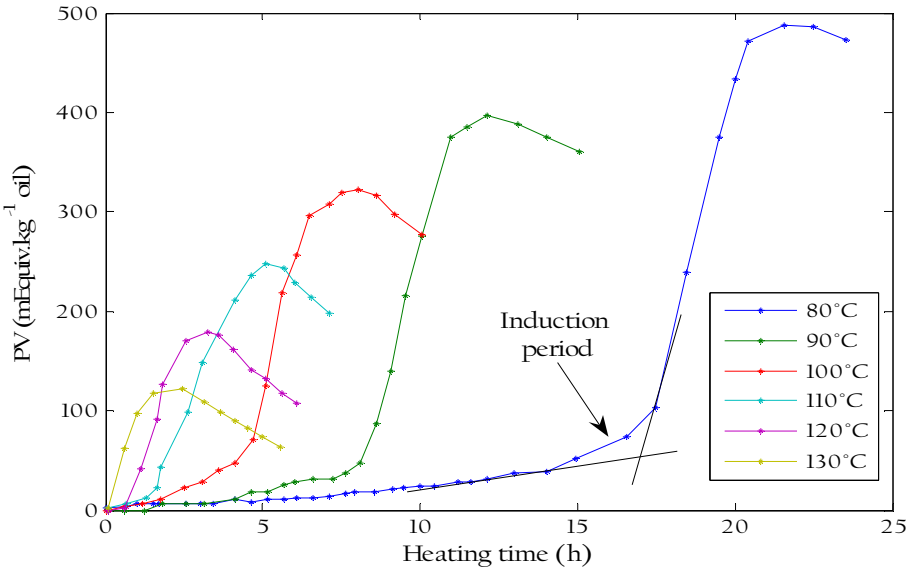

Figure 12: The effect of temperature on the oxidation of flaxseed oil (Kamal-Eldin et al., 2003), PV: Peroxide value

Another study shows that the lipid oxidation rate in relation to temperature can be well described by the Arrhenius equation (1) for the unrefined pollock oil (Sathivel et al, 2008) (Figure 13). In this case, lipid oxidation is followed by hydroperoxide formation for temperatures between 40 and 90°C. Similar relationship is found for unpurified salmon oil (Huang & Sathivel, 2008).

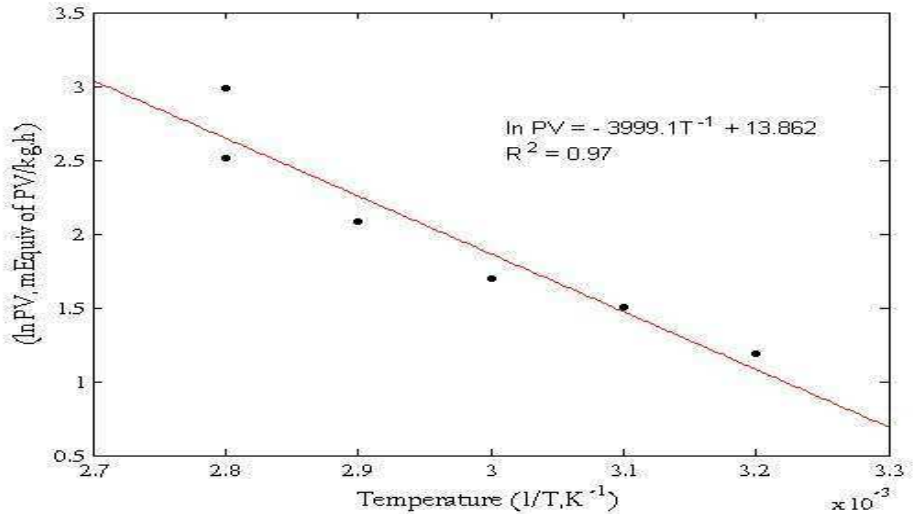

Figure 13: The Arrhenius plot for the peroxide values (PV) of the unrefined pollock oil (Sathivel et al., 2008)

A final example concerns the study of ten different vegetables oils analyzed at temperature ranging from 110-140°C. Once again, the rate of lipids oxidation is highly correlated with temperature (Tan et al, 2001).

It is worth noting that there is a strong interaction between temperature and oxygen. Indeed, as temperature increases, the solubility of oxygen decreases drastically (decreasing the oxidation rate) although all the oxidation reactions are accelerated (Labuza, 1971).

1.3 QUANTIFICATION OF LIPID OXIDATION

Oxidative decomposition is of major significance in regard to both the acceptability and nutritional quality of food products. Two major points are relevant regarding oxidation. The first one concerns the measurement of the present oxidative status answering the question of how far has a sample already been oxidized. The second one deals with a predictive measurement of oxidation in relation with its shelf-life. In this context, it is essential to dispose of several characterization methods to assess the variety of chemical compounds involved in the numerous reactions of the lipid oxidation process. Although these reactions appear to follow stepwise pathways, they often occur simultaneously and competitively. Numerous methods are available to give a quantitative or qualitative picture of the extent of lipid oxidation. Hydroperoxides are often measured to characterize the early stages of lipid oxidation. However, when hydroperoxide concentrations alone are considered, oxidation extent and kinetics may be underestimated. Other methods deal with the formation of secondary oxidation products which are often implied in the degradation of the sensory properties of food stuff. In this chapter, we will only discuss the methods used to characterize oil oxidation in bulk phase. Indeed, in food matrix, some molecules like proteins and sugars may interfere with lipids and make the tests less pertinent.

1.3.1 Classical methods for measuring lipid oxidation

The available methods to monitor lipid oxidation are based on physical or chemical tests, some of which are standardized and some of which use more sophisticated methods often needing specific instrumentation. Table 3 presents the main methods found in the literature to manage oxidation (Frankel, 2005) and Table 4 compares these methods. In this chapter, we will only discuss the studies on oil oxidation using the differential scanning calorimetry (DSC) technique.

Table 3: Main methods reported in the literature for the characterization of lipid oxidation of oils

	Compounds detected	Principle of measurement
Change in reactants	Loss of PUFA	-Change in fatty acid composition -Iodine value
	Weight gain	Increase in weight by addition of oxygen
	Oxygen consumption	Reduction of the oxygen pressure (headspace measurement) or oxygen concentration (electrochemical detection) due to oxygen uptake
Primary products of oxidation	Hydroperoxides	-Ability of the peroxides to liberate iodine from potassium iodide (iodometry) or to oxidize ferrous to ferric ions (thiocyanate method) -Stoichiometric reaction of triphenylphosphine with hydroperoxides and measurement of the absorption band by Fourier transform infrared spectroscopy (FTIR) -Reaction of hydroperoxides with chemiluminescent products (luminol and dichlorofluorescein) -Characterization of specific hydroperoxides by chromatographic techniques (gas chromatography (GC), high-performance liquid chromatography (HPLC))
	Conjugated dienes and trienes	Measurement of UV absorption at 234 and 268 nm, respectively
	Free radicals	Measurement of electron spin resonance (ESR): absorption of microwave energy by a sample placed in a varied magnetic field

Table 3: Main methods reported in the literature for the characterization of lipid oxidation of oils

	Compounds detected	Principle of measurement
Secondary products of oxidation	Anisidine value (*p*-AnV)	Color reaction of 4-methoxyaniline (anisidine, $ArNH_2$) with aldehydes (2-alkenals and 2,4 alkadienals)
	Thiobarbituric acid (TBA) test	Color reaction between TBA and TBA reactive substances (TBARS) (malondialdehyde, alkenals, alkadienals)
	Volatile organic acids	Formation of short-chain acids (formic acid and acetic acid) measured by the variation of water electrical conductivity when a stream of air is drawn through heated oil into a vessel containing water (oil stability index (OSI))
	Total carbonyl compounds	Color reaction with 2,4-dinitrophenylhydrazine to form hydrazones
	Volatile carbonyl compounds	Separation and identification of short chain aldehydes by headspace GC
	Epoxides	Reaction of hydrogen halides and the oxirane group
	Hydrocarbons	GC techniques for short-chain (C1-C5) hydrocarbons
Primary and secondary products of oxidation	Totox value	= 2 Peroxide Value + *p*-Anisidine Value
	Nuclear magnetic resonance (NMR) spectroscopy	Change of the molecular environment of proton (^{1}H) or carbon (^{13}C)

Table 4: Advantages and drawbacks of the main methods reported in the literature for the characterization of lipid oxidation of oils

	Advantages	Drawbacks
Loss of PUFA	Possible identification of fatty acids involved in the oxidative changes	-Difficult to use when the amount of PUFA is low -Determination of fatty acid composition by GC (necessity of a derivation step) -Poorly sensitive method compared with peroxide value
Weight gain	-Relatively quantitative during initial stages of autoxidation -Simple method -Low instrumentation cost	-Carefully monitor the working conditions (sample size, shape of container) -Weighing frequency when monitoring fast kinetics or low temperatures
Oxygen consumption	Simple and reproducible method	
Peroxide value (iodometry)	-Indicator of the early stages of oxidation -Good correlations may be obtained sometimes with development of oxidative off flavors -Standardized method	-Large amount of sample required -Generation of significant amount of waste -Lack of sensitivity in determining the titration endpoint -No systematic strict correlation with the level of off-flavor in the product -Time-consuming
Peroxide value (thiocyanate method)	-More sensitive method than the iodometric assay -Rapid not sensitive to ambient oxygen or light	Possible interference of the spectrophotometric measurements for colored samples

Table 4: Advantages and drawbacks of the main methods reported in the literature for the characterization of lipid oxidation of oils

	Advantages	Drawbacks
Peroxide value (FTIR)	-Highly precise method -Good correlation with iodometric method -No solvent and reagent needed	-High instrumentation cost -Need to assign wavelengths to more common molecular species
Conjugated dienes (CD)	-Good correlation with peroxide value (early stages of oxidation) -Simple and fast method -Small amounts of samples required	-Method not suitable for heated fat, for fat that already contains conjugated dienes, and for fats with a high content of oleic acid or low levels of linoleic acid -Method less specific than the peroxide value measurement
Free radicals (ESR)	-Characterization of free radicals originating in the early stages of oxidation and of the onset of primary oxidation -High sensitivity -Requires little sample preparation	Expensive instrumentation cost
Anisidine value	-Good correlation with the amount of total volatile compounds -Significant correlation with flavor scores	-More sensitive to unsaturated aldehydes than saturated aldehydes -Cannot be used to compare different types of oils -Toxicity of the anisidine reagent
Thiobarbituric acid test	Good correlation with the intensity of oxidized flavor in liquid milk	Presence of malonaldehyde not always present in oxidized systems

Table 4: Advantages and drawbacks of the main methods reported in the literature for the characterization of lipid oxidation of oils

	Advantages	Drawbacks
Total carbonyl compounds		-Necessity to reduce hydroperoxides to non carbonyl compounds prior to determination of carbonyls -Conducting the reaction at a low temperature.
Volatile carbonyl compounds	-Possibility to detect flavor notes (for example, 4-heptanal, 2,6- and 3,6-nonadienals) -Good correlation between hexanal content, sensory scores, and TBA values	Expensive instrumentation cost (headspace GC)
Volatile organic acids	-Automatic commercially instruments available (Rancimat, Oxidative Stability Instrument) -Useful comparative values when the same oil is used	-High level of oxidation required -Limited for predicting the stability of a range of oils
Totox value	Good estimation of the progressive oxidative deterioration of fats and oils	Combination of two indicators with different dimensions
NMR spectroscopy	Rapid and non-destructive method	-Expensive instrumentation cost -No direct quantification of the oxidation deterioration

1.3.2 THERMAL ANALYSIS METHODS FOR MEASURING LIPID OXIDATION

A number of novel methods have been developed to estimate the deterioration of oils. One of them is based on thermal analysis which comprises a group of methods based on the measurement of the exothermic events occurring during the oxidation reactions (Simon et al., 2000). The two main thermo-analytical techniques available are based on the measurement of temperature change by Differential Thermal Analysis (DTA) or heat flow variation by Differential Scanning Calorimetry (DSC). However, the thermal analysis approach can also measure other physical parameters (i.e., change of the mass or the gas volume); some of them are listed in Table 5. In the following, we will only focus on DTA and DSC methods to investigate the oxidative behaviour of oils.

Table 5: Main groups of thermo-analytical methods (Litwinienko, 2005)

Parameter measured	*Name*
Mass	*Thermogravimetry*
Temperature difference	*Differential thermal analysis*
Heat flux (enthalpy)	*Differential scanning calorimetry*
Volume of gaseous products	*Evolved gas analysis*
Dimension (length, volume) changes	*Dilatometry*
Mechanistic properties, deformations	*Thermo-mechanical analysis* *Dynamic mechanical analysis*

1.3.2.1 DIFFERENTIAL THERMAL ANALYSIS

In the case of DTA, the sample and the reference material are heated by the same heat source. The temperatures of the sample and of the reference are measured separately by two thermocouples (Figure 14).

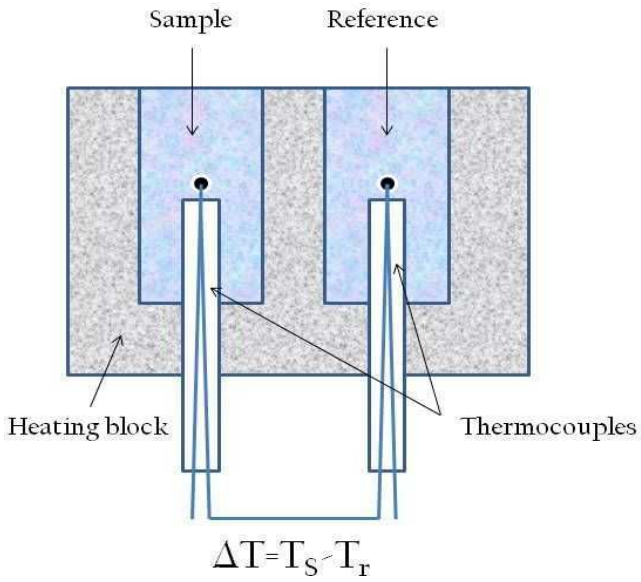

Figure 14: Schematic diagram of differential thermal analysis cell (Litwinienko, 2005)

The temperature difference between the sample and the reference (inert material), $\Delta T = T_S - T_r$, is measured either as a function of temperature or as a function of time, τ, when subjected to a programmed temperature ($T = T_0 + \beta\tau$, where T_0 is an initial temperature and β is a heating rate (in $K.min^{-1}$)). Thus, as long as no reaction or phase transition occurs, no difference between temperatures T_S and T_R is recorded and the experimental curve is flat (baseline). When the sample and reference are submitted to a temperature increase, the sample can undergo a chemical reaction or a phase transition. Its response in temperature varies compared with that of the reference. The thermocouple measures this temperature variation. In practice, in the case of a phase transition, the baseline changes into a peak, that returns to the baseline according with the ongoing process ending. If $T_S < T_r$, this means that the phase transition involves heat absorption and an endothermic peak is observed. On the contrary, if $T_S > T_r$, the reaction gives an exothermic peak, involving a heat release.

When DTA is programmed with a heating rate, the temperature difference between the sample and the reference is plotted as a function of temperature. When the system works in isothermal conditions (i.e., at constant temperature), the DTA curve is plotted as a function of time. Concerning the magnitude of ΔT, this value is proportional to the changes in enthalpy and heat capacity and to the total thermal resistance to the heat flow.

1.3.2.2 Different scanning calorimetry

DSC measures the heat capacity as a function of temperature, but, unlike with DTA, the sample and reference are keep at a constant temperature with two individual heaters in order to kept $\Delta T = 0$ at any time of the experiment (Figure 15).

The International Confederation of Thermal Analysis and Calorimetry (ICTAC) considers two types of DSC. In the case of the power-compensated DSC (Figure 15 a)), if an exothermal or endothermal reaction occurs in the sample, the power input compensates ΔT, and the amount of heat provided to the sample or the reference is recorded as heat flux (mW) dh/dt. In the case of the heat flux DSC

(Figure 15 b)), the temperature difference between the sample and the reference is measured, and the difference is proportional to the change in the heat flux. The heat flux DSC differs from DTA system since the thermocouples are attached to the base of the sample and reference holders. Thus, absorption or emission of heat by the sample causes a variation in heat flux through the heat sensitive plate. Then, the temperature difference between the heat sensitive plate and the furnace is recalculated into the enthalpy of the occurring process.

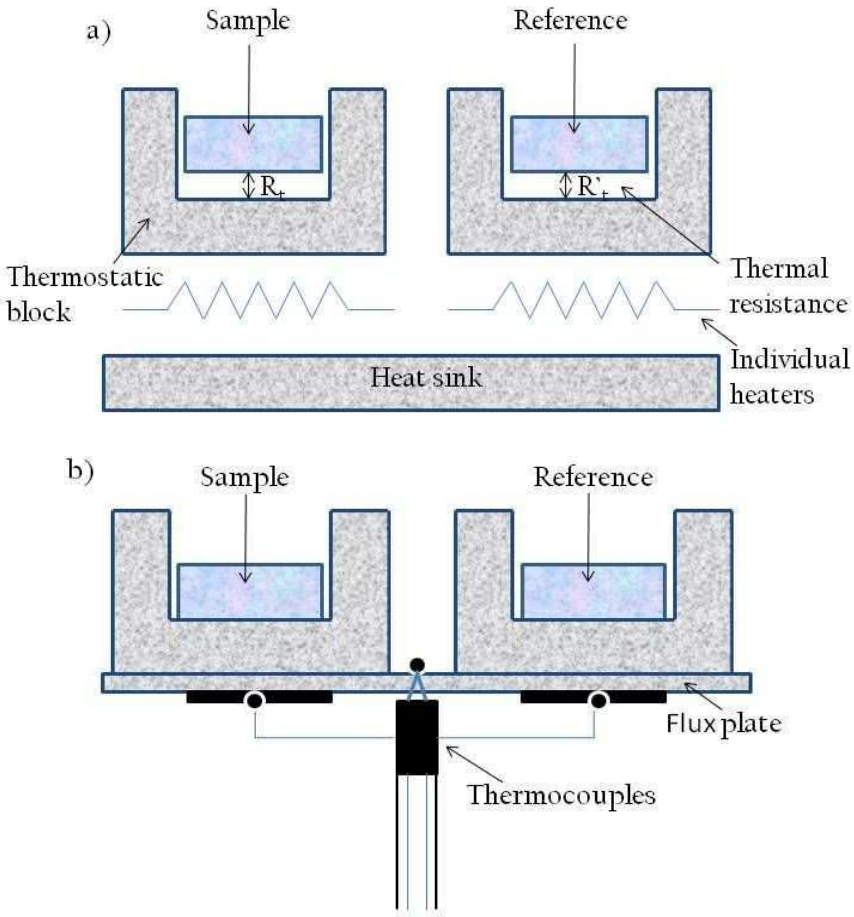

Figure 15: Schematic diagram of the sensitive part of differential scanning calorimeter, a) Power-compensated DSC, b) Heat flux DSC

1.3.2.3 THE CALORIMETRY PRINCIPLE

The sample to be measured is contained in an adapted vessel (an inert material such as aluminium recommended to avoid lipid oxidation) and the optimal weight

of the samples analyzed by the DSC should be lower than 10 mg to form a flat, thin layer on the bottom of the sample pan. The reference consists of the same vessel (same material and same size) but used empty. The measurement chamber that contains the sample is surrounded by a detector (thermocouple, resistance wires, and thermopiles) to measure the heat flux exchanged by the sample. This chamber is insulated in a surrounding heat sink made by a high thermal conductivity material. Since any temperature perturbation of the thermostatic block will affect the measurement, a symmetrical calorimeter is preferred.

Consequently, two identical calorimeter chambers hold the sample and the reference, placed in similar pans but the first one containing the material to be analyzed and the second one being empty. The two containers are placed in the thermostatic block at the same temperature (T_P). The heat flux difference is measured between the two chambers.

The heat flux $\frac{dh}{dt}$, produced by the transformation of the sample or the reaction, is given by:

$$\frac{dh}{dt} = -\frac{dq}{dt} + (C_s - C_r)\frac{dT_p}{dt} - R_t C_s \frac{d^2q}{dt^2} \quad (2)$$

C_s and C_r are the heat capacities of the sample + the container, and the reference + the container, T_s and T_r are the temperatures of the sample and the reference, respectively and $\frac{dq_s}{dt}$ and $\frac{dq_r}{dt}$ are the heat flux exchanged with the thermostatic block at a temperature T_p through a thermal resistance R_t, as follow,

$$\frac{dq}{dt} = \frac{T_r - T_s}{R_t} \quad (3)$$

where by derivation, it becomes:

$$R_t \frac{d^2q}{dt^2} = \frac{dT_r}{dt} - \frac{dT_s}{dt} \quad (4)$$

By combining the equations (2) and (3), the characteristic equation for the calorimetric measurement is obtained:

$$\frac{dh}{dt} = -\frac{dq}{dt} + (C_s - C_r)\frac{dT_p}{dt} - R_t C_s \frac{d^2 q}{dt^2} \quad (5)$$

If $\frac{dh}{dt}$ corresponds to an endothermic reaction, the heat flux is positive. It is negative if it corresponds to an exothermic reaction. If the calorimetry performance is isothermal, $\frac{dT_p}{dt}$ is equal to zero.

In a small perturbation of the temperature T_p of the thermostatic block, the corresponding thermal effect will be minimized if C_s and C_r heat capacities are similar.

The term $R_t C_s \frac{d^2 q}{dt^2}$ (thermal lag) depends on the thermal resistance or the time of response of the calorimeter.

1.3.3 DSC APPLIED TO OIL OXIDATION STUDY

DSC has been used to study oil oxidation due to the fact that oil oxidation implies a number of exothermic thermally induced transitions. Indeed, this method allows assessing the oxidation process in real time as well as in accelerated conditions. In addition, DSC methods in isothermal and non-isothermal conditions show good correlation with other accelerated methods and chemical analysis of oil oxidation (Akoh & Min, 2002; Cross, 1969; Kowalski et al., 1997; Tan et al., 2002; Vittadini et al., 2003).

1.3.3.1 DETERMINATION OF THE INDUCTION TEMPERATURE AND INDUCTION TIME

In non-isothermal conditions, DSC curves evidence different events: i) the onset temperature (that can be associated with the initiation step), ii) the temperature at which the reaction is maximum, and iii) the offset temperature of advanced oil oxidation (that may be related to the termination step) (Tan & Che Man, 2002)

(Figure 16). The oxidation stability may be evaluated through the onset temperature, i.e., the temperature before the increase of the heat flux due to the development of the lipid oxidation reactions.

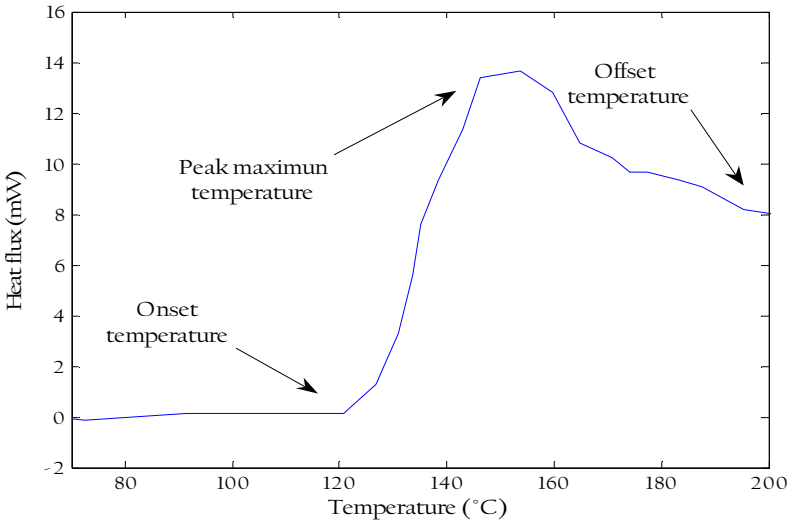

Figure 16: DSC curve of linseed oil in non-isothermal conditions (Litwinienko, 2001)

Similarly, in isothermal conditions, the oxidation stability may be evaluated through the time before the increase of the heat flux due to the development of the lipid oxidation reactions. This time is referred to as the induction time (Figure 17) and has been investigated in several works (Table 6).

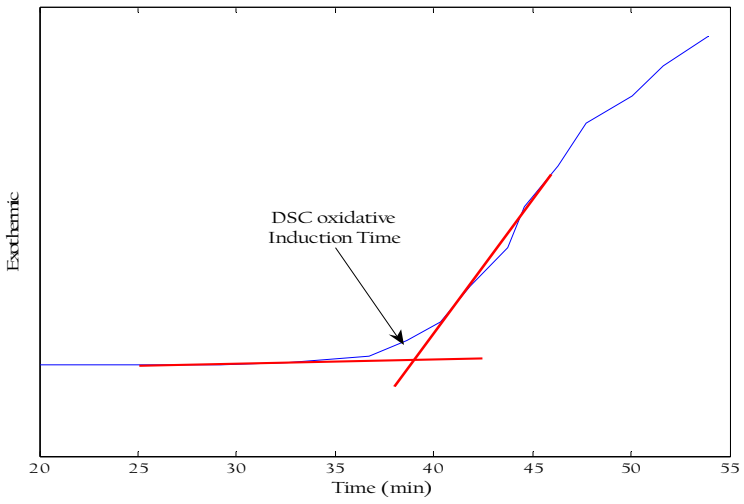

Figure 17: DSC oxidation curve of corn oil at 130°C (Tan et al., 2002)

Table 6: Induction time of different vegetable oils determined using DSC in isothermal conditions

Experimental conditions	Oil type	Induction time (min) at 110°C	Induction time (min) at 140°C	Reference
Pure oxygen (50 ml.min^{-1})	Coconut	325	44	Tan et al., 2002
	Canola	259	37	
	Corn	166	21	
	Grape seed	74	7	
	Olive	169	13	
	Palm kernel	539	70	
	Palm oil	515	82	
	Peanut	127	12	
	Safflower	88	8	
	Sesame	542	60	
	Soybean	124	20	
	Sunflower	131	19	
Pure oxygen (50 ml.min^{-1})	Bauhinia purpurea	483	48	Arain et al., 2009
	Cotton seed	172	20	
	Rice bran	132	18	
Pure oxygen (50 ml.min^{-1})	Buriti pulp	369	30	Pardauil et al., 2011
	Passion fruit	42	3	
	Rubber seed	51	3	

The induction times depend on the temperatures used in the experimental procedure (cf. § 1.2.4). Thus, the lower the experimental temperature applied, the longer the induction time value. More precisely, irrespectively of the oil studied, decreasing the temperature of 30°C increases the induction time by a factor 10.

Oil oxidation susceptibility is highly dependent on its fatty acid composition (cf. § 1.2.1). Because the induction time directly measures this susceptibility, then it is also function of the fatty acids present in the oil. For example, palm kermel and palm oils are characterized by high induction times (70 and 82 minutes, respectively, at 140°C) due to an elevated amount of saturated fatty acids (more than 50%) (Tan et al., 2002). In contrast, passion fruit and rubber seed oils with elevated proportions of PUFA (71% and 56%, respectively) are more susceptible to oxidation and present short induction times (3 minutes, at 140°C) (Pardauil et al., 2011).

However, as already mentioned (cf § 1.3.3.1), the accurate comparison of the oxidative stability of different oils and thus of induction times requires not only the knowledge of the fatty acid compositions but has also to take into account the presence of antioxidants. This is actually the case of sesame oil that, despite a high amount of PUFA (42.6 and 40.6% of linoleic acid and oleic acid, respectively), exhibited a quite good resistance to oxidation (induction time = 60 min at 140°C) probably due to the high amount of γ-tocopherol (predominant in 96-98%) and two naturally-occurring preservatives sesamol and sesamin (0.3 -1.2 %) that are the precursors of several phenolic antioxidants (Gunstone, 2003).

The induction time values can be correlated with other different oxidation measurement methods such as accelerated tests (Rancimat method, OSI) or volatile compound analysis. For example, a good correlation is found between OSI measurements and induction times for 4 different exotic vegetable oils at 4 temperatures ranging from 110 to 140°C (Pardauil et al., 2011).

1.3.3.2 STUDY OF THE KINETIC CONSTANTS OF LIPID OXIDATION IN OILS

As shown previously (cf. § 1.2.4), based on the *Arrhenius* equation, the reaction rate constant (k), the activation energy (E_a), the activation enthalpy (ΔH) and the activation entropy (ΔS) can be calculated. The determination of these kinetic parameters of the lipid oxidation of oils is important in order to optimize or at least maximize the quality of oil products during processing and storage. DSC technique has been successfully applied to obtain kinetics data on lipid oxidation of oils. Some of these works are summarized in Table 7.

The activation energy of the different oils studied varies from 48 to 104 kJ.mol^{-1}. A high activation energy implies that a small temperature change is required to induce a significant change in the rate of oxidation High energy values are often characterizing unsaturated oils because it reflects the energy required for the oxygen molecules to interact with the unsaturations.

1.3.3.3 . ADVANTAGES AND DRAWBACKS OF CALORIMETRY TO STUDY OIL OXIDATION

Calorimetry is largely used to follow oil oxidation because it presents numerous advantages (Kaletunc, 2009):

- The heat flow release by the chemical reactions (ΔH) is directly measured. The experimental results are not model dependent.

- Materials do not have to be optically transparent or to have chromophores as required by spectroscopic methods.

- Calorimetry does not require elaborated or destructive sample preparation.

- Small lipid samples are used.

- The time of analysis may be short when high temperatures are applied.

- The experimental procedure is simple.

- There is the possibility to work with a wide temperature range and with different heating programs.

- The theory behind the technique is well developed, which facilitates interpretation of the data.

- In case calorimetry is correlated with other chemical characterization methods, it avoids the use of organic solvents.

However, calorimetry also presents some drawbacks:

- It is not always easy to match the time scale of the events to be detected with the experimental time scale, especially in dynamic systems or in poor oxidative systems.

- If the magnitude of the heat flux (energy) associated with the transition is small, it needs the use of detectors with high sensitivity.

- In classical calorimeter device, the ratio volume/surface of the sample is imposed.

In this context, the design of a more versatile microcalorimer will compensate these different drawbacks.

Table 7: Determination of the kinetic constants of oils by DSC methods

Experimental conditions	Oil type	Activation energy ($kJ.mol^{-1}$)	Reference
1400 kP of pure oxygen	Rapeseed	81.9	Kowalski et al., 2000
Pure Oxygen ($100\ ml.min^{-1}$)	Mustard	90.6	Litwinienko, 1998
Pure Oxygen ($100\ ml.min^{-1}$)	Corn	104.0	Litwinienko et al., 1995
	Peanut	62.3	
	Rapeseed	48.3	
	Soybean	66.7	
Pure Oxygen ($50\ ml.min^{-1}$)	Coconut	86.9	Tan et al., 2001
	Canola	86.0	
	Corn	88.1	
	Grape seed	99.9	
	Peanut	99.1	
	Palm oil	79.9	
	Palm kernel	89.4	
	Safflower	104.3	
	Sesame	88.8	
	Soybean	80.8	
304 kP of pure oxygen ($100\ ml.min^{-1}$)	Castor	77.0	Kasprzycka-Guttman & Odzeniak, 1992
	Cod-liver	59.7	
	Linseed	56.3	
	Olive	74.9	
Air ($100\ ml.min^{-1}$)	Soybean	89.6	Thurgood, et al., 2007

CHAPTER 2

OIL CHARACTERIZATION

2.1 MATERIALS

2.1.1 CAMELINE OIL

Virgin, cold pressed Cameline oil used in this study is produced from seeds of *Camelina sativa* plants. It is provided by Philippe Vigean Company (France) and bought from a local organic supplier. At reception, the oil is discarded into 5-ml vials, flushed with nitrogen and stored in darkness at 4 °C until use.

Fatty acid composition of the Cameline oil used in this work was determined by GC by the Fat and Oil Institute (ITERG, Pessac). The distribution of the fatty acids on the glycerol backbone was determined after hydrolysis of the TAG by pancreatic lipase (Table 8).

γ-Tocopherol is an antioxidant naturally occurring in Cameline oil. Its amount was determined by HPLC (ITERG, Pessac) and found equal to 864 $mg.kg^{-1}$ of oil.

2.1.2 OTHER PRODUCTS

For DSC analysis, three different paraffins are used. Two paraffins characterized by a well-defined melting point of 46-48°C and 52-54°C, respectively, are from Merck. The third one for food use (jam making) is from EMB (France). Thermal grease (thermal conductivity 0.71 $W.m^{-1}.K^{-1}$) from Radiospare is used to facilitate the heat transfer between the thermopiles and the containers as well as between the thermopile and the hot plate. Skamotec 225 from Skamol is used as thermal insulating material for the microcalorimeter aparatus.

The different analyses of oil oxidation need the use of chemicals. The solvents used are: hexane (purity 96 %) from Scharlau, chloroform from Sigma Aldrich, and butan-1-ol from Carlo Erba. Glacial acetic acid is purchased from Carlo Erba as well as potassium iodure and Iotech. 4-Methoxy aniline (para-anisidine) is from Alfa Aesar, TBA reactive from Merck, and sodium thiosulfate from Fluka.

Table 8: Total fatty acid composition of Cameline oil and distribution in triacylglycerols

Fatty acid	Total fatty acids (wt %)	Total fatty acids ($mg.g^{-1}$ of oil)	Proportion of the fatty acid in internal position
14:0	0.10	0.574	0
15:0	0.04	0.210	0
16:0	7.75	46.302	2.11
16:1 (n-9)	0.06	0.358	0
16:1 (n-7)	0.15	0.889	0
17:0	0.06	0.339	0
17:1	0.03	0.191	0
18:0	2.71	16.185	5.89
18:1 (n-9)	16.14	96.418	52.17
18:1 (n-7)	0.97	5.819	13.52
18:2 trans	0.04	0.241	57.93
18:2 (n-6)	25.78	153.993	56.38
18:3 (n-6)	0.138	0.827	41.67
18:3 (n-3)	27.43	163.859	32.36
20:0	1.62	9.694	0.84
20:1 (n-9)	11.86	70.842	1.43
20:1 (n-7)	0.43	2.567	0
20:2 (n-6)	1.60	9.533	4.34
20:4 (n-6)	0.69	4.103	0
22:0	0.28	1.647	0
22:1 (n-9)	2.14	12.810	0

2.2 METHODS

2.2.1 HYDROPEROXIDE INDEX

Hydroperoxide index is determined according to the standardized method AFNOR T60-220. A known mass of Cameline oil (ranging from 2.0 to 2.5 g) is dissolved into 10 ml of chloroform and stirred for a few minutes. Fifteen ml of acetic acid and 1 ml of a saturated potassium iodure solution (1.5 $g.ml^{-1}$) are then added. The mixture is stirred for 1 minute and left 5 minutes in the dark at room temperature. The following reaction between the iodine ion (I^-) and the hydroperoxides (LOOH) is involved:

$$LOOH + 2CH_3COOH + 2K^+ + 2I^- \longrightarrow I_2 + LOH + 2CH_3COO^- + 2K^+ + H_2O \quad (6)$$

Water (75 ml) is added to stop the reaction. Iodure liberated is titrated by a sodium thiosulfate solution (0.01 N) under stirring, in presence of endpoint indicator (Iotech). During the titration, the following reaction occurs:

$$2(S_2O_3^{2-}Na^+) + I_2 \longrightarrow S_4O_6^{2-}2Na^+ + 2I^- \quad (7)$$

All reactant solutions (chloroform, acid acetic, and potassium iodure solution) are deprived of oxygen by flushing nitrogen. A standard test is performed without oil in the same conditions to check the presence of residual oxygen in the reactants. The acidic conditions (excess acetic acid) prevent formation of hypoiodite (analogous to hypochlorite), which would interfere with the reaction.

Peroxide index (PI) is expressed as milliequivalents of active oxygen per kg of oil and is given by:

$$PI = \left(\frac{(V-V') * T}{m}\right) * 1000 \quad (8)$$

with

V: ml of sodium thiosulfate solution used for the oil titration

V': ml of sodium thiosulfate solution used for the reactant titration

T: exact normality of the sodium thiosulfate solution

m: mass (in g) of the Cameline oil sample

PI is measured on Cameline oil at 25°C and 37°C, in daylight conditions and darkness during 2 days. The measurements are performed in duplicate on each sample.

2.2.2 CONJUGATED DIENE MEASUREMENT

During the formation of hydroperoxides from unsaturated fatty acids, conjugated dienes are produced due to the rearrangement of the double bound. This formation of conjugated dienes (Figure 18) in oils gives rise to an absorption peak in the UV region.

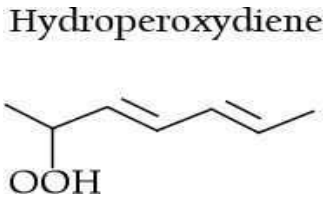

Figure 18: Hydroperoxydiene formation

Cameline oil is dissolved in hexane to a final lipid concentration of 2 $mg.ml^{-1}$. The lipid solution is immediately scanned from 300 nm to 200 nm for absorbance with a Hitachi (U-2810) double beam spectrophotometer equipped with background correction. A typical absorption spectrum obtained for a Cameline oil sample is given in Figure 19. An intense absorption is observed at 228-233 nm corresponding to the diene formation. The absorbance at 265-268 nm reflects the presence of conjugated trienes.

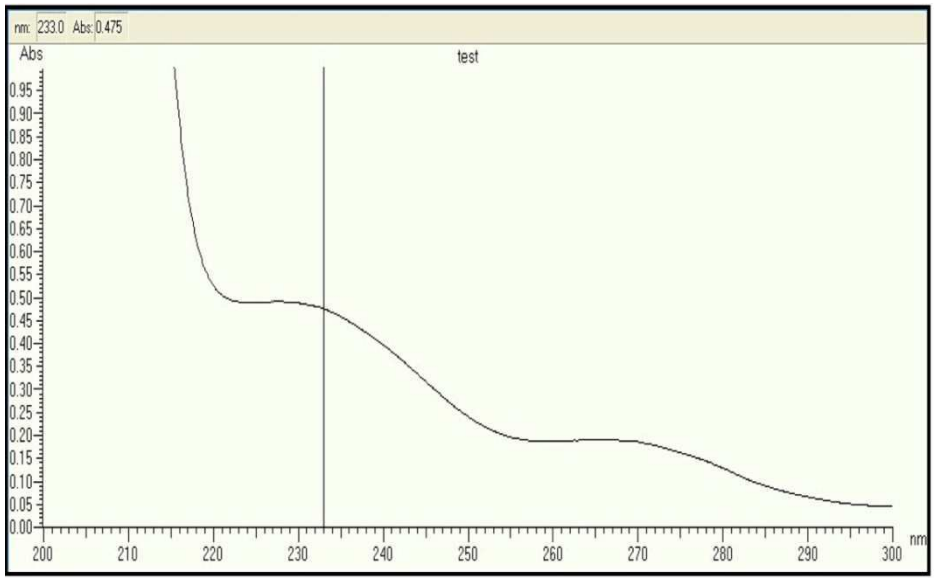

Figure 19: Absorption spectrum from Cameline oil

For the different oil samples, only the absorbance at 233 nm is recorded. If the absorbance value at 233 nm is higher than 1, then the sample is diluted once again in hexane. Three measurements are performed on each sample. In order to compare the different samples, absorbance measured at 233 nm is standardized for 1 $mg.ml^{-1}$ of oil.

Two types of samples are analyzed:

- Several oil samples (1 g) placed in identical containers are left in an incubator for 48 hours at different temperatures (60, 80 and 120°C). Every hour, one sample is taken out of the incubator and analyzed for its conjugated diene content;

- Samples are placed in the microcalorimeter in isothermal conditions (100°C) for 35 hours (cf. § 4.1.4). Every hour, a sample is withdrawn and the oil analyzed. These experiments are performed with three different copper container sizes in order to study the influence of the surface/volume ratio on the oil oxidation.

2.2.3 ANISIDINE VALUE

p-Anisidine value is determined according to the standardized method NF-ISO 6885 that can be applied to determine the amount of aldehydes (principally 2-alkenals and 2,4-alkadienals), as secondary oxidation products, produced by the decomposition of the hydroperoxides in oils and fats. The yellowish products are formed after the reaction of para-anisidine and the aldehydes compounds in the sample (Figure 20). They are detected in an acetic solution at 350 nm.

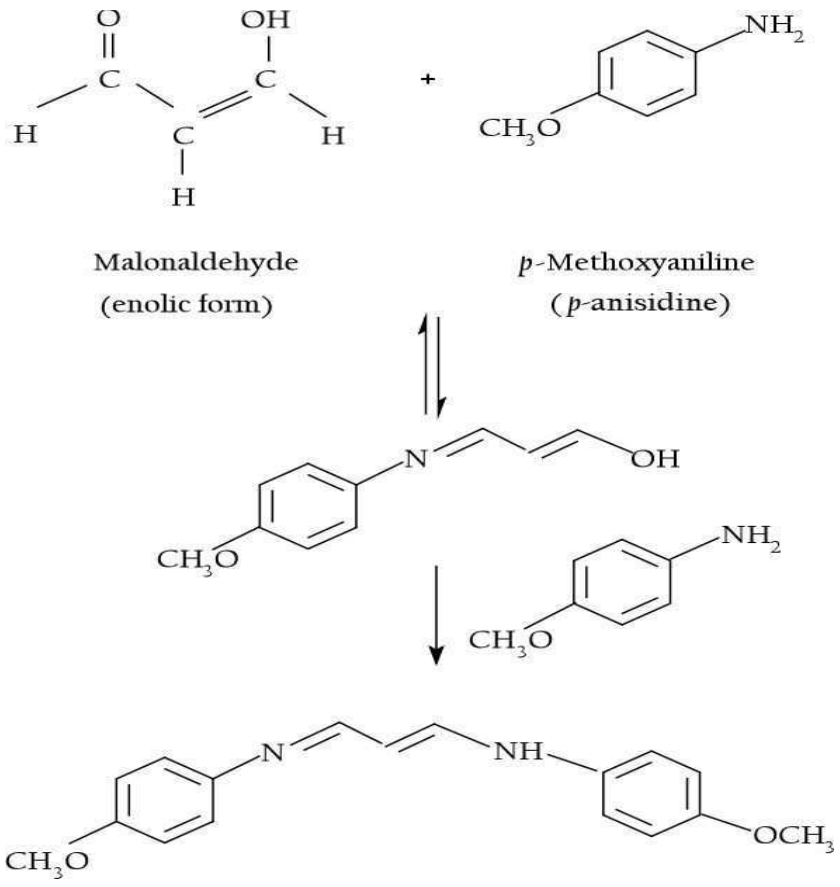

Figure 20: Possible reactions between p-anisidine reagent and malonaldehyde (Shahidi & Zhong, 2005)

In the standardized method, a known mass of Cameline oil (ranging from 0.5 to 4.0 g) is dissolved in hexane in a volumetric flask of 25 ml. The absorbance (Ab) of

the solution is measured with the spectrophotometer at 350 nm with a cell containing hexane as a reference. Then, 5 ml of hexane are introduced in a test tube and 1 ml of the *p*-anisidine solution (2.5 $g.ml^{-1}$ of acetic acid) is added. The same procedure is applied to 5 ml of the oil in hexane. After stirring, the samples are left for 10 minutes. Then, the absorbance of the oil sample (Ab) is measured against the *p*-anisidine solution in hexane. If the absorbance is higher than 1 at 350 nm, the initial oil mass is reduced.

The p-anisidine value (*p*-AnV) is given by:

$$p-\text{AnV}=\frac{25*(1.2*As-Ab)}{m} \quad (9)$$

with:

As: Absorbance of the oil after the reaction with *p*-anisidine reagent

Ab: Absorbance of the oil dissolved in hexane

m: mass of the oil (in g)

Because the amounts of aldehydes in our samples were high, it was necessary to validate that the procedure was applicable to oil quantities lower than that advocated by the standardized method. Several samples left for 2 hours at 98°C are analyzed. Figure 21 shows that similar *p*-anisidine values are obtained for samples ranging from 0.025 to 0.125 g.

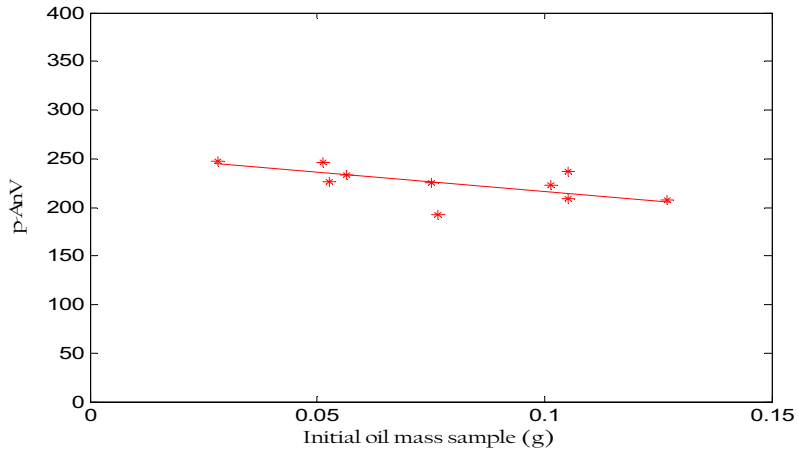

Figure 21: p-Anisidime values for different masses of Cameline oil samples

The samples analyzed are those recovered from the microcalorimetry experiments (isothermal conditions T=100°C, duration of the experiment = 25 hours, diameter of the copper container = 29 mm). The measurements are performed in triplicate on each sample.

2.2.4 THIOBARBITURIC ACID TEST

During the oil oxidation, the degradation of polyunsaturated fatty acids leads to the formation of malonaldehyde (MA), a minor component of fatty acids with 3 or more double bonds. MA reacts with TBA to form a pink MA-TBA complex that can be measured spectrophotometrically at its maximum absorption at 530-535 nm (Figure 22).

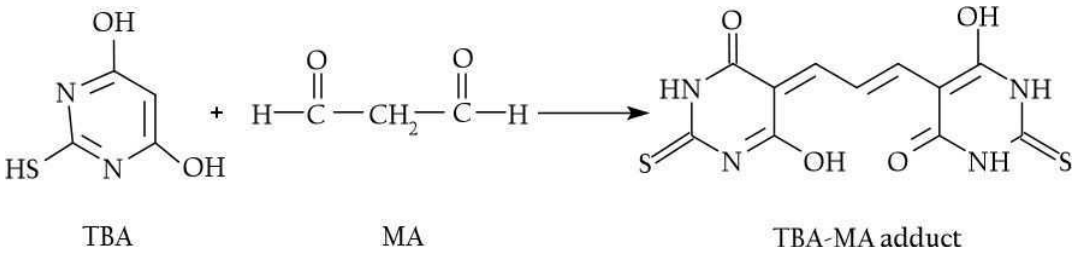

Figure 22: Reaction of thiobarbituric acic (TBA) and malonaldehyde (MA)(Shahidi & Zhong, 2005)

A known mass of Cameline oil (ranging from 20 to 80 mg) is placed in a volumetric flask of 10 ml and dissolved in butan-1-ol. Five ml of this solution is added to 5 ml of TBA (2 $g.ml^{-1}$ in butan-1-ol). The reference consists of the TBA solution in butan-1-ol. The tubes are placed in a heat bath at 95°C for 120 min and then cooled to room temperature. After cooling to room temperature, the absorbances of the sample and the TBA reference are measured at 530 nm with a reference cell containing distillated water.

TBA value is expressed as mg of MA equivalents per mg of oil and is given by:

$$TBAvalue = \frac{20 * (A - B)}{m} \quad (10)$$

with

A: Absorbance of the oil sample

B: Absorbance of the TBA reference

m: mass of the oil (in mg)

20: dilution factor corresponding to 10 ml of sample and 1 cm of thickness of the cell

2.2.5 DSC ANALYSIS

The DSC principle is explained in detail (cf. § 1.3.2.2). DSC experiments are performed on a Setaram instrument (model 131 EVO). Samples of paraffin (≈ 15 mg) are placed in aluminum pans. The samples are heated to different temperatures (40-130°C), at 0.15°C.min^{-1}. Heat flux is recorded as a function of increasing temperature and also in isothermal conditions (110, 120 and 130°C).

2.2.6 MICROCALORIMETRY ANALYSIS

The microcalorimetry method is explained in detail (cf. § 3.1). Samples of Cameline oil (≈ 1 g) are placed in copper containers with different sizes, i.e. 14, 24 and 29 mm of internal diameter (Figure 23) in order to study the influence of the surface/volume ratio on the oil oxidation. The samples are heated in isothermal conditions (100°C) and left under this temperature for 35 hours. Heat flux is recorded as a function of time.

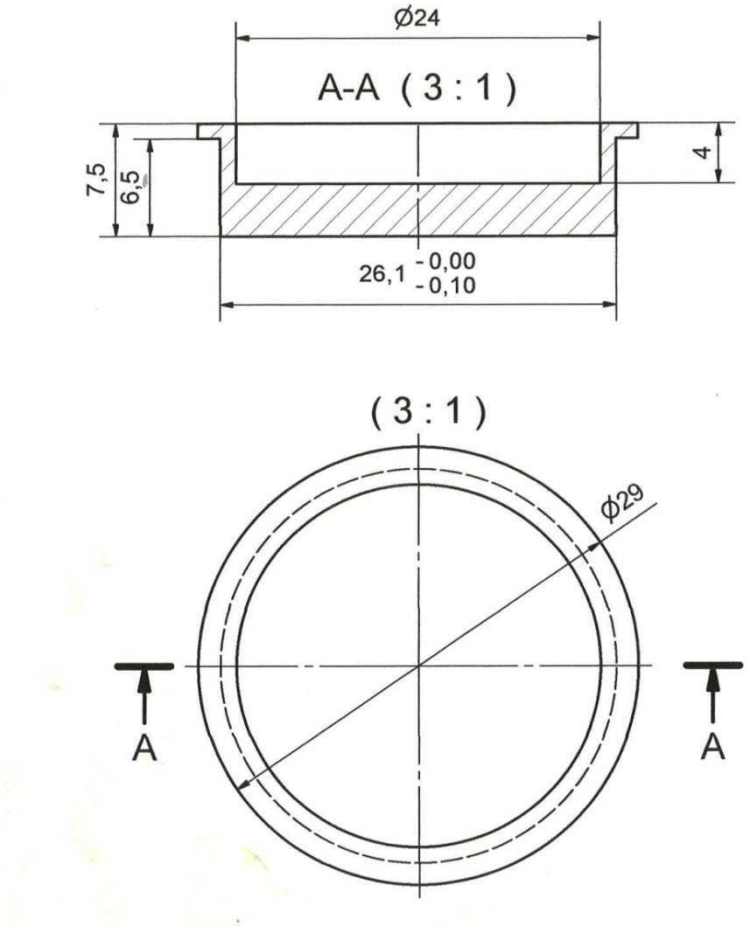

Figure 23: Scheme of the copper containers used in the microcalorimetry experiments

CHAPTER 3

MICROCALORIMETER CONCEPTION

3.1 EXPERIMENTAL DEVICE

3.1.1 GENERAL PRESENTATION

The principle of the measurement is based on the DSC which was already presented in detail in (cf. § 1.3.2.2). The microcalorimeter is a differential one with two thermopiles, one for the measurement of the chemical reaction and the second for the reference. The temperature of the system is regulated by a thermostat bath circulation. The heat flux as a function of time for the sample and the reference are recorded and subtracted. When the chemical reaction or phase change occurs in the system involving release or evolution of heat as in the case of oil oxidation, the differential heat flux between the reference and the sample varies. This variation allows the possibility to get information about the kinetic of the chemical reaction, as well as the pick of the enthalpy of the reaction as a function of time or temperature.

In the case of non-isothermal system, for the study of phase change of an inert material this pick will change and the information about the change phase temperature, enthalpy of the phase transition and transformation rate can be deduced.

The developed microcalorimeter is described in the Figure 24.

The microcalorimeter is designed with three different reaction rooms, each of them containing two thermopiles (fluxmeters) for the measurement of the dissipated heat flux, one for the measurement of the chemical reaction and the second one for the reference. This allows following the heat flux evolution of the system. The system also allows working with one thermopile as the reference and the other 5 thermopiles with the studied samples.

a)

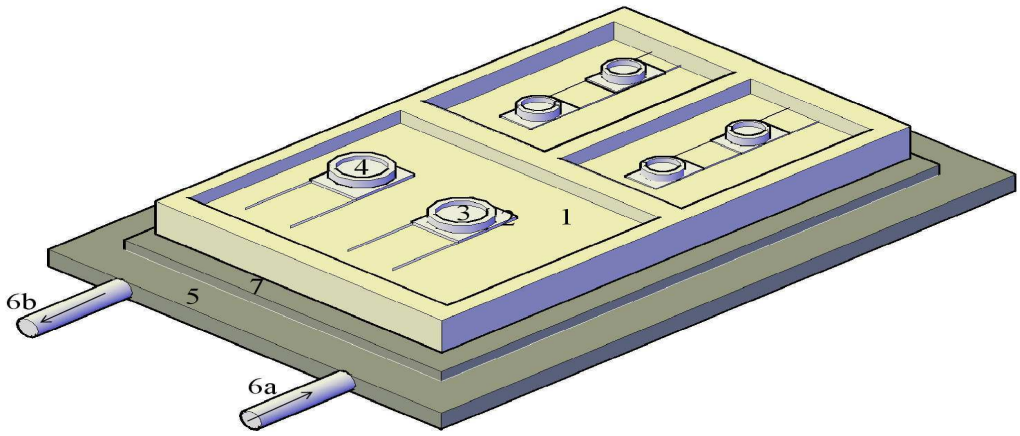

b)

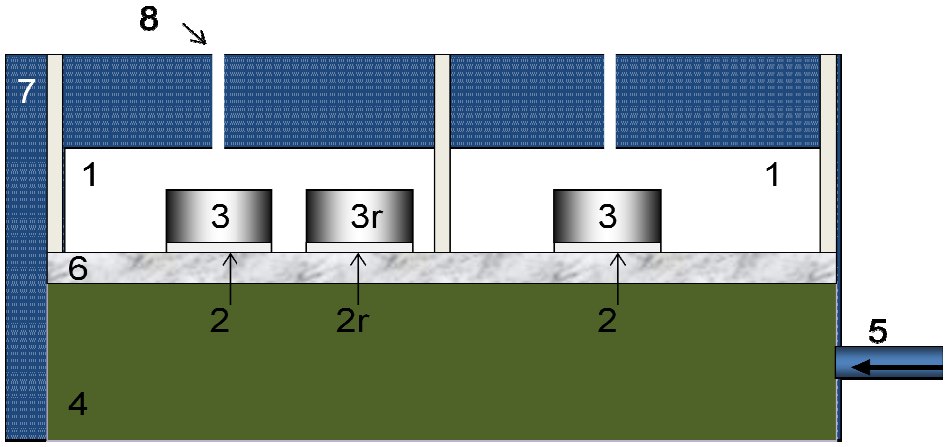

Figure 24: Scheme of the differential microcalorimeter: a): 3D-view and b): Cross section: (1) reaction room, (2) thermopile, (2r) thermopile reference, (3) sample container, (3r) reference, (4) heat exchanger plate, (5) thermostatic flow circulation, (6) metal plate, (7) thermal insulating foam, (8) syringe groove for the sample injection.

The microcalorimeter structure is made by aluminium due to its good thermal conductivity (120-180 $W.m^{-1}.K^{-1}$) with wall thickness of 5 cm allowing a very good global thermal stability of the system. All the surrounding is insulated with foam (skamotec 225) in order to limit the heat exchange with the environment. A groove is placed on the top of each reaction room through the insulating material; this allows injecting a well known volume of product and knows the starting point of the chemical reaction. A high conductive metal plate of aluminum is

placed between the hot plate and the system to avoid temperature variations across the hot plate and the thermopile (Peltier).

3.1.2 Acquisition and calibration

The tensions given by the thermopiles are recorded by a digital multimeter model Agilent 34410A with 6 digits resolution (1 µV). The frequency of acquisition is around 2 seconds. The measurement corresponds to the difference between the tension given by the chemical reaction and the reference one. This difference of tension is proportional to the heat flux releases by the chemical reaction of oxidation or the heat flux dissipated by a phase change. As a consequence, a coefficient of calibration has to be determined in order to get the value of the heat flux in W from the value given by the thermopile in Volt. This coefficient is determined by an electrical calibration (by Joule effect) of the microcalorimeter (cf. § 3.3.2). This calibration coefficient is obtained by the injection of a well known heat flux from an electrical heat source through the thermopile by Joule effect. A flexible laminar heater is used as a heat source, stuck to the thermopile with thermally conductive thermal grease to avoid thermal gradient between the resistive element and the heat sink (Figure 25). A Power Supply model Agilent 3631A is used to generate the tension from the electrical heat source.

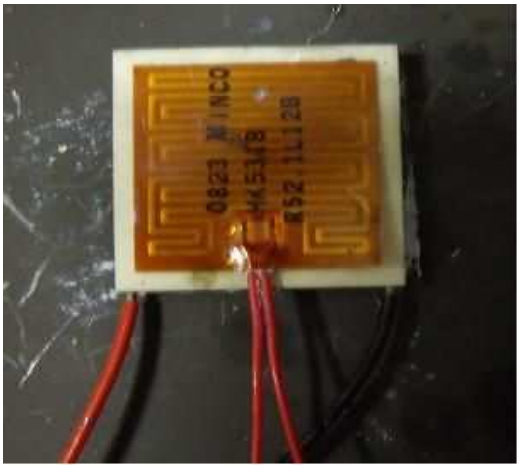

Figure 25: Flexible laminar heater used for the electrical calibration

3.2 SET UP AND PROPERTIES

3.2.1 REGULATION SYSTEM

In order to impose the temperature of the chemical reaction, a thermal regulation is used. The regulation of the working temperature is set up with a heating thermostat bath circulation from Lauda heating system model ECO Gold 4G. The flow rate is controlled by a pressure pump and six flow/rates levels can be selected. The higher power level is chosen to keep the temperature difference between the bath and the rest of the system as small as possible. Silicone oil from Lauda is used as the heat transfer liquid to perform experiments at a large temperature scale (from room temperature to 200 °C). This silicone oil is sent to the hot plate through two viton hoses.

With this regulation system, the measurements are done, either in an isothermal mode with an imposed temperature (T_{imp}) or in a non-isothermal (transient state) mode with temperatures ranging from room temperature to 130 °C. It is important to consider the time necessary to achieve the imposed temperature in the system. As it is shown in Figure 26, the thermal regulation of the system makes a time response of around 1 h to stabilize the system. The temperature of the system is recorded thanks to a thermocouple placed in the surface of the hot plate level.

Different flow/rates levels of heat transfer liquid are available to heat the hot plate. In this work, the maximum flow/rates levels are arbitrarily chosen to guarantee the maximal homogeneity and effectiveness of the heater in order to perform the experiments. A very stable system is achieved with no perturbation during the time.

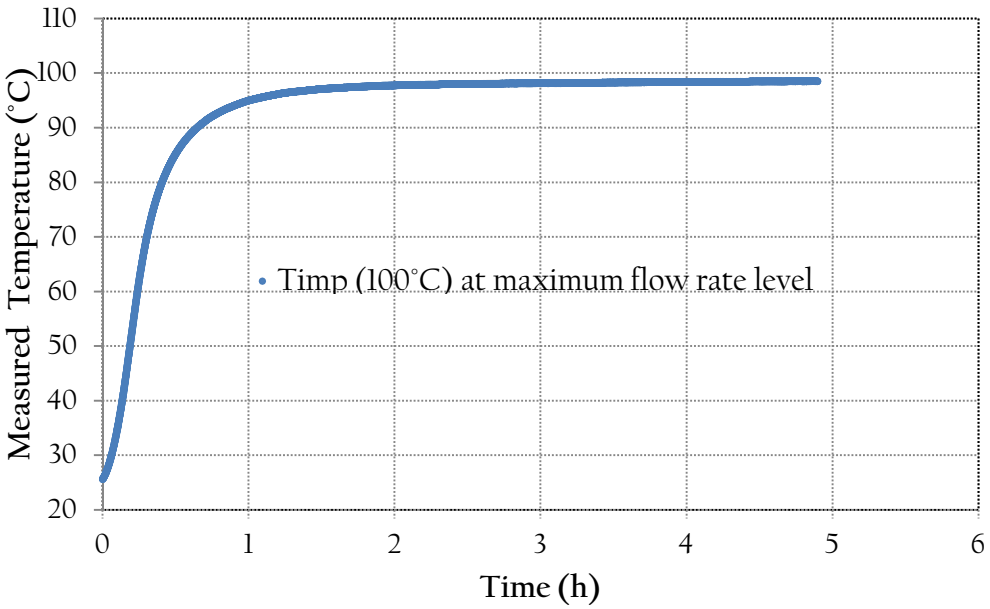

Figure 26: Measured temporal evolution of the temperature in the hot plate with an imposed temperature (Timp) for the Lauda system and the maximum flow/rate level of the pressure pump

.

3.2.2 FLUXMETER (THERMOPILE)

Fluxmeters or thermopiles are placed between the metal plate and the sample container (Figure 27). This allows the measurement of the voltage dissipated from the chemical reaction by the Peltier effect. The heat flux is measured according to the temperature gradient from the chemical reaction in the top of the thermopile and the imposed temperature of the plate, this thermoelectric Peltier effect will generate a tension proportional to the gap of temperatures between the top and the bottom of the thermopile.

Thermal grease with a thermal conductivity of 0.71 $W.m^{-1}.K^{-1}$ is used to improve the conductive heat transfer between the thermopiles and the containers and between the thermopile and the hot plate. The thermopiles used for this device, are a model GM 200127- 10-25 (Radiospares) with a maximum temperature performance of 200°C. The sensitivity is closed to few µW of resolution; the dimensions are 30 mm x 30 mm x 3.7 mm and there are 127 junctions.

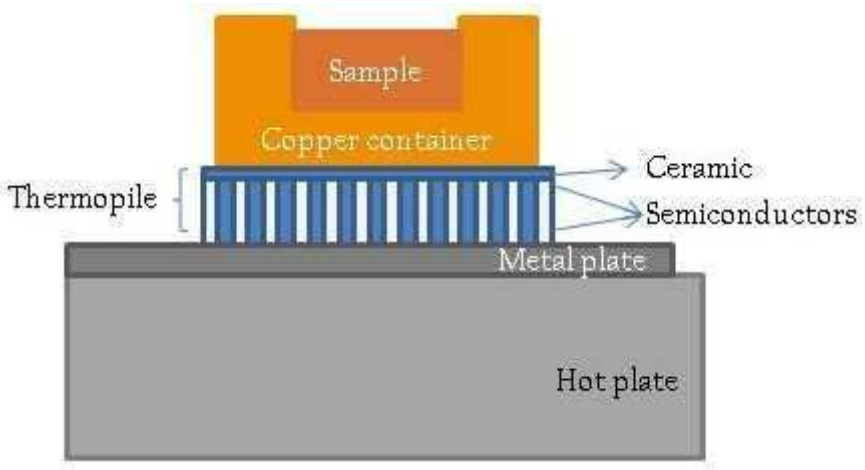

Figure 27: Location of the thermopile in one of the three reaction rooms

3.2.3 ISOLATION, SAMPLE INJECTION AND SECURITY MEASUREMENTS

Insulating foam and skamotec, with good insulating properties and high temperature resistance (1100°C T_{max} and thermal conductivity of 0.12 $W.m^{-1}.K^{-1}$) are used in order to avoid the heat loses and the heat fluctuation due to the room temperature. This material is placed around the aluminium structure, and also above each reaction room where a grove is placed in order to carry out sample injection with a syringe. This syringe fitted with a needle long enough to pass through the skamotec (≈4 cm), is used in order to minimize the heat loses and to ensured that the heat flux from the reaction is acquired as soon as the reaction begins.

The microcalorimeter and the Lauda heating system are placed into a box made with an aluminium structure in order to avoid the risk for the operators due to the high temperature work conditions (from room temperature to 200°C). This structure has two separates areas, one for each part of the system connected by two viton hoses for the flow of the heat transfer liquid. A first area containing the Lauda heating system is open and small groves for the ventilation of the engine

and the pump are placed; the second one containes the hot plate and the rest of the system is closed and insulated thanks to foam and skamotec. Transparent windows are placed in order to provide an easy control of the system.

Figure 28 presents the system. The Lauda system in one of the areas and the hot plate in the other can be observed. At the top of the structure a cover is placed easy to remove when the sample needs to be injected.

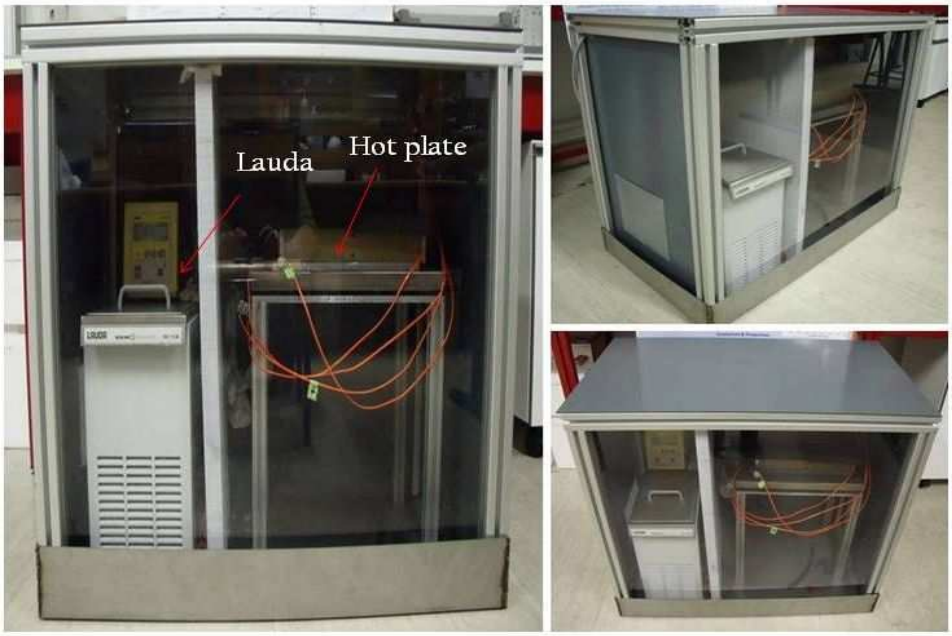

Figure 28: Pictures of the microcalorimeter

3.3 PERFORMANCE OF THE MICROCALORIMETER

3.3.1 GENERAL USE

The device operation can be divided into three steps:

1° ***Temperature stabilization***: As mentioned in (cf. § 3.2.1), the homogenization of the temperature needs at least one hour to be achieved so the first requirement to work with the microcalorimeter is to get a constant signal between the

subtraction of the reference and the thermopile. After this step the system is ready for the sample injection.

2° ***Sample injection***: The sample pre-weighted in the syringe is injected manually through the skamotec directly into the copper container placed between the thermopile and the skamotec. This is the moment considered as the starting point of the reaction.

3° ***Measurement of the heat released***: the heat flux release from the chemical reaction is recorded for about 50 h of data acquisition in the form of a tension (Volt). This tension is then multiplied by the calibration coefficient in order to get the temporal evolution of the heat flux in W.

3.3.2 CALIBRATION

The calibration of the microcalorimeter is a key factor in this kind of measurements due to the variations of the performance of the device affected by the temperature and its components (thermopile, regulation system, heat exchange, etc). For this reason, even if the supplier of the thermopile gives a calibration coefficient as function of the temperature (Figure 29), a calibration coefficient of the whole device is recommended in order to get a global calibration as function of the heat transfer of the global system.

This calibration consists in the generation, by Joule effect of different heat fluxes from an electrical heat source through the thermopile in order to simulate the heat flux provided by the chemical reaction (generated by the sample) and to measure the voltage variation corresponding to each power.

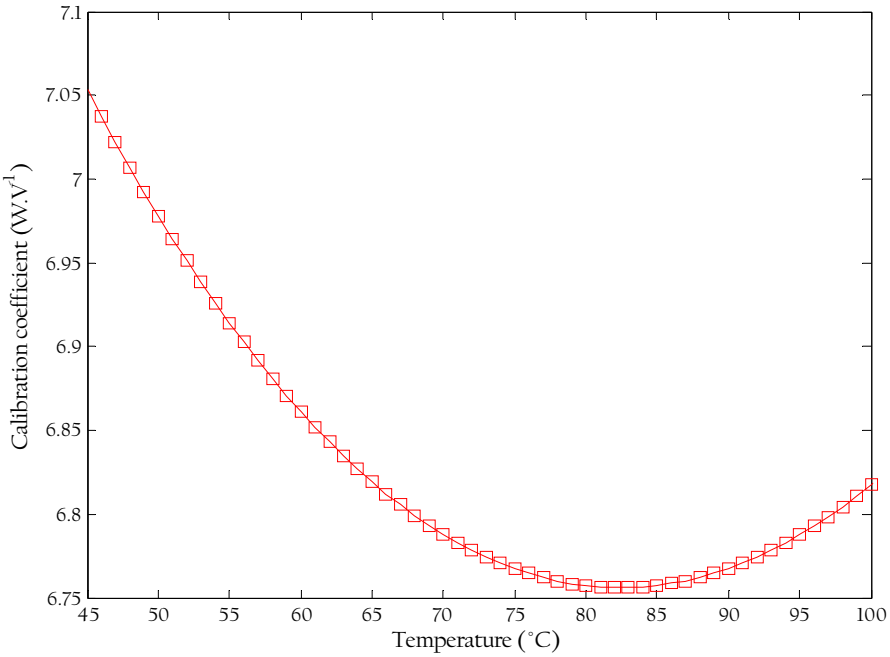

Figure 29: Calibration coefficient of the thermopile given by the supplier

These values allow the estimation of a calibration coefficient in $W.V^{-1}$ that is going to be used to get the heat flux in W from the measured tension in Volts. This coefficient is measured at different temperatures due to the fact that the thermal properties of the thermopile are function of the temperature.

From the measured voltage with the thermopiles and from a calibration coefficient determined at several temperatures; the quantitative heat flux is deduced according to the following relationship:

$$Q_M = \alpha U_M \qquad (11)$$

with Q_M (W) the measured heat flux dissipated from the chemical reaction, U_M (V) the measured voltage given by the thermopile and α ($W.V^{-1}$) as the calibration coefficient.

3.3.3 DATA ACQUISITION

The instrumental control and data acquisition are operated with a computer using Labview software version 9.0. A GUI (Graphical User Interface) is developed using this graphical programming environment software which allows operating all the experimental steps of work: i) Stabilization of the device, ii) Calibration at different temperatures, iii) Chemical reaction data acquisition, and iv) Temperature monitoring. The different GUI used are presented in Figure 30.

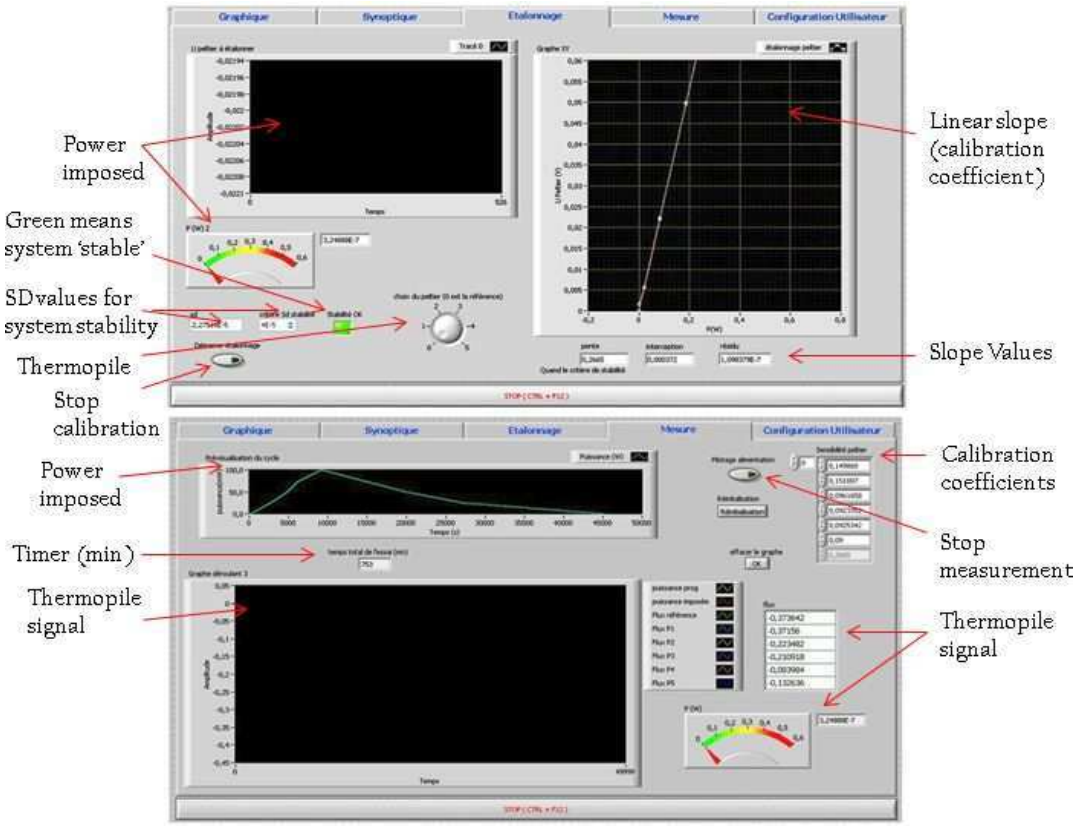

Figure 30: Interface to control the microcalorimeter

This GUI allows programming the power that then will be injected from a flexible laminar heater, and allows getting the calibration coefficient as the linear regression between the power v/s voltages, explained in (cf. § 3.5). Finally, the GIU gives the graph of the heat generated flux from the chemical reaction in real time, considering that oxidation follows a flow reaction kinetics with a huge amount of data to be analyzed.

3.4 THERMAL MODELLING OF THE SYSTEM

3.4.1 THERMAL PROBLEM

The main problem of the measurement comes from the fact that the temperature in the hot plate is not spatially homogeneous. In order to study the homogeneity of temperature due to the shape of the tube inside the hot plate and the influence of the high conductive metal plate of aluminium placed between the hot plate and the system, an Infrared camera (FLIR Orion SC7000) and Altair and Cirrus softwares are used (Figure 31).

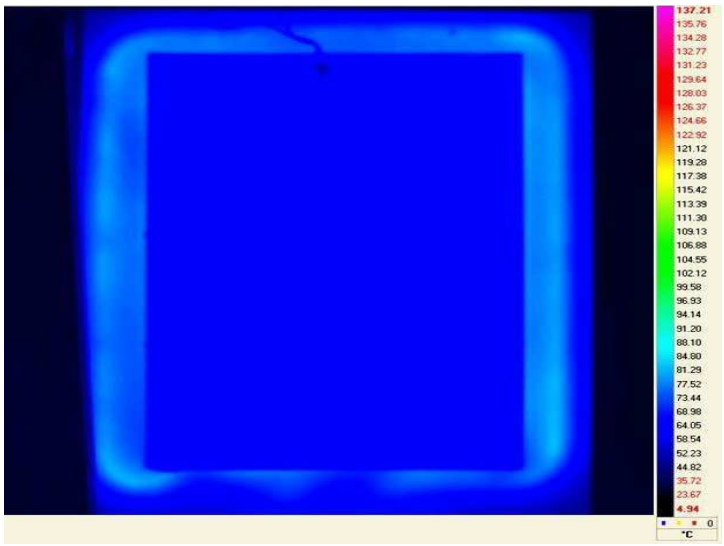

Figure 31: Infrared image of the hot plate

From the recording with the IR camera it can be seen that the time evolution of the temperature varies depending on the position (variation of around 20°C) (Figure 32).

This amplitude of temperature can be due to the Lauda system heat regulation that works with a tube inside the hot plate which carries out the heat transfer liquid (silicone oil) as a serpentine (Figure 33).

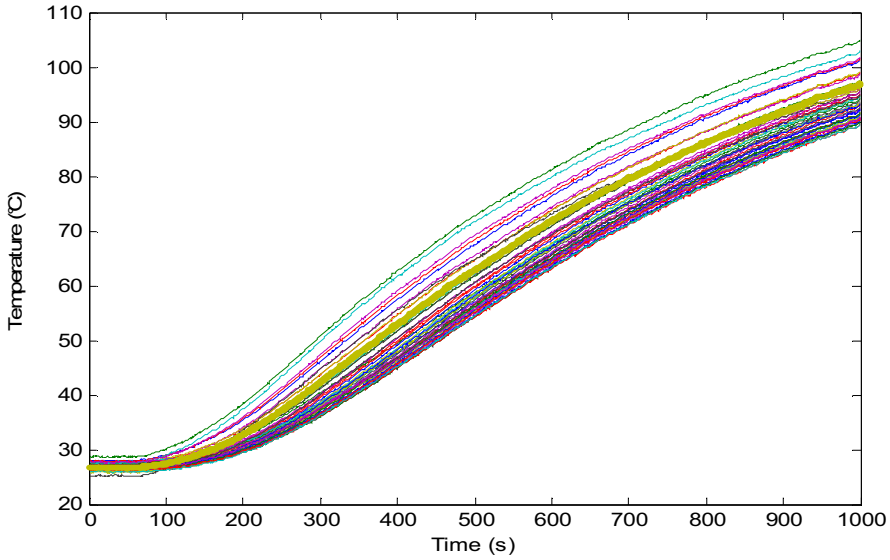

Figure 32: Temperature development in the hot plate

This particular shape gives a difference in the homogeneity of the temperature in the surface due to the variation of the intensity of the heat flux related with the shape of the tube. Thus, there is a gradient of temperature in the tube between the heat transfers liquid that goings into and goings out of the heat plate.

On the other hand the time delay depends of the deepness of the tube inside the hot plate. This is the time it is requires for the heat flux to arrive to the surface of the plate.

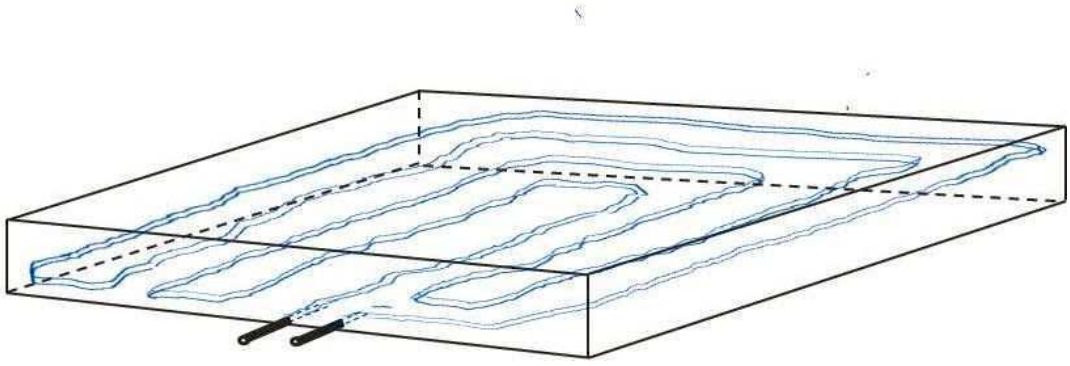

Figure 33: Tube inside the hot plate with the heat transfer liquid

In order to control this drawback, the same asymptotic expansion as described before is developed (cf. § 3.4.2) where A is defined as the amplitude variations of the system due to heterogeneous heat flux inside the hot plate and τ is defined as the delay of the time/response of the combined system (Lauda and thermopile). The idea is to find the best zone with the maximum temperature homogeneity where the model will better suit.

3.4.2 Representation of the amplitude (A) and the time/response (Tau)

To be able to improve the homogeneity in temperature in the hot plate an analytical representation is done. This analytical representation allows choosing the best position where the thermopiles can be placed. The hot plate is divided in *n* number of squares with the same size as the thermopile (3 x 3 cm) and one of the surfaces is arbitrary chosen as reference which is then subtracted to the rest of the surfaces squares.

Thus, the delay of the time/response (τ) (Figure 34) and the amplitude variations (A) (Figure 35) of the heat flux going to the surface of the hot plate is calculated with Equation (22) and the most homogeneous part is used to place the thermopiles.

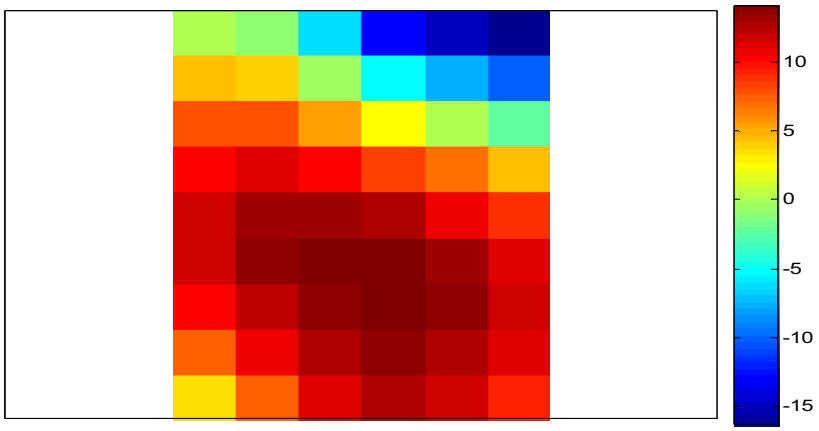

Figure 34: Development of the time delay (τ) of the heat flux in the hot plate

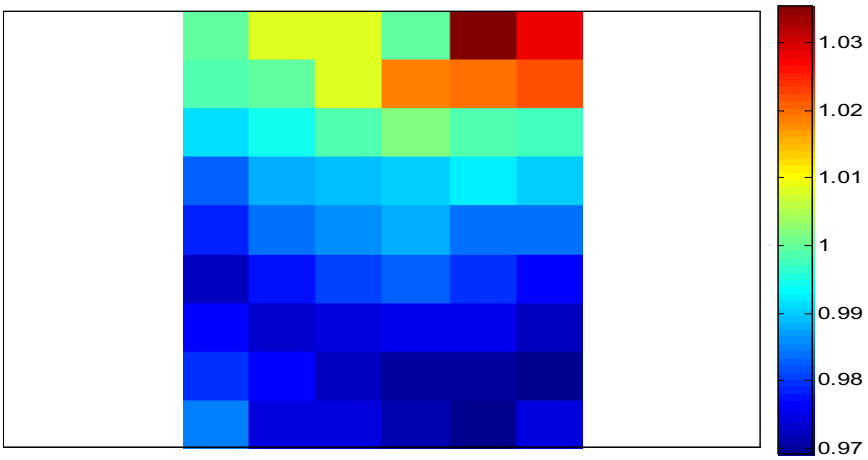

Figure 35: Development of the intensity (A) of the heat flux in the hot plate

3.4.3 Analytical solution

A 1-D transient model is considered to represent the evolution of the heat transfer in the system described by Equation (12). This set of equations permits to obtain the spatial distribution of the temperature as well as its temporal evolution as a function of the thermal properties of the system. We consider that the heat losses at the top of the container are neglected.

$$\begin{cases} a_z \dfrac{\partial^2 T(z,t)}{\partial z^2} = \dfrac{\partial T(z,t)}{\partial t}; a_z = \dfrac{\lambda_z}{\rho C_p} \\ T(z, t=0) = 0 \\ -\lambda_z \left.\dfrac{\partial T(z,t)}{\partial z}\right|_{z=0} = \varphi_0 f(t) - h(T - T_0) \\ T(z=e,t) = T_{imp}(t) \end{cases} \quad (12)$$

For the resolution of the thermal model, the system is considered as an unique homogeneous media (Figure 36), where T is the temperature (K), λ is the thermal conductivity ($W.m^{-1}.K^{-1}$), C_p is the heat capacity ($J.kg^{-1}.K^{-1}$), ρ is the density ($kg.m^{-3}$) and a is the thermal diffusivity ($m^2.s^{-1}$) in the z direction.

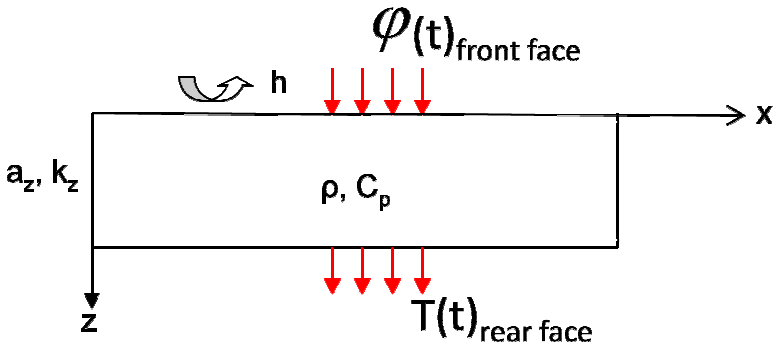

Figure 36: Representation of thermal problem

In this way, it is assumed that the heat flow is going through the system from the front side as $\varphi_0 f(t)$ released by the chemical reaction and going out as $T_{imp}(t)$ released by the heat exchanger.

A Laplace transformation is applied to the system Equation (13) in order to remove the time partial derivative by an algebraic term accounting for the initial condition.

$$\theta(z,p) = \int_0^\infty T(z,t)\exp(-pt)\,dt \tag{13}$$

$$F(z,p) = \int_0^\infty f(z,t)\exp(-pt)\,dt \tag{14}$$

With $p = i\omega$ as the Laplace variable.

In the transformed space of Laplace, and assuming T_0=0, the system is rewritten as follows:

$$\begin{cases} \dfrac{d^2\theta(z,p)}{dz^2} - \left(\dfrac{p}{a_z}\right)\theta(z,p) = 0 \\ -\lambda_z \left.\dfrac{d\theta(z,p)}{dz}\right|_{z=0} = \varphi_0 F(p) \\ \theta(z=e,p) = \theta_{imp}(z=e,p) \end{cases} \tag{15}$$

Then, the general solution of the system is:

$$\theta(z,p) = A\exp(-\beta z) + B\exp(\beta z), \quad with \quad \beta = \sqrt{\frac{p}{a_z}} \tag{16}$$

The constant terms A and B are obtained from the boundary conditions.

This equations can be solved by the quadrupole method (Fudym et al., 2002, Maillet *et al.*, 2000, Fudym *et al.*, 2007) which permits to convert this differential system in an algebraic problem by the resolution of an inverse transformation of a lineal system. This method allows relating the temperature and the heat flux at the front face with the temperature and heat flux at the rear face (Figure 36) at $z = e$.

From Equations (15) and (16), the formulation based on the thermal quadrupole terms is as follow:

$$\begin{Bmatrix} \theta_0 \\ \varphi_0 F(p) \end{Bmatrix} = \begin{bmatrix} e^{\beta e} \\ e^{\beta e} \end{bmatrix} \begin{bmatrix} A & B \\ C & D \end{bmatrix} \begin{Bmatrix} \theta_{imp} \\ \phi_e \end{Bmatrix} \tag{17}$$

where:

$$A = D = \frac{1+e^{-2\beta e}}{2}, \quad B = \frac{1-e^{-2\beta e}}{2}, \quad C = \lambda s \beta \frac{1-e^{-2\beta e}}{2} \tag{18}$$

This formulation used the exponential form of the hyperbolic functions.The use of this exponential form is shown to be convenient in order to performs a numerical computation (Pailhes et al., 2012).

From the matrix Equation (17), the front face temperature and the heat flux at the rear face are obtained.

$$\theta_0 = \frac{2\theta_{imp} e^{-\beta e}}{(1+e^{-2\beta e})} + \frac{\varphi_0 F(p)(1-e^{-2\beta e})}{\lambda s \beta (1+e^{-2\beta e})} \tag{19}$$

$$\phi_e = \frac{2\varphi_0 F(p) e^{-\beta e} - \lambda s \beta (1-e^{-2\beta e})\theta_{imp}}{1+e^{-2\beta e}} \tag{20}$$

Thanks to these equations it is possible to deduce the heat flux measured by the thermopile when the imposed temperature $\theta_{imp}(p)$ in the rear is already known.

A numerical inverse Laplace transformation based on the DenIseger algorithm (Den Iseger, 2005) is finally used in order to obtain the solution in the time-space.

3.4.4 THERMAL MEASUREMENT METHOD

The main idea of the proposed method is to use a differential measurement of the heat flux. As it was mentioned before (cf. § 3.1.1), a thermopile is used as a reference and the other ones are devoted to measure the chemical reaction. As both the thermal properties and the imposed temperature due to the Lauda system of each thermopile are different, the differential measured heat flux deduced is depicted by a first order asymptotic expansion that represents a transfer function between two thermopiles:

$$Q_i(t) = A_i\left(Q_{Ref}(t) + \tau_i \frac{dQ_{Ref}(t)}{dt}\right) \quad (21)$$

Where Q_i is the measured heat flux of the i^{th} thermopile, Q_{Ref} is the measured heat flux of the reference one, A_i is the amplitude variations of the system (due to heterogeneous heat flux inside the hot plate) and τ_i corresponds to a delay (time response) of the combined system (Lauda and thermopile).

When a chemical reaction occurs inside the system, the chemical measured heat flux takes the following form:

$$Q_{C_i}(t) = Q_{M_i}(t) - A_i\left(Q_{Ref}(t) + \tau_i \frac{dQ_{Ref}(t)}{dt}\right) \quad (22)$$

Where Q_{C_i} is the deduced chemical heat flux and Q_{M_i} the measured heat flux of the i^{th} thermopile without chemical reaction.

From this measurement, the reaction enthalpy can be estimated:

$$\Delta H(t) = \int Q_{C_i}(t)dt \quad (23)$$

The reaction energy can be estimated from Equation (23) where the total flux release for the chemical reaction (W) is integrated in function of time in order to obtain the energy in Joule (J). The energy dissipated by the chemical reaction of oxidation in function of time refers to the area under the curve taking for the base line the onset and offset temperatures as explained for the DSC method in the oil oxidation measurement (cf. § 1.3.2.2). The results are standardized by dividing the enthalpy value by the amount of oil.

3.5 SENSITIVITY AND PERFORMANCE OF THE MICROCALORIMETER

3.5.1 THERMOPILE CALIBRATION

In order to estimate the amplitude (A) and time delay (τ) of each thermopile, a calibration is performed. A heat flux is imposed with the Lauda, and the response of each thermopile is recorded. From this response and with the asymptotic expansion Equation (21), the coefficients (A and τ) are estimated according to a Levenberg-Marquardt quadratic minimisation (More, 1978). These values are obtained without chemical reaction and for the heat flux only measured from the hot plate. Based on these results, the minimization is performed. The signal given for the thermopile fits well with the signal calculated with (Equation(21)) (Figure 37). In the following, A and τ values (Table 9) are used for the calculation of the chemical heat flux (Equation (23)).

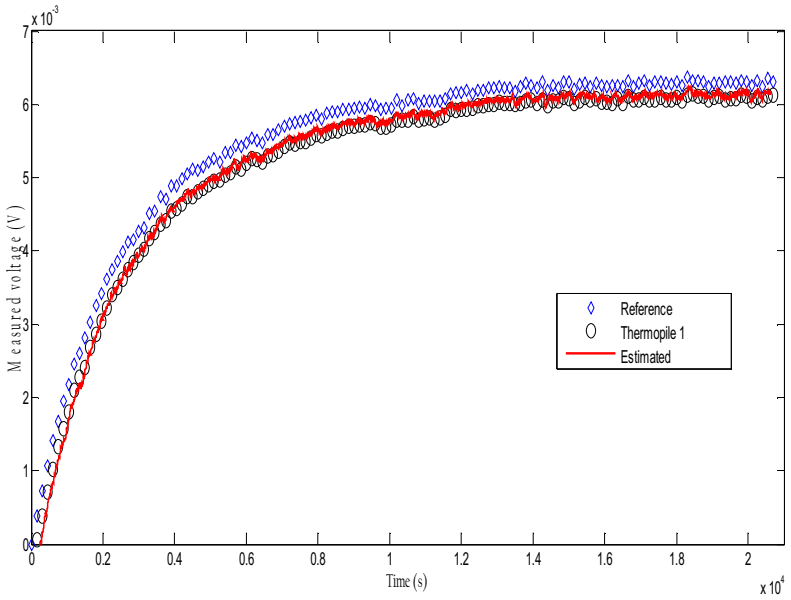

Figure 37: Signal given for the thermopile (O) and for the reference (◊). The line represents the signal calculated with Equation (22)

Table 9: A and τ values determined for the thermopile calibration

Thermopile	1	2	3	4	5
A (wu)	1.0533	0.7391	0.7584	0.6790	0.8705
τ (s)	8.1319	1.2068	1.4625	6.7598	11.5076

wu: without units

3.5.2 ELECTRICAL CALIBRATION OF THE MICROCALORIMETER

In order to get the variation in the performance of the thermopile due to the temperature variation, a calibration coefficient (α) is determined.

$$\alpha = Q_M / U_M \quad (24)$$

Where Q_M is the delivered power (W) and U_M the measured voltage (V). This calibration coefficient is obtained by the injection of a known heat flux from an electrical heat source through the thermopile by Joule effect. A flexible laminar heater is used as a heat source, stuck to the thermopile with conductive thermal grease to avoid thermal gradient between the resistive element and the heat sink. In order to calibrate the microcalorimeter by Joule effect, we impose different electrical power (from 0 to 0.6 W) by the use of a power supply (Agilent E3631A) at 46°C, 71°C and 97°C thanks to the regulation system. The heat flux through the system is measured by the thermopile as a function of time. Figure 38 shows the linear regression of the imposed heat flux versus the measured voltage and allows the determination of the calibration coefficient as the slope of the line. This coefficient varies with the performance of the thermopile and temperature (Table 10). These data are used to deduce the chemical heat flux of the oxidation reaction.

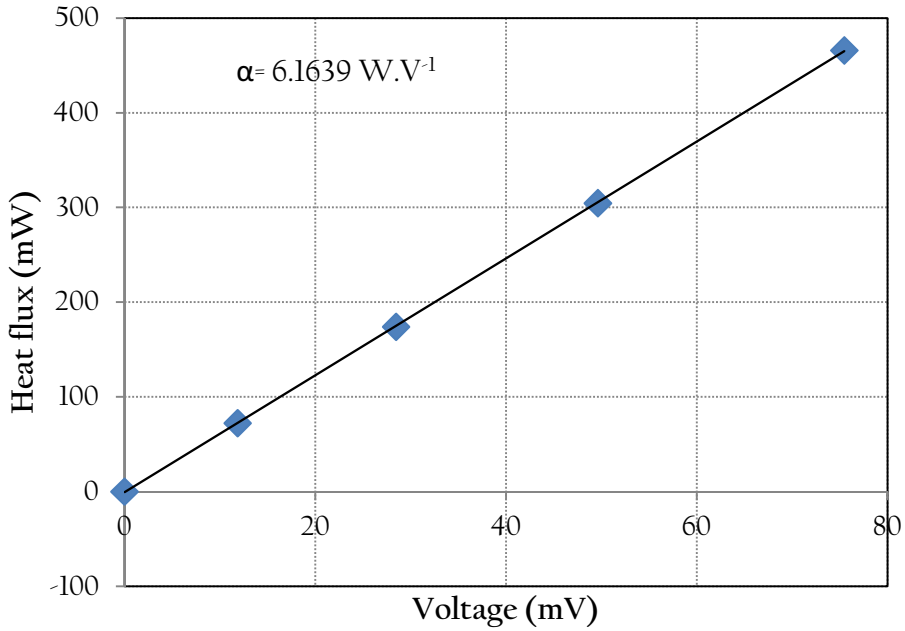

Figure 38: Imposed heat flux versus measured tension at 46 °C. The solid line corresponds to the linear regression. The slope gives the calibration coefficient α.

Table 10: Experimental calibration coefficient measured at different temperatures

Temperature (°C)	Calibration coefficient **α** ($W.V^{-1}$)
46.0961	6.1639
71.1111	7.0689
97.3874	6.9639

Related to the global thermal stability, Figure 39 presents the evolution of the different thermopile responses (W) during a long period of time (45 h) by the calibration coefficient in isothermal conditions (97°C). The response is showed for the thermopile placed as reference and also for the other 5 without sample. It can be observed that the system is very stable and thus it can be used for long experimental d.

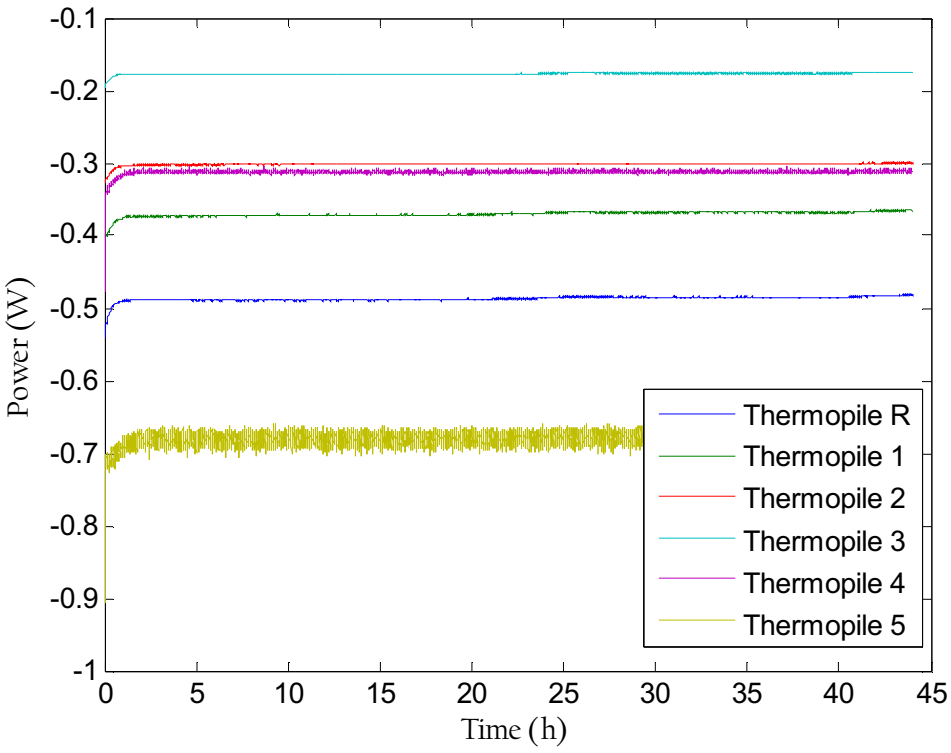

Figure 39: Thermal stability of the different thermopiles at 97°C

3.5.3 SENSITIVITY OF THE HEAT FLUX MEASUREMENT

In order to get the accuracy of the calibration coefficient and the measurement of the heat flux, the errors in the measurement using a known heat flux are calculated. Figure 40 shows the deviation between the imposed heat flux and the experimental one for 4 different values of imposed power (0.4, 4, 40 and 400 mW). The experimental errors are calculated and reported in Table 11 for the 4 different cases.

Table 11: Comparison between the imposed and measured heat fluxes

Imposed heat flux (mW)	0.4 (a)	4 (b)	40 (c)	400 (d)
Standard deviation between imposed and measured heat flux (mW)	6.57E-02	8.77E-02	4.76E-01	5.17
Injected energy (J)	1.470	13.89	136.8	1 027
Measured energy (J)	1.166	14.67	135.4	1 039
Relative errors between imposed and measured energy	20.66 %	-5.68 %	0.96 %	-1.18 %

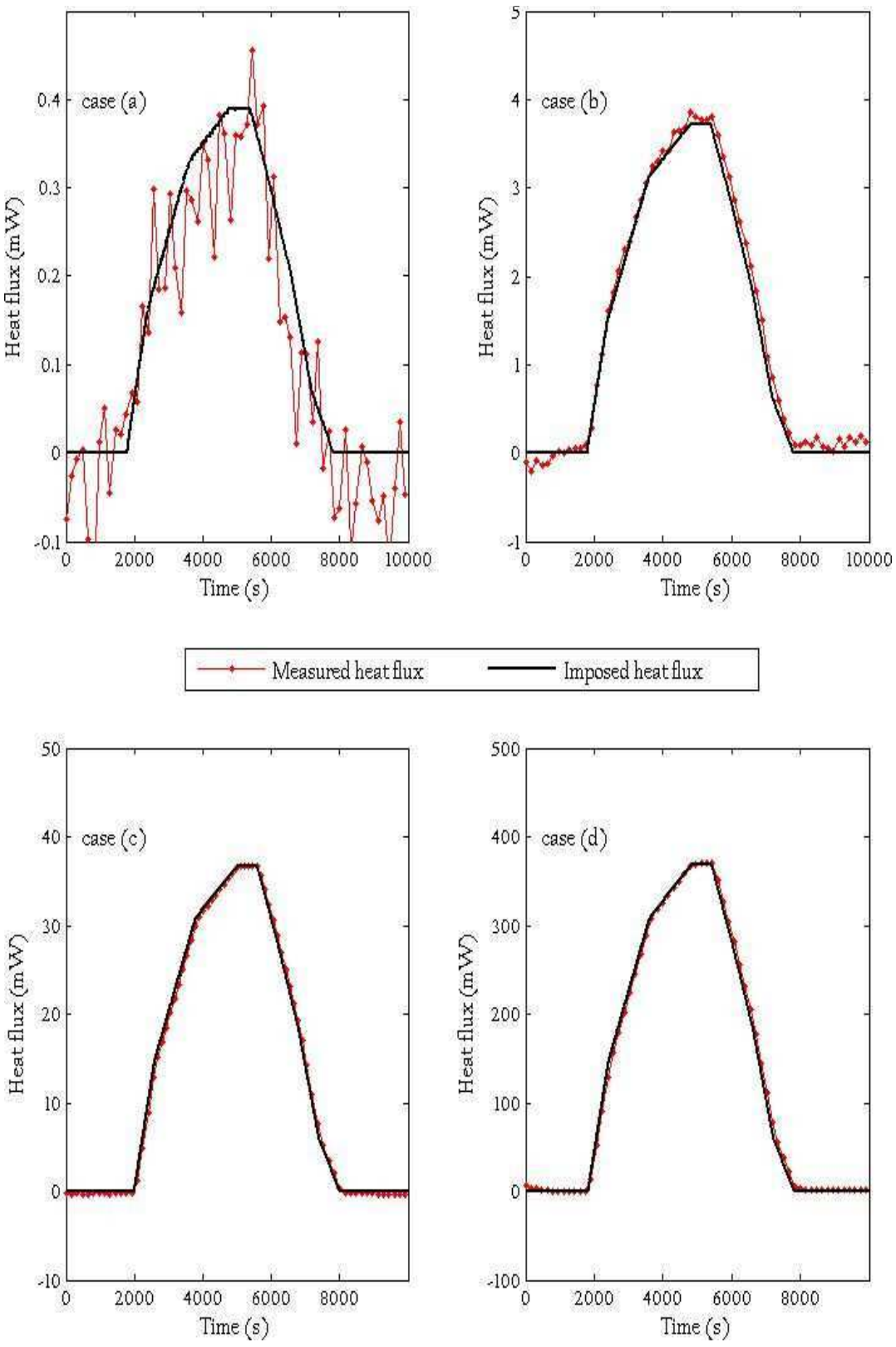

Figure 40: Heat flux imposed from the electrical heat source and heat flux measured by the thermopile for different imposed heat flux

3.6 VALIDATION AND EVALUATION OF METHOD UNCERTAINTY BY THE USE OF A PARAFFIN

From Equation (24) and the value of the calibration coefficient, heat flux values can be calculated and enthalpy deduced by integration. The obtained values are compared with those determined using the classical DSC technique on well-defined matters. Figure 41 presents the melting behavior of a jam making paraffin. Similar values of 132 $J.g^{-1}$ and 140 $J.g^{-1}$ are found for the melting enthalpy of the jam making paraffin with the microcalorimeter and the DSC, respectively. The slight discrepancy between the two experimental values can be explained by a different accuracy of the calculation of the enthalpy (surface area under the curve determined from different onset and offset temperatures). The microcalorimeter validation is also assessed with the determination of the melting temperature of two well-characterized paraffins. The melting curve profiles give similar points of the paraffins, i.e. 46-48°C and 52 to 54°C (Figure 42) to that given by the supplier. One the whole, these measurements allowed the validation of the microcalorimeter device and the method of heat flux measurement.

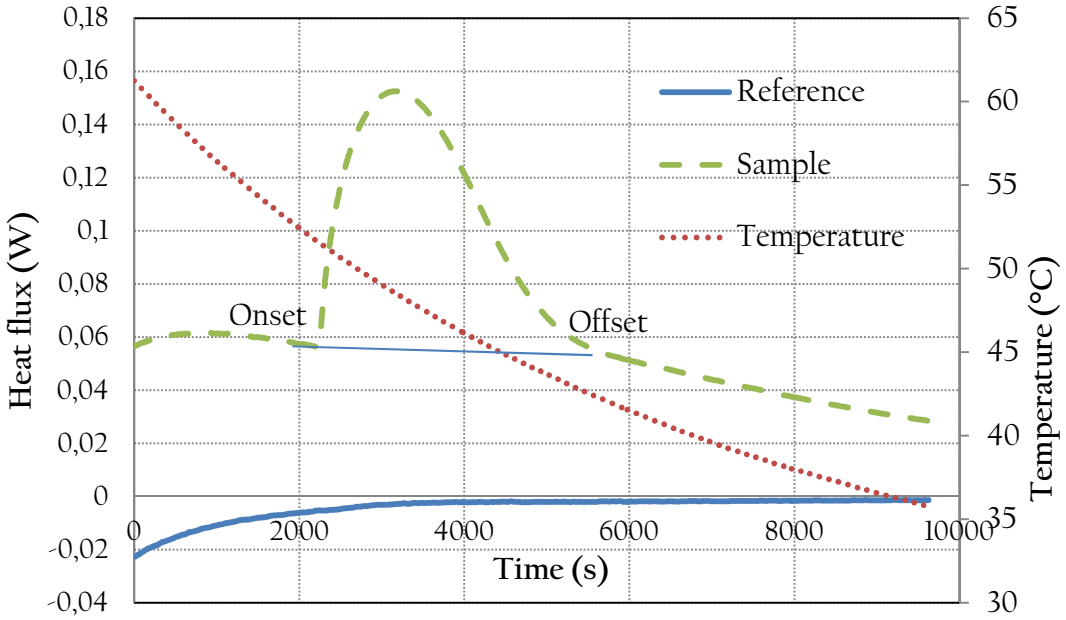

Figure 41: Experimental curve obtained the microcalorimeter device

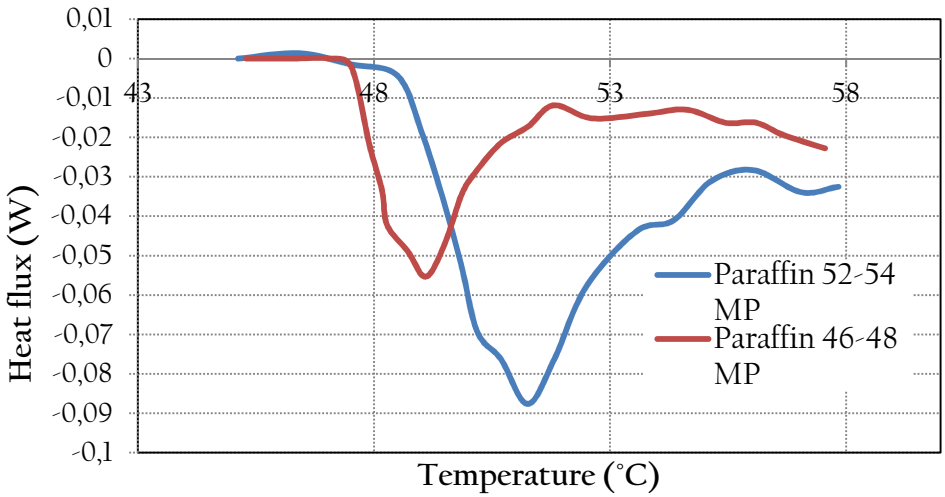

Figure 42: Melting profile of two paraffin wax characterized by two different melting point ranges

3.7 Conclusion

We have designed a microcalorimeter that shows an optimization of the classical DSC device in terms of heat flux measurements and versatility for sample management. The microcalorimeter presented has a good sensitivity and precision in the heat flux measurement like the DSC device. It is also very stable during long periods of time (cf. § 3.5.1). This is of great interest in our case because cameline oil used in this work shows a very slow oxidation kinetics that requires continuous measurements for at least two days (cf. § 4.1). In addition, the microcalorimeter has the versatility of work with different samples at the same time. Moreover, the ratio volume/surface that significantly affects the oil oxidation kinetic can be varied using different designs for the oil containers. In particular, this allows determining if oxygen is the reaction limiting factor and studying the kinetics of oxygen diffusion into the oil.

On the whole, the developed device provides an adaptable, sensitive, and solvent-free method for the measurement of lipid oxidation, particularly suitable for the fast screening of a large set of samples. Finally, compared with DSC, the microcalorimeter designed in the laboratory is low cost (less than 10 000 € for the microcalorimeter vs 30 000 to 100 000 € for the DSC device).

CHAPTER 4

RESULTS AND DISCUSSION

This project deals with the study of the oxidative behavior of Cameline oil. This oil is chosen because of its high amount of α-linolenic acid among the linolenic vegetable oils (Table 12).

Table 12: Composition (wt% total fatty acids) in α-linolenic acid (18:3 n-3) of several vegetable oils (Couëdelo, 2011)

Vegetable oils	18:3 (wt % total)
Perilla	65
Inca inchi	48
Linseed	47
Cameline	27
Hemp	18
Blackcurrent seed	13
Walnut	12
White mustard	10
Rapeseed	10
Soya	7

Cameline oil is produced from seeds of *Camelina sative* plants. The plant is known as false flax and gold of pleasure (Figure 43). Native to Northern Europe and to Central Asian areas, it has been also introduced in North America. It is a summer annual oilseed plant in the family *Brassicaceae. Camelina sative* seeds contain about 30-40 % of oil dry matter basis (Zubr, 2009).

The oil has a yellow color and mustard like odor. It is very rich in natural antioxidants, such as tocopherols, making it very stable to oxidation and rancidity. Moreover, it is a naturally rich source of essential fatty acids, with favorable nutritional implications and beneficial physiological effects.

Likewise, this oil is very attractive because of its very low cost of production compared with other vegetable oils, making it a potential biodiesel, an environmentally friendly alternative to petroleum diesel and gasoline.

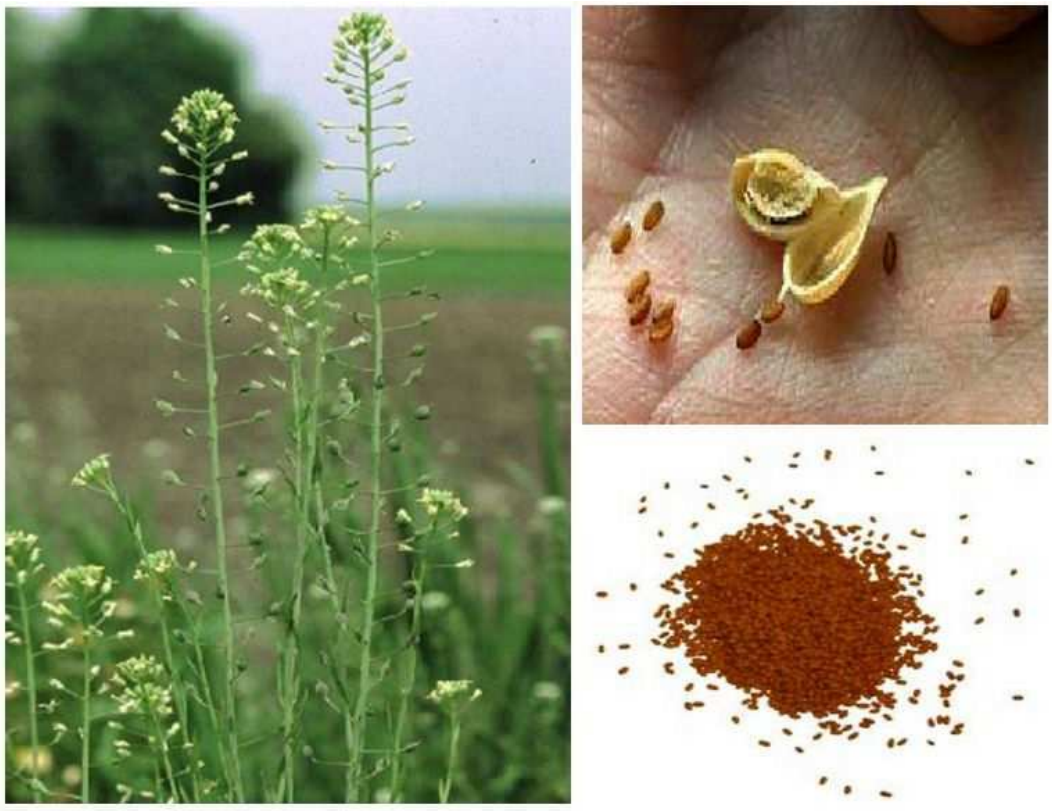

Figure 43: Cameline plant, capsule and seeds inside the capsule

4.1 CAMELINE OIL OXIDATION

4.1.1 IMPORTANCE OF MANAGING CAMELINE OIL SAMPLES ON OXIDATION RESULTS

By means of the conjugated diene amount, two different batches of Cameline oil (batch 1 and batch 2 corresponding to deadlines for an optimal use of 15/06/2010 and 15/05/2011, respectively) are analyzed and compared in Figure 44.

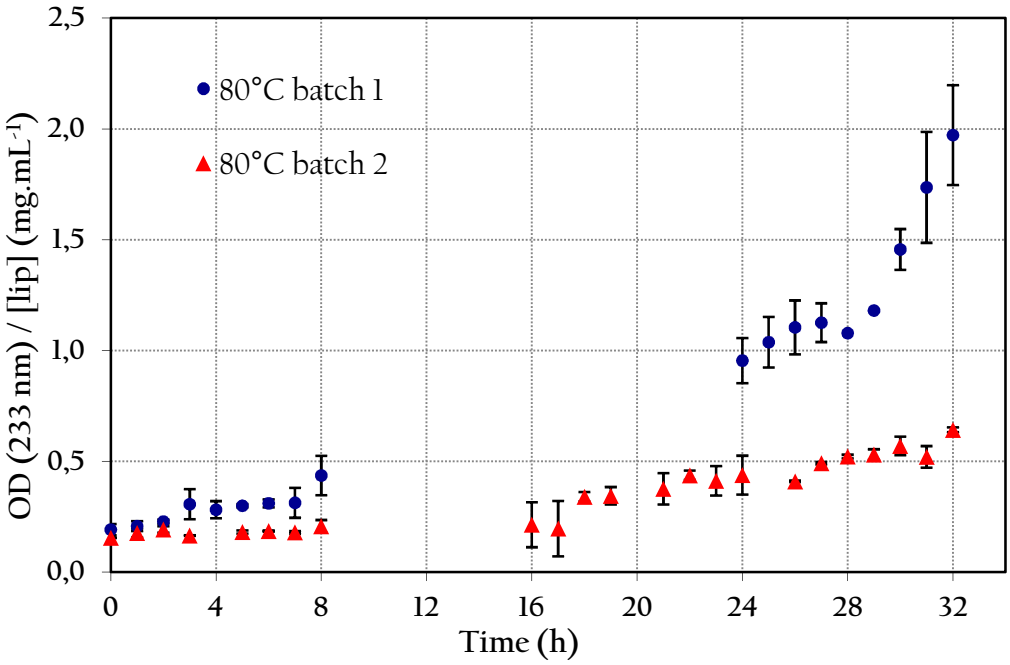

Figure 44: Conjugated diene amount in Cameline oil samples from two different batches (deadlines for an optimal use: batch 1 15/06/2010 and batch 2 15/05/2011) stored at 80°C in the dark.

The conjugated diene formation is higher in the oldest batch (deadline for an optimal use of 15/06/2010) compared with most recent one (deadline for an optimal use 15/05/2011). This may be due to a different amount of active vitamin E in the two batches. Indeed, Vitamin E presents anti-oxidative properties due to its ability to produce phenolic hydrogen to lipid free radicals. The tocopheroxyl radical formed is considered to be non reactive towards the unsaturated lipids and thus limits the propagation reactions.

These data show the importance to work on well characterized samples especially regarding the amount of vitamin E. To limit the oil evolution, small aliquots were prepared as soon as the oil was purchased and flushed with nitrogen. It is thus assumed that samples issued from the same batch are comparable. However, when the two batches are considered, the comparison is no more possible.

4.1.2 Influence of light on Cameline oil oxidation

By means of the peroxide index, the presence and type of light on the formation of primary oxidation products, versus time of storage is presented in Figure 45.

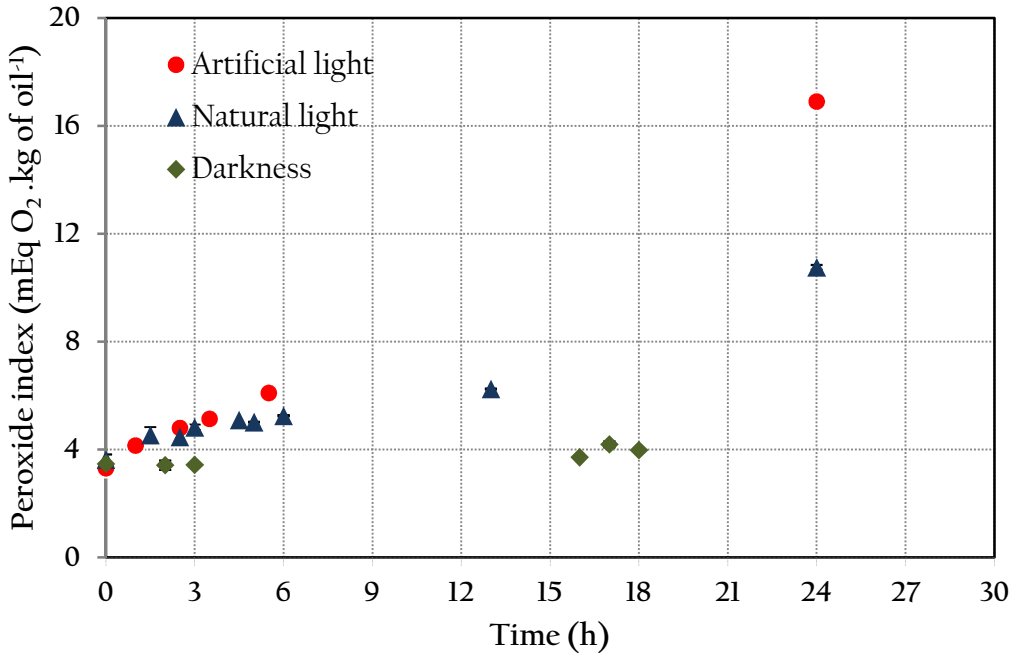

Figure 45: Influence of the presence and the type of light on primary oxidation of the Cameline oil stored at 37°C

Cameline oil is characterized by an initial peroxide index of 3.45 ± 0.45 mEq $O_2.kg^{-1}$ (n = 27). This value is considered as satisfactory for a crude oil according the European regulation.

Figure 45 shows that Cameline oil exposed to artificial light is oxidized more rapidly and to a greater extent compared with samples stored under natural light or in the dark. This is in agreement with studies showing that light favors the oxidation process (cf. § 1.1.1.) In particular, Cameline oil was stored at 8°C under daylight and darkness for a period of storage of several months (350 days) (Abramovic & Abram, 2005). It was shown that the peroxide value of fresh oil

was 2.38+/-0.01 mEq $O_2.kg^{-1}$, then, after a month in darkness the PI was 8.12+/-0.08 mEq $O_2.kg^{-1}$ while in daylight the oil reached 21.0+/-0.1 mEq $O_2.kg^{-1}$.

4.1.3 Influence of temperature on cameline oil oxidation

By means of the peroxide index, the effect of the storage temperature on the formation of primary oxidation products versus time of storage is presented in Figure 46. Temperature is a factor promoting the formation of primary oxidation products as already mentioned (cf. § 1.2.4).

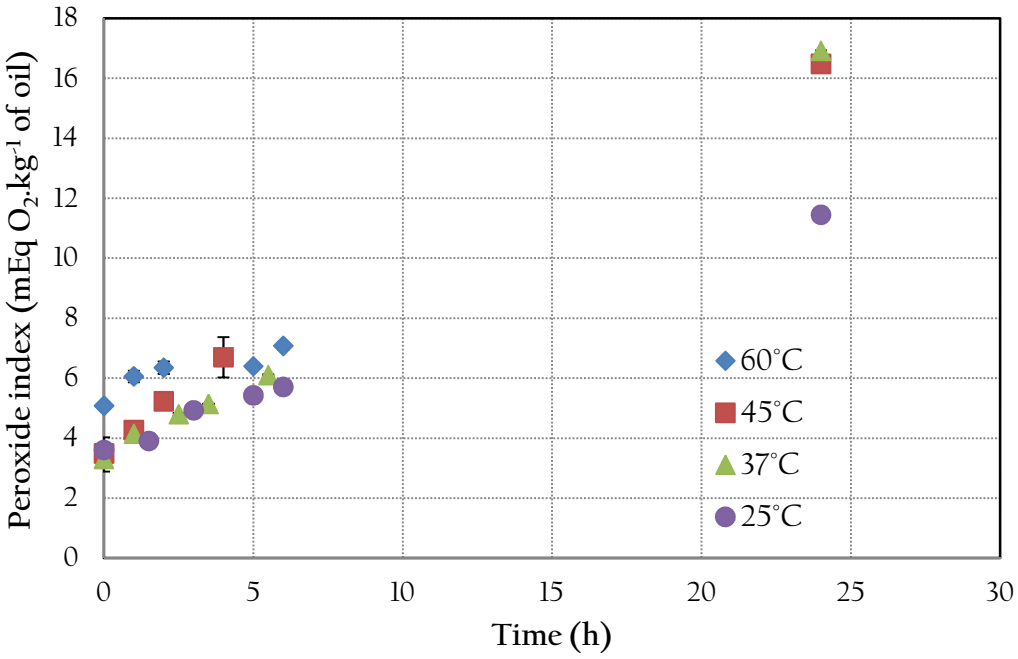

Figure 46: Influence of temperature on primary oxidation of the Cameline oil with light

Moreover, Figure 47 shows that the formation of the primary oxidation products is proportional to the temperature increase.

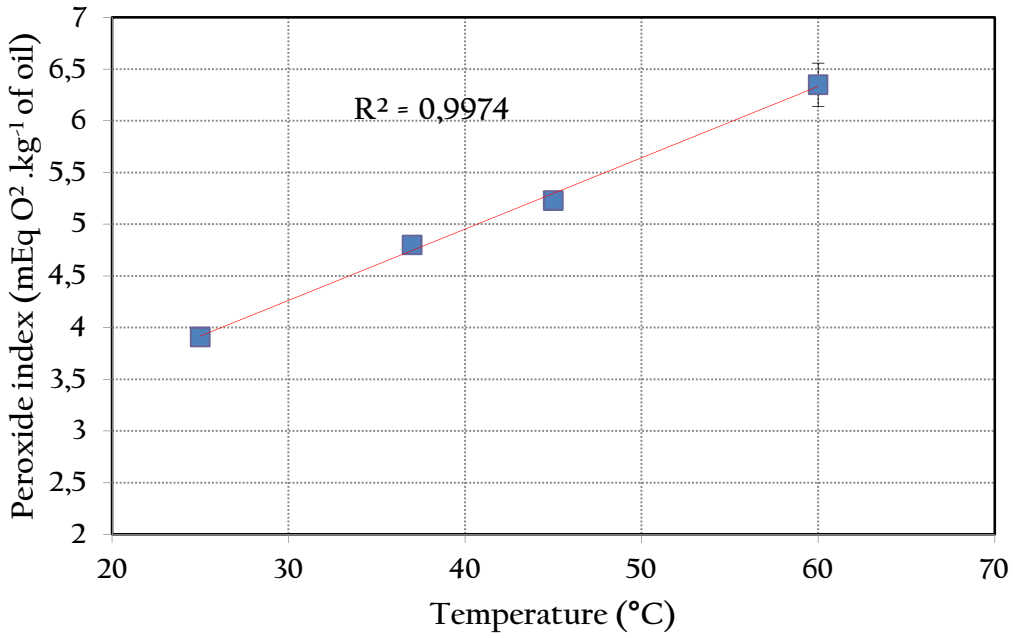

Figure 47: Correlation between the apparition of the primary oxidation products and temperature in Cameline oil after 2 hours of storage with light

Because the peroxide index determination uses a huge quantity of organic solvents and because its accuracy questionable for high amounts of peroxides, another method of quantification of the formation of primary oxidation products based on UV measurements was used especially when high temperatures are investigated. This method also presents the advantage of being quicker than the peroxide index. Thus, more samples can be assayed. Figure 48 presents the evolution of the conjugated diene amount for Cameline oil stored at two temperatures 80 and 120°C.

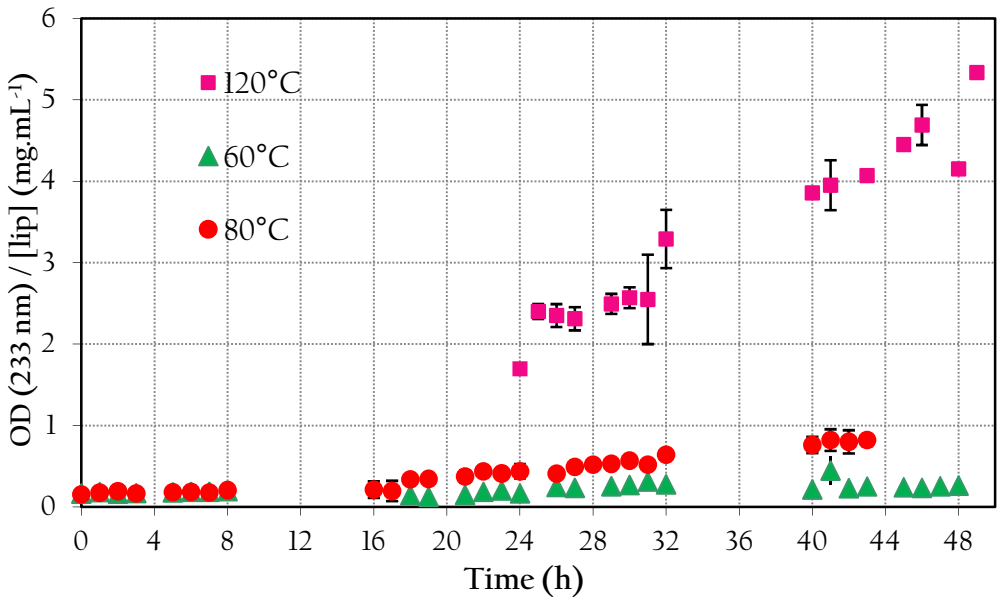

Figure 48: Effect of temperature on the conjugated diene formation (UV method) of Cameline oil (storage in the dark)

Once again, the results obtained by the UV method show the effect of temperature on the formation of the primary oxidation products. It is worth noting, that at 120°C, for storage time higher than 24 hours, results present high variability. This can be due to thermo-oxidation leading to polymeric compounds (Velasco & Dobarganes, 2002). Indeed, visual observations of the samples show a change in the color and the viscosity of the samples.

4.1.4 CHARACTERIZATION OF THE SAMPLES ISSUED FROM MICROCALORIMETRY EXPERIMENTS

Different samples issued from the microcalorimetry experiments are obtained and characterized.

Samples corresponding to continuous heat flux measurement are regularly taken from the microcalorimeter. In contrast, for samples corresponding to discontinuous measurement, the experiments are stopped. No difference in terms

of primary oxidation products is observed between the samples that are taken every hour from the microcalorimeter in order to be analyzed and those whose are left only at the end of the experience (Figure 49).

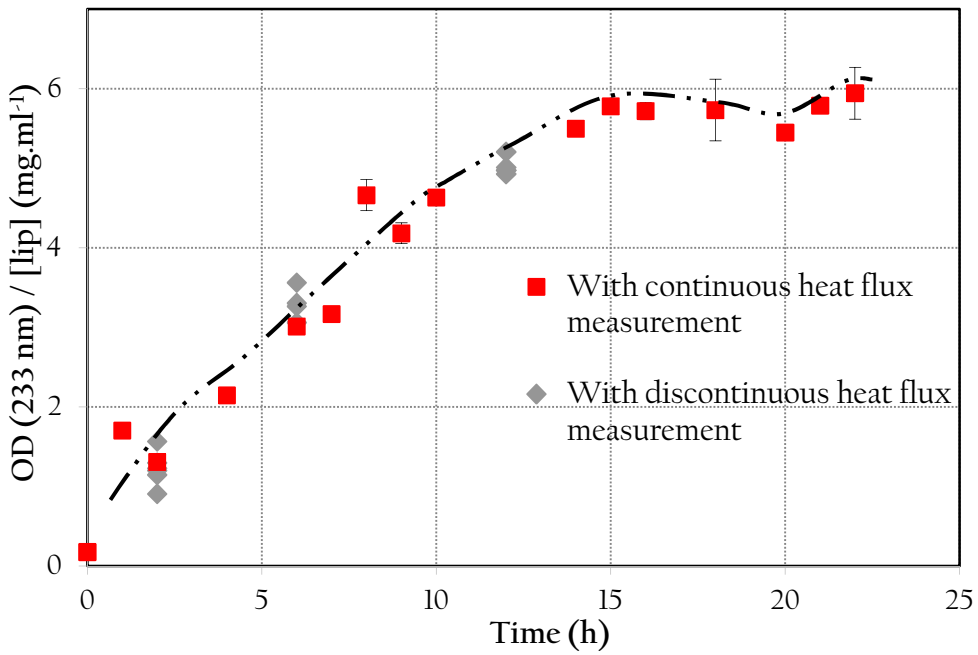

Figure 49: Effect of experimental procedure on the conjugated diene hydroperoxide formation (UV method) of the oil, (container diameter of 24 mm at 100°C)

On the other hand, Figure 50 shows the evolution of the p-anisidine value for Cameline oil taken from the microcalorimeter every hour, during a period of time of 25 h. The amount of aldehydes rapidly increases during the first 4 h then stabilizes up to 14 h to decrease afterwards. This decrease may be due to the degradation of the aldehydes already formed. Thus, this method permits to follow the formation of secondary products only in the first 14 h of oxidation.

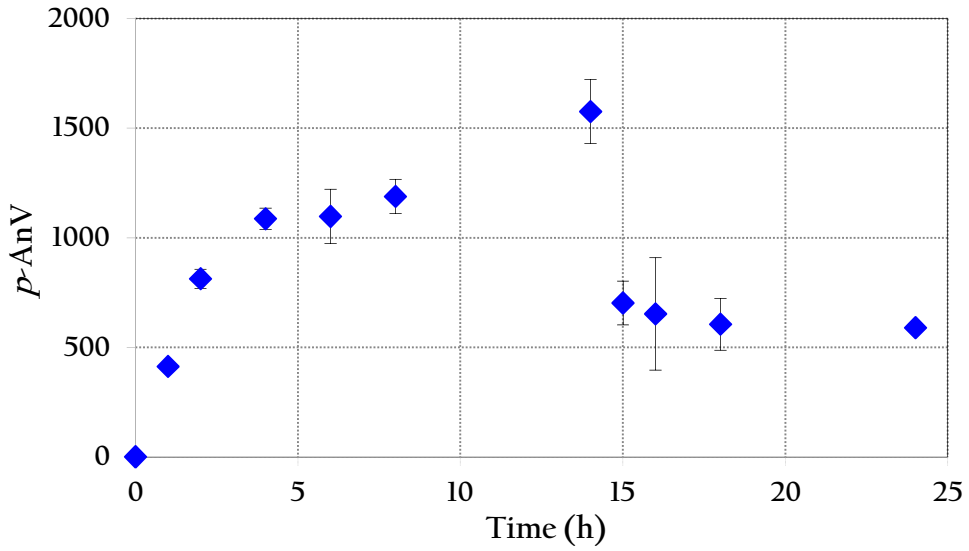

Figure 50: Evolution of p-anisidine value with time for Cameline oil (container diameter= 29mm; isothermal conditions T = 100°C)

Figure 51 shows the evolution of the TBA test value for Cameline oil samples taken every hour from the microcalorimeter. As the p-anisidine value, TBA test measures secondary oxidation products. A similar curve pattern is observed for the two types of measurements. However, TBA is less pertinent than p-anisidine because its values decrease as soon as 4 hours of storage.

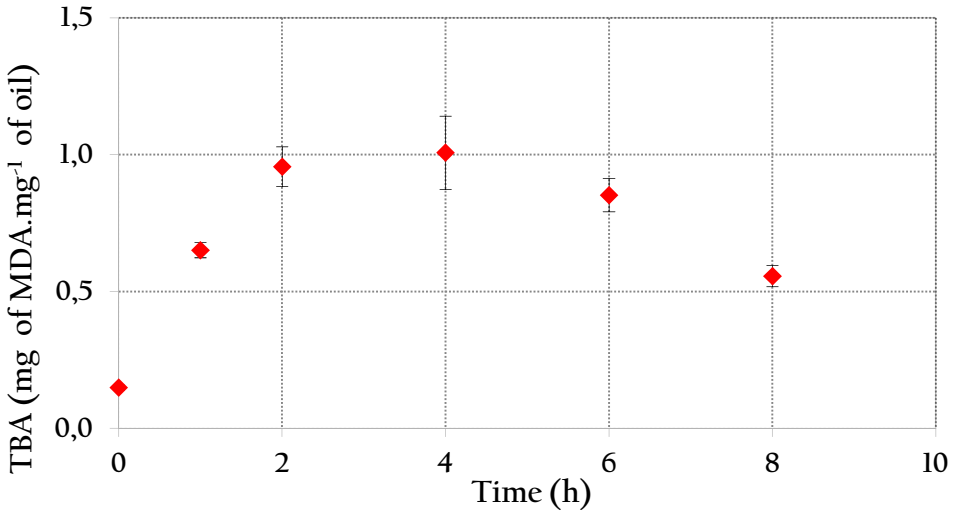

Figure 51: Evolution of TBA value with time for Cameline oil (container diameter= 29mm; isothermal conditions T = 100°C)

The conjugated diene hydroperoxide method is used to investigate the influence of the the surface/volume ratio on the formation of primary oxidation products (Figure 49). A higher surface/volume ratio slightly promote the oxidation process will be faster.

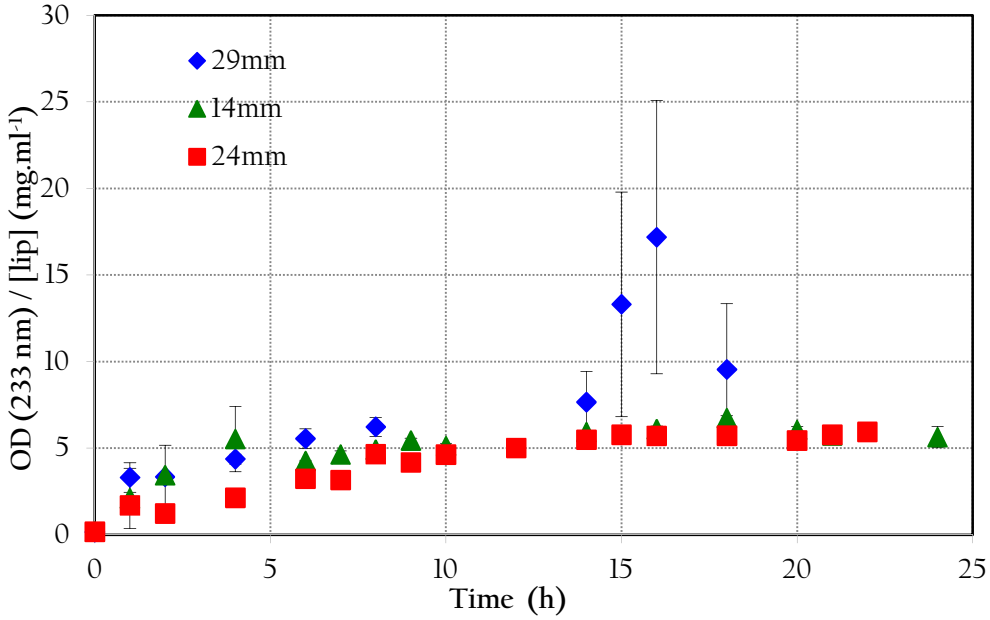

Figure 52: Influence of the surface/volume ratio on primary oxidation of the Cameline oil (isothermal conditions T = 100°C)

In conclusion, Cameline oil is a good model for studying the oxidative process since it is possible to investigate the role of light, and temperature. However, a peculiar attention must be paid on the amount of vitamin E if studies have to deal with different batches of oil production. Among the different methods used for studying lipid oxidation, the UV method appears to be the more reliable and sensitive one.

4.2 CHARACTERIZATION OF OIL OXIDATION BY DSC AND MICROCALORIMETRY

In order to characterize the Cameline oil oxidation as a function of its thermal behavior, the samples are analyzed by DSC and microcalorimetry developed in this study. The measurements are carried out directly on the oil in bulk phase.

The conditions for the experiments with DSC and microcalorimetry are in accordance with the time required to observe the chemical oxidation of Cameline oil (40 h) in isothermal conditions (DSC at 110, 120 and 130°C and microcalorimetry at 100°C).

Aluminum (DSC) and copper (microcalorimetry) containers are chosen for the oil oxidation study due to their very high thermal conductivity (400 $W.m^{-1}.K^{-1}$ and 209.3 $W.m^{-1}.K^{-1}$, respectively) despite the fact that, from the oil oxidation point of view, metals can act as a catalyst of the reaction (Andersson & Lingnert, 1998b; Osborn-Barnes & Akoh, 2003).

The Cameline oil samples inside the DSC apparatus and the microcalorimeter are deprived of light that is a catalyst of oil oxidation as shown previously (cf. §4.1.2).

4.2.1 DSC ANALYSIS

A DSC-oxidation curves of Cameline oil at isothermal conditions (110, 120 and 130°C) is shown in Figure 53.

From the curves, 4 different parameters can be described:

The induction time: Since the Cameline oil has a high content of polyunsaturated fatty acids (cf. § 1.2) it leads to a reduced oxidation stability as it can be seen in the rapid onset of the oxidation and reduced induction time.

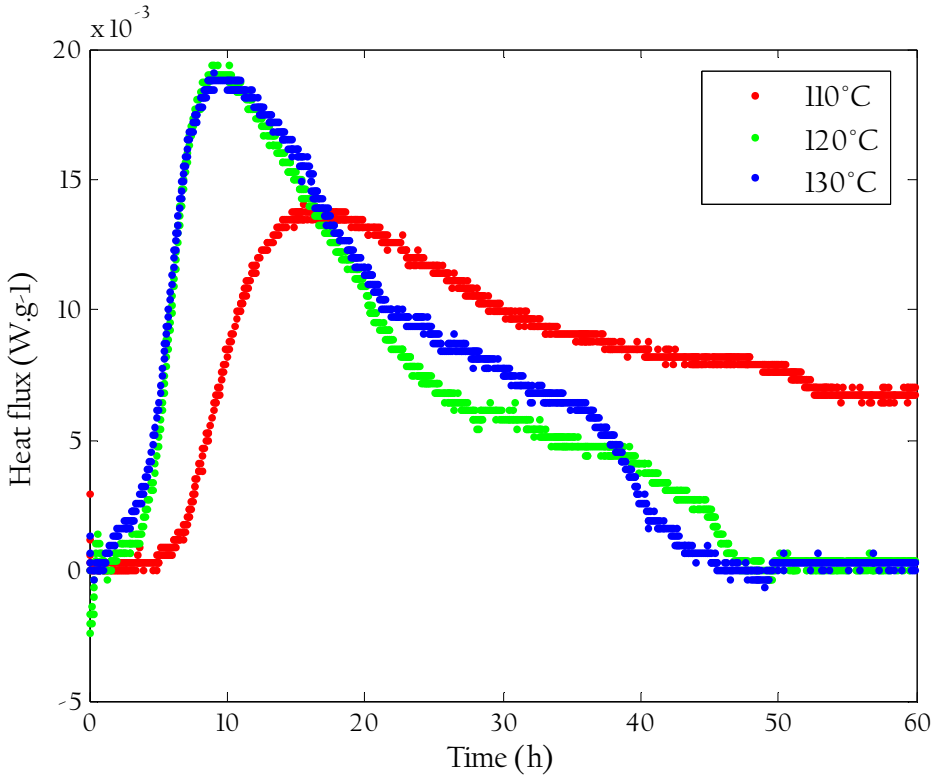

Figure 53: DSC-oxidation curves of isothermal of Cameline oil

Temperatures of 120 and 130°C lead to much shorter induction period values than at 110°C, this is in accordance with what was reported (cf. § 1.3.3.1); thus, oxygen is supplied to the oil from the media by interphase mass transfer and is consumed in the oxidation process so, at higher temperatures, the maximum peak of the oxidation will be achieved faster.

The thermal profile (curve morphology): At 120 and 130°C, the curves are quite similar and that both exhibited two well distinguishable exothermic events.

The major or maximum peak is at the same magnitude of heat probably due to the fact that at this point of the process, the high unsaturations degree of Cameline oil and all the oxygen available from the media are reacting at a rapid rate.

Thus, the oxygen is diffusing in the sample thanks to its solubility and all the species are reacting with the alkylperoxide radical (LOO•) present, which is the most common species at atmospheric pressure and at moderate temperature. Once the oil oxidation is initiated, the reaction with oxygen is very quick and the

hydroperoxide (LOOH) is being formed faster than its decomposition rate (cf. § 1.1.1). Indeed, it can be seen that this phenomenon is already catalyzed by the temperature but independent of its magnitude, since at 120 and 130°C the same behavior is observed. In addition, a second bearing can be observed in the graphic which can represent the species that are formatting. This formation corresponds to the auotacatalyzed chain reaction where probably the hydroperoxide decomposition and/or the set of termination reactions produce a high variety of compounds of different polarity, stability and molecular weight (cf. § 1.1.1.3). Thus, these species are dependent on the temperature since at 130°C this bearing is observed before than at 120°C.

On the other hand, at 110°C, the time characteristic and the heat flux released are completely different. The reaction process involved is catalyzed in a complete other range. The maximum peak level is observed with a lag of magnitude and time. A second bearing can be also observed but with a smaller magnitude and the termination of the reaction is not clear after 40 h of measurement.

The reaction time: About the onset and offset of the oxidation process at 120 and 130°C the heat flux releases by the reactions are almost the same, what gives the idea that the same kind of behavior is occurring in both reactions. All the species have reacted at the same time (before t=20 h). It can be deduced that at 120 and 130°C the oxidation process of all the species in the oil are the same and not too much temperature dependant. The offset of the reaction can be clearly identified at 120 and 130°C after 50 h. This means that all the media is saturated in oxygen and all the species are already oxidized.

On the opposite, at 110°C the onset and the offset of the oxidation process are different (the species are still interacting with the oxygen of the medium after 60 h). This can be due to the fact at 110°C the species are all reacted with a lag of time. So it can be deduced that there are some species that need the temperature above 120°C to be catalyzed.

Taking into account the fact that oxidation implies numerous reactions and the DSC corresponds to the total heat flux release by the whole reactions, more

specific analysis have to be done in order to identify the kind of species catalyzed by the temperature above 120°C. As already mentioned above thus temperature, thermooxydation may occurs.

Energy profile: In terms of the influence of temperature and the energy released by the oxidation process (Figure 54) the same magnitude of energy is released in the three cases but, there are faster at higher temperature (considering the first 60 h of measurement). At 110°C, the plateau of the energy released is observed even after 60 h of experiment suggesting that the oxidation reactions are not finished.

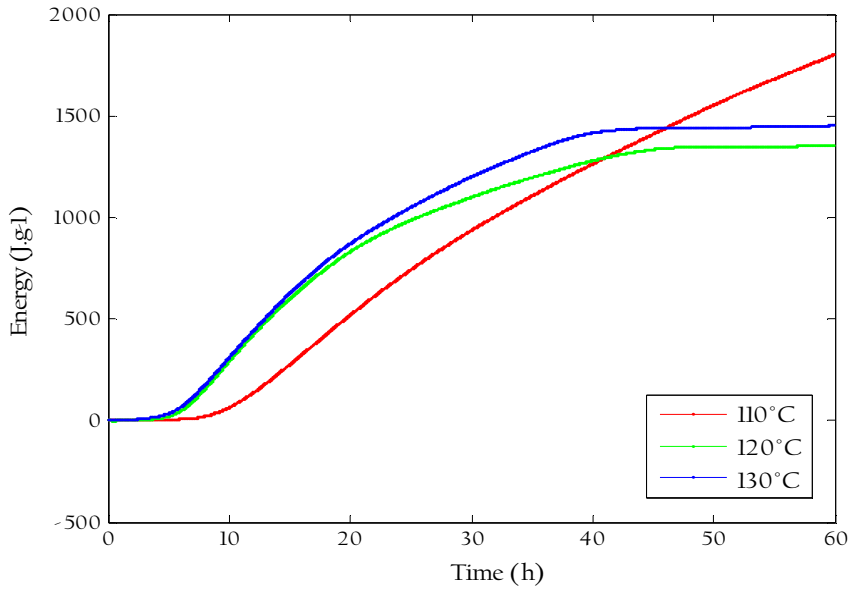

Figure 54: Energies released by the oxidation of Cameline oil at 110, 120 and 130°C by DSC

Another aspect to be considered, from the curves (Figure 54) is the quality of the measurement. The base line has to be neat because it is subtracted to the measurements in order to have the real behavior of the reaction and to subtract the noise. It is important to notice that the measured heat flux and the resolution of our 8bit-DSC device have the same order of magnitude. Thus, the exchanged energy during the oxidation processes can be under our instrument resolution. This may explain the difference between the curves at 120 and 130°C.

The Figure 55 shows zoomed images where the discretization of the measurement used by the DSC device resolution is clear by evidenced. This order of magnitude can be well observed in the Figure 55 a). This difference multiplied by the 60 h of

experimentation gives us a lack of error in the order of 100 $J.g^{-1}$ (Figure 55 b)) which corresponds to the energy releases by the sample.

a) b)

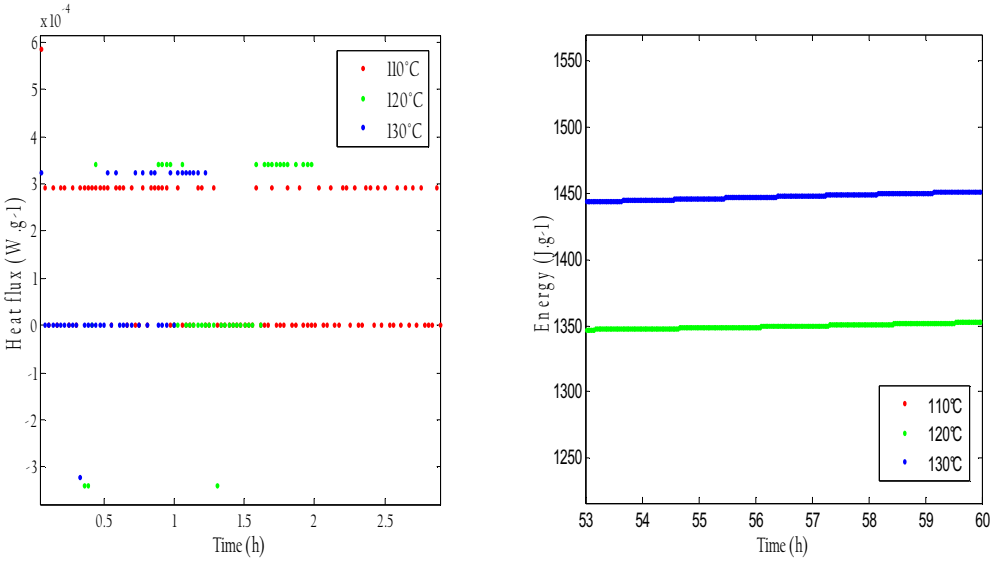

Figure 55: Zoom of the Figure 4.8 a) and Figure 4.9 b) to show theexperimental error

Since the chemistry of the oxidation at temperatures higher than 110°C is much more complex since both thermal and oxidative reactions are involved simultaneously and polymeric compounds are formed, we will only focus on the study of Cameline oil at isothermal condition for a temperature of 100°C.

4.2.2 MICROCALORIMETRY ANALYSIS

Figure 56 shows the heat flux as a function of time for a sample of Cameline oil in isothermal condition (100 °C) and a copper container of 14 and 24 mm.

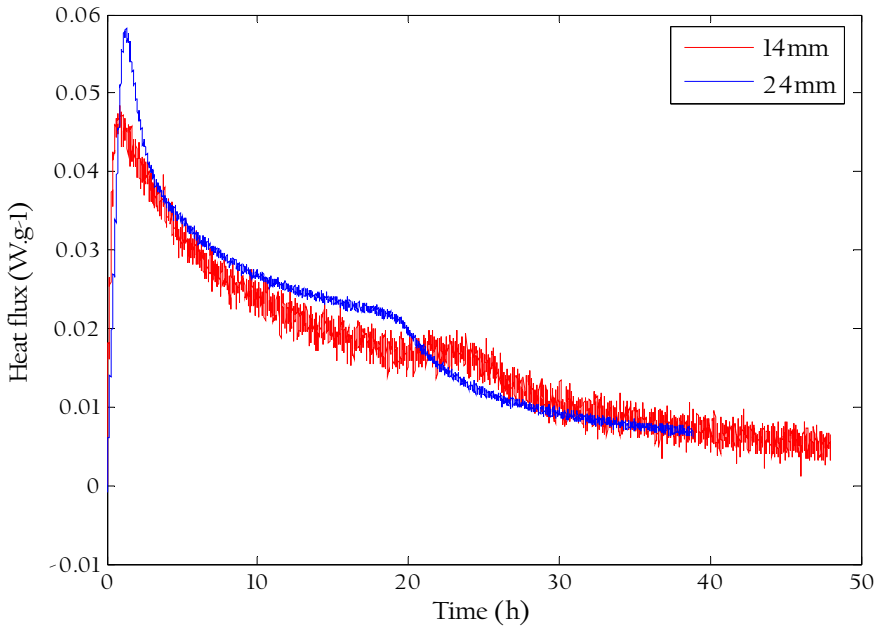

Figure 56: Signal acquisition by the thermopile from the oxidation of cameline oil at 100°C (container diameter 14 and 24 mm)

As in the case of DSC curves, 4 parameters can be described for the curves obtained by microcalorimetry.

The induction time: A higher surface/volume ratio gives a greater amount of oxygen consumed. Moreover, then the oxygen saturation of the system shows an induction time shorter than the induction time observed with the DSC (Figure 53).

This induction period is even hard to well identified maybe due to the fact that at t=0 all the system is already saturated by the oxygen present in the medium and ready to be consumed by the oil oxidation.

The reaction time: Once the oxidation is started, the diffusion of the oxygen present in the surface interface with the air takes place. This renewal of the oxygen can be modelled as follows:

$$N_{O_2} = \Delta O_2 \cdot K \cdot a \qquad (25)$$

where N_{O_2} is the interphase mass transfer flux of the oxygen, ΔO_2 the interface potential, K the mass transfer coefficient constant ($kg.m^{-2}.s^{-1}$) and a the area of the

exchange (m^2). Thus, the transfer of the oxygen is determined by the area of the exchange. According to this the fastest transfer rate is observed at the biggest container diameter of 24 mm (around 23 times higher the case of the DSC where the diameter is only 5 mm).

The thermal profile (curve morphology): The curve (Figure 56) shows the multiple rising and decreasing of the dynamic autocatalytic reactions of oxidation which are the results of the sequences of multiples reactions from the species involved. Each peak observed depends on the rate of diverse reactions as a function of time and is not easy to individualize.

Thus, after a fast thermalization of the sample in the microcalorimeter, the measured heat flux presents a profile with significant variations. If we assume that the measured heat flux consists in the summation of source terms of the involved chemical reactions, each of these source terms is equal to the product of a conversion rate by the enthalpy of reaction. Therefore, the heat flux pattern strongly suggests that several oxidation reactions occur with time. At the end of the kinetics, the formation of non- radicals and the termination of the oxidation reaction can be identified when the curve reachs the base line level.

The shape of the curve and the peak observed are the results of the overlapping effect from the oil composition. In other words, the proportion of several and different fatty acids which are components of this oil have different oxidation rates that influence in global the total heat flux dissipation from the chemical reaction.

Moreover, it must be taken into account the influence of the interaction between the fatty acids in the glycerol backbone. Thus, the number and position of the double bonds of the fatty acid or the location of the fatty acid (cf. § 1.2) should affect the global heat flux dissipation. Thus, each fatty acid present and the factors that influence the oxidation should determine the rate of oxidation of Cameline oil.

Since the oxidation is a very complex chemical reaction, it is impossible to determine unequivocally the amount or the origin of a peak in the curve.

Energy profile: From Figure 57, it can be observed that for two different diameter containers there is the same magnitude in the energy released by the oxidation of the Cameline oil. This probably means that in both cases there is the same reaction sequence that gives, at the end, the same order of energy since composition and the species present are similar and react almost into the same period of time.

Taking into account the energy profile from the DSC and microcalorimetry (Figure 54 and Figure 57), the same order of energy are obtained but with a range of different for the temperatures of 110°C and 100°C, respectively. Even if a difference in the container diameter can be the source of some error, it strongly suggests that, in the case of microcalorimetry the thermal calibration and control of the temperature is absolutely essential.

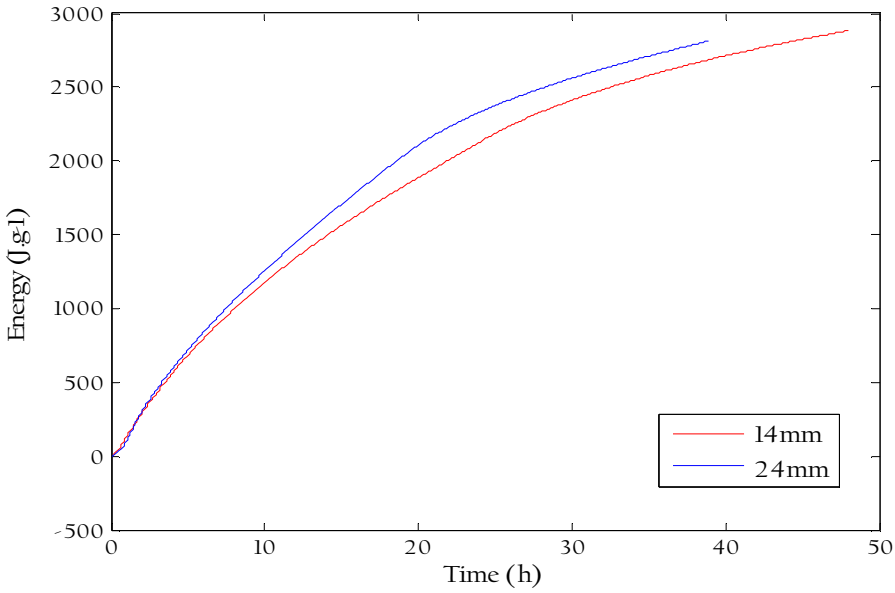

Figure 57: Energies released by the oxidation of Cameline oil by the microcalorimeter developed and for two different container diameters

The oil cannot be treated as homogeneous substance for the study of the oxidation kinetics since different compounds will react at different reaction times. As a consequence, a model of representation is done in order to mimic the oxidation process and to be able to correct the base line.

4.2.3 KINETIC MODEL DEVELOPMENT

This model of representation allows us to mimic the reaction of oxidation and to improve the signal by means of the amelioration of the base line. Even if there is a thermal calibration development of the microcalorimeter presented in detail before (cf. § 3.1). The fitting of the model developed here shows that the measurement can be still improved.

A kinetic model has been developed based on mass balance accounting for both kinetic laws of chemical reactions and mass transfer of oxygen between ambient air and the bulk phase, in which the reactions occur. This model aims to reproduce our experiment. We think that the complete reaction scheme, such as that shown in Figure 10 may be inadequate because of its complexity, number of chemical intermediate species and to unknown kinetic laws. Considering this, the following simplified chemical processes are taking into account, for which we consider that an oil (L_1) can be oxidized *n* times successively. For each of these steps, the involved reaction is characterized by a kinetic law (partial order of one for each reactant) and an enthalpy of reaction. Moreover, the volume of the liquid is assumed to be constant versus time, so that the mass balance can be written in terms of concentration.

We can explain qualitatively the influence of the surface area in contact with the air, (the area interfaces between the oil and the ambient oxygen) and the rate of the oil oxidation. This model will give us the behavior of the oxygen transfer from the saturation of the surface to the saturation in all oil present in the container, considering a constant deepness during the study and considering the limited amount of oxygen from the environment.

Thus, in the kinetic study of the oil oxidation observed from Figure 56, a reaction scheme is defined as follows:

$$\begin{cases} L_1 + O_2 \longrightarrow L_2 + \mathcal{Z}_1, & \Delta H_1 \\ L_2 + O_2 \longrightarrow L_3 + \mathcal{Z}_2, & \Delta H_2 \\ \quad \vdots \quad \vdots \quad \vdots & \\ L_n + O_2 \longrightarrow L_{n+1} + \mathcal{Z}_n, & \Delta H_n \end{cases} \tag{26}$$

Then, if we consider the container as an homogeneous media, the resulting set of mass balance equations for each component, may be expressed as follows:

For the oil concentration variation

$$\begin{cases} \dfrac{d[L_1]}{dt} = -k_1[L_1][O_2] \\ \dfrac{d[L_2]}{dt} = -k_2[L_2][O_2] + k_1[L_1][O_2] \\ \quad \vdots \quad \vdots \quad \vdots \quad \vdots \quad \vdots \\ \dfrac{d[L_n]}{dt} = -k_n[L_n][O_2] + k_{n-1}[L_{n-1}][O_2] \end{cases} \tag{27}$$

Where k is the mass transfer coefficient ($kg.m^{-2}.s^{-1}$).

And from the balance equation:

$$\frac{dE}{dt} = \Phi = -\sum_{p=1}^{n} \nu_p \Delta H_p = -\sum_{p=1}^{n} k_p \left[L_p\right][O_2]\Delta H_p \tag{28}$$

Taking into account also the oxygen variation the expression is:

$$\frac{d[O_2]}{dt} = -\sum_{p=1}^{n} k_p \left[L_p\right][O_2] + K \cdot A \cdot \Delta O_2 \tag{29}$$

And the oxygen concentration potential is defined by:

$$\Delta O_2 = [O_2]^s - [O_2] \tag{30}$$

Where, $[O_2]^s$ is the concentration when the media is saturated in oxygen.

The set of ordinary differential equations is solved using a classical Runge-Kutta method. From this point, an optimization algorithm may be used in order to obtain a set of parameters (k_p, ΔH_p, K) to simulate a process of oil oxidation close to that observed experimentally.

Then, some simulations are achieved with a view to highlight the impact of interfacial area a on the energy release, global heat flux and dimensionless amount in oxygen.

First, related to the energy release as a in function of time (Figure 58) it depends on the surface/volume ratio since the diameter used in the case of the DSC measurement and in the microcalorimeter measurement suggests (at similar temperature ranges 100°C for the microcalorimeter and 110°C for the DSC) a rate that increases with the increase in the surface in interface with the oxygen in the medium.

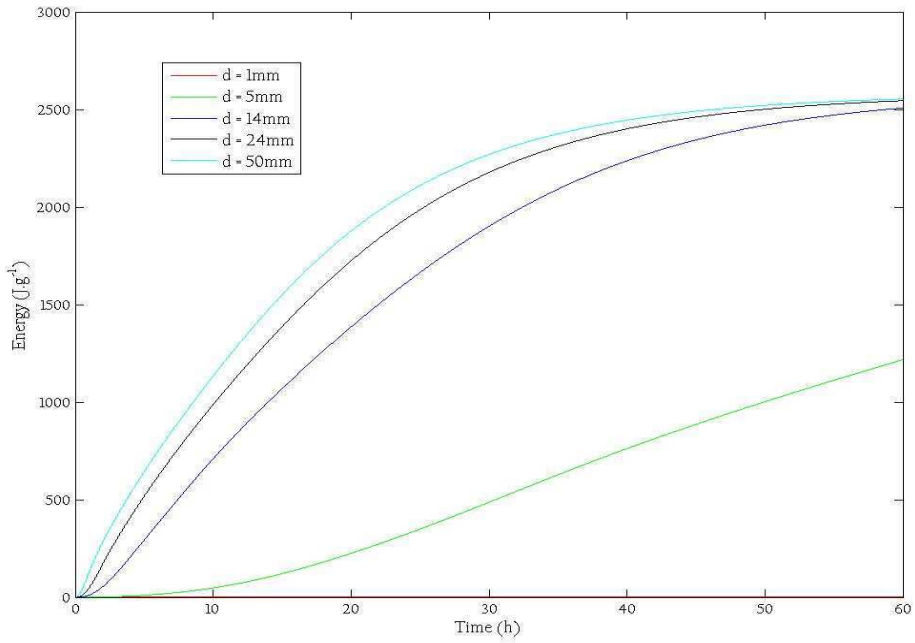

Figure 58: Energy releases for different surface/volume ratios for the oxidation of Cameline oil

Secondly, taking into account the morphology of the reaction, in Figure 59, the surface/volume rate clearly increases the rate of the oxidation process. However, the same range of heat flux released and the same kind of behavior are finally

observed only differentiated by different lag of times. Thus, higher the surface/volume rate interfaces to oxygen, faster the oxidation process occurs.

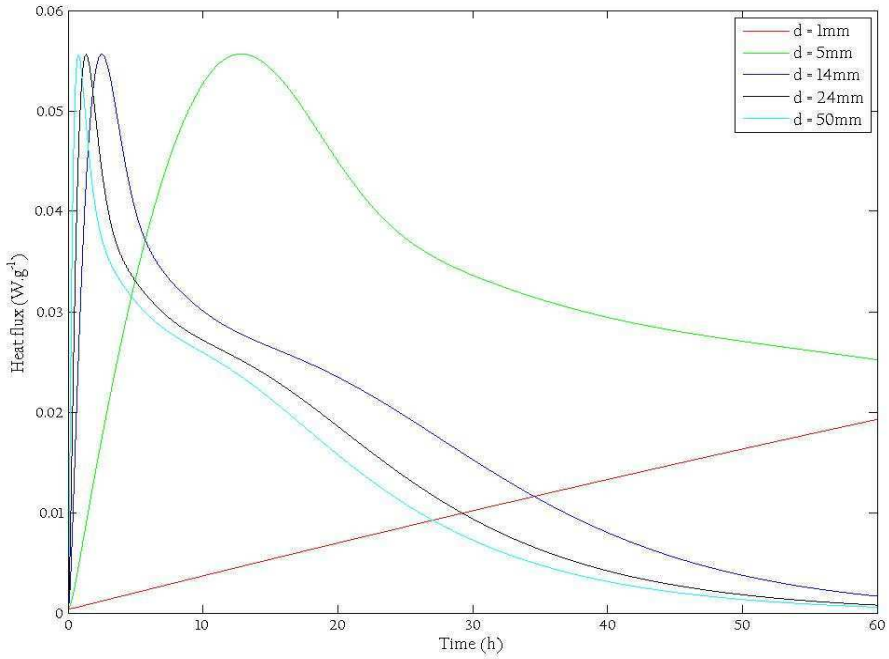

Figure 59: Heat flux releases for different surface/volume ratios in the oxidation of Cameline oil

Considering this, the developed model shows that the amount of oxygen available for the oxidation plays an important role in the formation of the different compounds and in the rate at which this formation occurs. Hence, as showed before, this rate depends on the surface/volume ratio interfaces with the oxygen in the medium, there is a moment when all this level stay remains stable showing the moment when the system is saturated in oxygen and all the oxidation reaction have already been done (Figure 60).

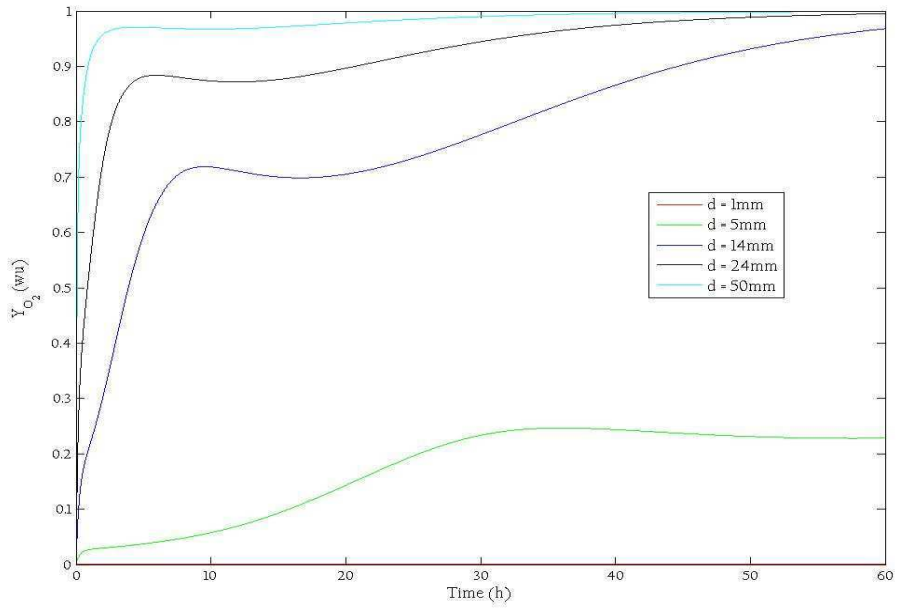

Figure 60: Influence of the oxygen concentration on the oxidation ratio of Cameline oil at different surface/volume

Finally, the 'limiting' case, corresponding to an infinite interfacial area, leads to a constant value of the concentration in oxygen (equal to $[O_2]^s$) and reveals that both energy releases and heat flux are tending to a 'maximum' rate (Figure 58 and Figure 59). Then, it suggests that the initial modeling may be simplified in neglecting the evolution versus time of oxygen.

Considering the following change in the choice of variables, another simplified model is developed.

$$Y_p = \frac{[L_p]}{[L_1]_0}, \qquad p = 1,2\ldots n \tag{31}$$

$$k'_p = s^{-1}$$

Where $[L_1]_0$ is the initial L_1 oil concentration.

And the new set of mass balance equations for each component may be expressed as follows:

$$\begin{cases} \dfrac{dY_1}{dt} = -k'_1 \cdot Y_1 \\ \dfrac{dY_2}{dt} = k'_1 \cdot Y_1 - k'_2 \cdot Y_2 \\ \vdots \quad \vdots \quad \vdots \quad \vdots \\ \dfrac{dY_n}{dt} = k'_{n-1} \cdot Y_{n-1} - k'_n \cdot Y_n \\ \dfrac{dE}{dt} = \sum_{p=1}^{n} \Delta H_n k'_n \cdot Y_n \end{cases} \tag{32}$$

This set of mass and energy balances is a linear mode. Therefore, if we introduce:

$$\mathcal{X} = \begin{bmatrix} Y_1 \\ Y_2 \\ \vdots \\ \vdots \\ Y_n \\ E \end{bmatrix} \quad M = \begin{bmatrix} -k'_1 & 0 & \cdots & \cdots & 0 & 0 \\ k'_1 & -k'_2 & \ddots & & \vdots & \vdots \\ 0 & \ddots & \ddots & \ddots & \vdots & \vdots \\ \vdots & \ddots & \ddots & \ddots & 0 & \vdots \\ 0 & \cdots & 0 & k'_{n-1} & -k'_n & \vdots \\ \Delta H_1 k'_1 & \cdots & \cdots & \cdots & \Delta H_n k'_n & 0 \end{bmatrix} \tag{33}$$

$$\mathcal{X}(t=0) = \mathcal{X}_0 = \begin{bmatrix} 1 \\ 0 \\ \vdots \\ \vdots \\ 0 \\ 0 \end{bmatrix} \tag{34}$$

Finally:

$$\mathcal{X}(t) = \exp(M \cdot t) \cdot \mathcal{X}_0 \tag{35}$$

This analytical solution can be easily computed by method Buffham & Kropholler, (1971) which allows us to integrated the differential system about 100 time faster than the previous one.

Thus, optimization method can be used in order to identify k'_p, that represents inverse of time characteristics, and ΔH_p enthalpy of the reaction.

4.3 CORRELATION BETWEEN THERMAL/CHEMICAL METHODS

The microcalorimetry gives us the information about the energy released during the chemical reaction of oxidation. However, this technique does not provide information about products that exist before and after the process. In consequence another technique must be coupled to correlate the thermal results obtained.

A variety of analytical techniques has been developed to study primary oxidation products of lipid oxidation in bulk fats and oils (cf. § 1.3). During the formation of hydroperoxides from unsaturated fatty acids, conjugated dienes are produced as a result of the rearrangement of the double bonds which gives rise to an absorption peak at 230-235 nm (Shahidi & Zhong, 2005). During the isothermal measurement of heat flux, oil samples are regularly withdrawn and analyzed for their content in conjugated diene hydroperoxides. Two diameters of container are studied: 14 mm, 24 mm.

The integration of the energy curve from the injection time to the sampling is correlated with the amount of conjugated diene hydroperoxides products (Figure 61).

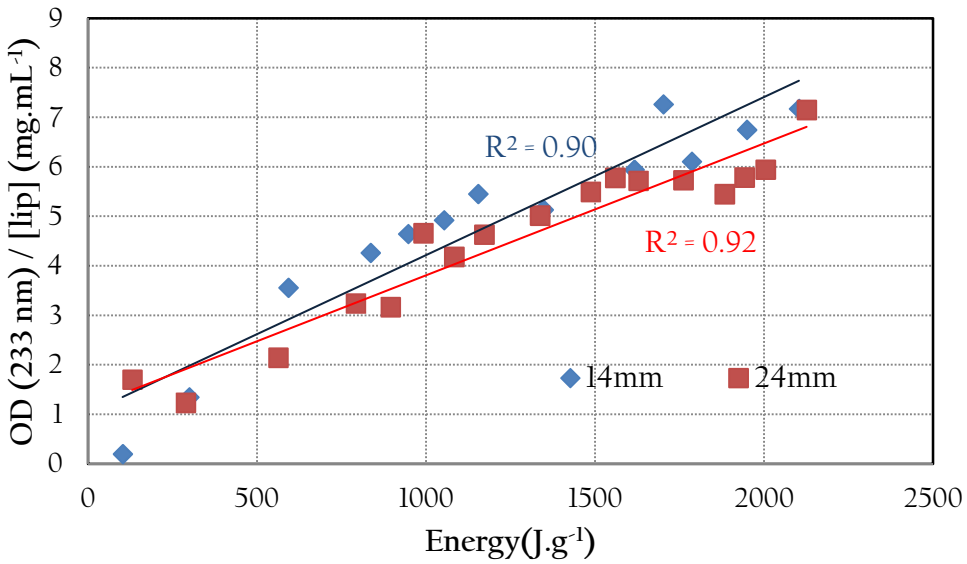

Figure 61: Correlation between the enthalpy and the amount of conjugated diene hydroperoxide from oxidation of Cameline oil (T=100°C)

The quite good correlation (R^2 = 0.92 and 0.90 for 14 and 24 mm, respectively) obtained suggested that the energies of the different reactions involved are nearly equal from one to each other and that the resulting integration of the energy curve is proportional to the conversion rate.

Another point to be considered from the Figure 61 is that beside the linearity that represents the correlation between the two different types of measurements, on one side the physicochemical one and on the other side the thermal one, at least three different sequences of reactions are occurring. The first one an straight lines before 1300 $J.g^{-1}$, a second one between 1500 and 1700 $J.g^{-1}$ and finally the rest of the reaction. These three sequences are already very well evidenced in the cf. § 4.2.2 well the original signal as heat flux where is suggested that several reactions are occurring and overlapping between them.

CHAPTER 5

GENERAL CONCLUSION AND PERSPECTIVES

Lipids are compounds used in numerous domains like food, pharmaceutics, cosmetics and oleochemical industry. However, as raw material and in formulation into products, lipids are susceptible to oxidation reactions. This non-controlled process is one of the most important technological problems in the industry due to the deterioration of the functional and chemical properties of polyunsaturated fatty acids that are part of the triglycerides in fats and oils. Thus, the development of quantification methods either to characterize the oxidation process or to predict the oxidative stability of fats and oils is of great scientific, technological and economical concern.

In this context, in the present study, a microcalorimeter is designed and developed for the study of lipid oxidation, with the particularity to be sensible enough to detect the thermal reactions occurring during the oxidation process. This new non-destructive experimental method is based on a thermo-analytical method, capable to follow the oil oxidation in real time through the direct measurement of the heat flux releases from the reactions. The heat flux pattern obtained allows getting the whole oxidation kinetics. In addition, the development of a model of representation permitted to mimic the reaction of oxidation and to improve the signal by means the amelioration of the base line. Further work to determine if the different events present in the curve could be assigned to specific oxidation reactions is presented as one of the improvement to be considered in a future work. The validation of the method is performed by Joule effect and by comparison with the classical differential scanning calorimetry technique on well-characterized paraffins. For Cameline oil chosen as an example of a polyunsaturated material, the enthalpy values obtained under isothermal condition (100°C) are correlated with the diene conjugated hydroperoxide amount measured by their absorbance at 233 nm.

The developed device is designed to gain more versatility of use than DSC. Indeed, several samples can simultaneously be examined owing to the parallelization of the thermopiles so that the device appeared to be particularly suitable for the fast screening of a large set of samples. In addition, compared with DSC apparatus, the microcalorimeter presented in this work is low cost. Moreover, it gives the possibility to vary the sample geometry (area interface between lipid phase and air) using various container sizes.

Compared with chemical analysis, the thermo-analytical approach presents the advantage to be a solvent-free method. Moreover, this method is independent of the oil absorbance, a drawback in the case of spectrophometric methods.In this work, we focus on a specific oil rich in polyunsaturated fatty acids, i.e Cameline oil. The obtained results are very promising but have to be consolidated using other experimental conditions. In particular, the temperature range from 37°C (physiological temperature) to 110°C (limit of the thermooxydative process) has to be investigated and the correlation between the thermal data and the chemical analysis validated.

This study has also to be widened first to other vegetable oils (for example, flaxseed and rapeseed oils) and second to animal oils (fish oils). This will allow the validation of the thermal analysis independently of the fatty acid type present in the oil. In this case, if the oxidative behavior of the different oils is to be compared, it will be necessary to take into account the presence of antioxidants naturally occurring in the oils. This will require to deprive the oils from tocopherols and to reincorporate them at various but well defined amounts. As soon as the thermal method is validated on different oils, specific oxidative conditions (presence of oxygen and/or light, presence of metals) could be investigated.

Finally, because of the high sensitivity of the technique, the characterization of lipid oxidation directly in oil-in-water emulsions could be forseen. Indeed, at present, the characterization of the oxidative status of emulsified oil requires an extraction step. Having at our disposal a method avoiding this time consuming step would be very innovative.

REFERENCES

Abramovic, H., & Abram, V. (2005). Physico-chemical properties, composition and oxidative stability of camelina sativa oil. *Food Technology and Biotechnology*, *43*(1), 63-70.

Akoh, C., & Min, D. (2002). *Food lipids: chemistry, nutrition and biotechnology*. (Casimir C. Akoh & D. B. Min, Eds.)*Journal of the American Chemical Society* (Vol. 121, p. 914). Marcel Dekker, Inc.

Andersson, K., & Lingnert, H. (1998a). Influence of oxygen concentration on the flavour and chemical stability of cream powder. *Lebensmittel-Wissenschaft und-Technologie*, *31*(3), 245-251.

Andersson, K., & Lingnert, H. (1998b). Influence of oxygen and copper concentration on lipid oxidation in rapeseed oil. *Journal of the American Oil Chemists' Society*, *75*(8), 1041–1046.

Andersson, K., & Lingnert, H. (1999). Kinetic studies of oxygen dependence during initial lipid oxidation in rapeseed oil. *Journal of Food Science*, *64*(2), 262-266.

Arain, S., Sherazi, S., Bhanger, M., Talpur, F., & Mahesar, S. (2009). Oxidative stability assessment of Bauhinia purpurea seed oil in comparison to two conventional vegetable oils by differential scanning calorimetry and Rancimat methods. *Thermochimica Acta*, *484*(1-2), 1-3.

Buffham, B., & Kropholler, H. (1971). The evaluation of the exponential matrix. *Conference on line computer methods relevant to chemical engineering*. University of Nottingham.

Choe, E., & Min, D. (2006). Mechanisms and factors for edible oil oxidation. *Comprehensive Reviews In Food Science And Food Safety*, *5*, 169-186.

Colakoglu, A. (2007). Oxidation kinetics of soybean oil in the presence of monoolein, stearic acid and iron. *Food Chemistry*, *101*(2), 724-728.

Cross, C. (1969). Oil stability: A DSC alternative for the active oxygen method. *Journal of the American Oil Chemists' Society*, *47*, 229-230.

Den Iseger, P. (2005). Numerical transform inversion using gaussian quadrature. *Probability in the Engineering and Informational Sciences*, *20*(01), 1-44.

Endo, Y., Hoshizaki, S., & Fujimoto, K. (1997). Oxidation of synthetic triacylglycerols containing eicosapentaenoic and docosahexaenoic acids: effect of oxidation system and triacylglycerol structure. *Journal of the American Oil Chemists' Society*, *74*(9), 1041-1045.

Frankel, E. (1980). *Lipid oxidation* (Pray. Lipi., Vol. 19, pp. 1-22). Pergamon Press Ltd.

Frankel, E. (1984). Lipid oxidation: Mechanisms, products and biological significance. *Journal of the American Oil Chemists' Society*, *61*(12), 1908-1917.

Frankel, E. (1993). Formation of headspace volatiles by thermal decomposition of oxidized fish oils vs. oxidized vegetable oils. *Journal of the American Oil Chemists' Society*, *70*(8), 767-772.

Frankel, E. (2005). *Lipid oxidation* (second., p. 470). The oily press.

Frankel, E., Neff, W., & Miyashita, K. (1990). Autoxidation of polyunsaturated triacylglycerols. II.Trilinolenoylglycerol. *Lipids*, *1*(1), 40-47.

Fudym, O., Ladevie, B., & Batsale, J. (2002). A Seminumerical approach for heat diffusion in heterogeneous media: One extension of the analytical quadrupole method. *Numerical Heat Transfer: Part B: Fundamentals*, *42*(4), 325-348.

Fudym, O., Pradere, C., & Batsale, J. (2007). An analytical two-temperature model for convection–diffusion in multilayered systems: Application to the thermal characterization of microchannel reactors. *Chemical Engineering Science*, *62*(15), 4054-4064.

Gray, J. (1978). Measurement of lipid oxidation: A review. *Journal of the American Oil Chemists' Society*, *55*(6), 539-546.

Gunstone, F. (2003). *Vegetable oils in food technology: composition, properties and uses*. *Food Research International* (Vol. 36, p. 337). Blackwell Publishing Ltd.

Hess, P., & Ohare, G. (1947). Oxidation of linseed oil temperature effects. *Industrial & Engineering Chemistry Research*, *42*(7), 1424-1431.

Huang, J., & Sathivel, S. (2008). Thermal and rheological properties and the effects of temperature on the viscosity and oxidation rate of unpurified salmon oil. *Journal of Food Engineering*, *89*(2), 105-111.

Kaletunc, G. (2009). *Calorimetry in food processing: Analysis and design of food systems* (p. 414). Wiley-Blackwell.

Kamal-Eldin, A. (2006). Effect of fatty acids and tocopherols on the oxidative stability of vegetable oils. *European Journal of Lipid Science and Technology*, *108*(12), 1051-1061.

Kamal-Eldin, A., Makinen, M., & Lampi, A. (2003). The challenging contribution of hydroperoxides to the lipid oxidation mechanism. In A. Kamal-Eldin (Ed.), *Lipid oxidation pathways* (pp. 1-36). AOCS Press.

Kasprzycka-Guttman, T., & Odzeniak, D. (1992). Thermoanalytical investigation of edible oils. *Thermochimica Acta* (Vol. 204, pp. 303-310).

Kimoto, H., Endo, Y., & Fujimoto, K. (1994). Influence of interesterification on the oxidative stability of marine oil triacylglycerols. *Journal of the American Oil Chemists' Society*, *71*(5), 469-473.

King, M., Boyd, L., & Sheldon, B. (1992). Antioxidant properties of individual phospholipids in a salmon oil model system. *Journal of the American Oil Chemist's Society*, *31*(6), 295-551.

Knothe, G., & Dunn, R. (2003). Dependence of oil stability index of fatty compounds on their structure and concentration and presence of metals. *Journal of the American Oil Chemists' Society*, *80*(10), 1021-1026.

Kowalski, B., Gruczynska, E., & Maciaszek, K. (2000). Kinetics of rapeseed oil oxidation by pressure differential scanning calorimetry measurements. *European Journal of Lipid Science and Technology*, *102*, 337-341.

Kowalski, B., K, R., Miciula, A., & Krygier, K. (1997). Monitoring of rapeseed oil autoxidation with a pressure differential scanning calorimeter. *Thermochimica Acta*, *307*(2), 117-121.

Labuza, T. (1971). Kinetics of lipid oxidation in foods. *CRC Critical Reviews in Food Technology*, *2*, 355-405.

Le Grandois, J., Marchioni, E., Zhao, M., Giuffrida, F., Ennahar, S., & Bindler, F. (2010). Oxidative stability at high temperatures of oleyol and linoleoyl residues in the forms of phosphatidylcholines and triacylglycerols. *Journal of Agricultural and Food Chemistry*, *58*(5), 2973-9.

Lee, J., Chung, H., & Chang, P. (2007). Development of a method predicting the oxidative stability of edible oils using 2,2-diphenyl-1-picrylhydrazyl (DPPH). *Food Chemistry*, *103*(2), 662-669.

Litwinienko, G. (1998). A DSC study on thermoxidation kinetics of mustard oil. *Thermochimica Acta*, *319*(1-2), 185-191.

Litwinienko, G. (2001). Autooxidation of unsaturated fatty acids and their esters. *Journal Of Thermal Analysis*, *65*, 639-646.

Litwinienko, G. (2005). Analysis of lipid oxidation by differential scanning calorimetry. In A. Kamal-Eldin & J. Pokorny (Eds.), *Analysis of lipid oxidation* (pp. 152-193). AOCS Press.

Litwinienko, G., Kasprzycka-Guttman, T., & Jarosz-Jarszewska, M. (1995). Dynamic and isothermal DSC investigation of the kinetics of thermooxidative decomposition of some edible oils. *Journal of Thermal Analysis*, *45*, 741-750.

Maillet, D., Andre, S., Batsale, J., Degiovanni, A., & Moyne, C. (2000). *Thermal quadrupoles, solving the heat equation through integral transforms* (p. 384). Wiley-Blackwell.

Malcolmson, L., Vaisey-Genser, M., Przybylski, R., & Eskin, N. (1994). Sensory stability of canola oil: Present status of shelf life studies. *Journal of the American Oil Chemists' Society*, *71*(4), 435-440.

Marcuse, R., & Fredriksson, P. (1968). Fat oxidation at low oxygen pressure: I. Kinetic studies on the rate of fat oxidation in emulsions. *Journal of the American Oil Chemists' Society*, *45*(5), 400-407.

Marcuse, R., & Fredriksson, P. (1969). Fat oxidation at low oxygen pressure: II. Kinetic studies on linoleic acid oxidation in emulsions in the presence of antioxidants. *Journal of the American Oil Chemists' Society*, *46*, 262-268.

Marcuse, R., & Fredriksson, P. (1971). Fat oxidation at low oxygen pressure: III. Kinetic studies on linoleic acid oxidation in emulsions in the presence of added metal salts. *Journal of the American Oil Chemists' Society*, *48*(9), 448-51.

More, J. (1978). The Levenberg-Marquardt algorithm: Implementation and theory. *Lecture notes in mathematics* (pp. 105-116). Springer.

Naghshineh, M., Ariffin, A., Ghazali, H., Mirhosseini, H., & Mohammad, A. (2009). Effect of saturated/unsaturated fatty acid ratio on physicochemical properties of palm olein–olive oil blend. *Journal of the American Oil Chemists' Society*, *87*(3), 255-262.

Neff, W., & El-Agaimy, M. (1996). Effect of linoleic acid position in triacylglycerols on their oxidative stability. *Lebensmittel-Wissenschaft und-Technologie*, *29*(8), 772-775.

Neff, W., Frankel, E., & Miyashita, K. (1990). Autoxidation of polyunsaturated triacylglycerols. I. Trilinoleoylglycerol. *Lipids*, *25*(1), 33-39.

Neff, W., Mounts, T., & Rinsch, W. (1997). Oxidative stability as affected by triacylglycerol composition and structure of purified canola oil triacylglycerols from genetically modified normal and high stearic and lauric acid canola varieties. *Lebensmittel-Wissenschaft und-Technologie*, *30*(8), 793-799.

Osborn-Barnes, H., & Akoh, C. (2003). Copper-catalyzed oxidation of a structured lipid-based emulsion containing α-tocopherol and citric acid: Influence of pH and NaCl. *Journal of Agricultural and Food Chemistry*, *51*(23), 6851-6855.

Pailhes, J., Pradere, C., Battaglia, J.-L., Toutain, J., Kusiak, A., Aregba, A. W., & Batsale, J.-C. (2012). Thermal quadrupole method with internal heat sources. *International Journal of Thermal Sciences*, *53*, 49-55. Elsevier Masson SAS.

Pardauil, J., Souza, L., Molfetta, F., Zamian, J., Rocha Filho, G., & da Costa, C. (2011). Determination of the oxidative stability by DSC of vegetable oils from the Amazonian area. *Bioresource Technology*, *102*(10), 5873-7.

Santos, J., Santos, I., Conceiçao, M., Porto, S., Trindade, M., Souza, A., Prasad, S., et al. (2004). Thermoanalytical, kinetic and rheological parameters of commercial edible vegetable oils. *Journal of Thermal Analysis and Calorimetry*, *75*(2), 419-428.

Sathivel, S., Huang, J., & Prinyawiwatkul, W. (2008). Thermal properties and applications of the Arrhenius equation for evaluating viscosity and oxidation rates of unrefined pollock oil. *Journal of Food Engineering*, *84*(2), 187-193.

Schaich, K. (2005). Lipid oxidation: Theoretical aspects. In F. Shahidi (Ed.), *Industrial Oil and Fat Products* (Sixth., pp. 269-355). John Wiley & Sons, Inc.

Shahidi, F., & Zhong, Y. (2005). Lipid oxidation: measurement methods. In F. Shahidi (Ed.), *Bailey's industrial oil and fat products: industrial and nonedible products from oils and fats* (Sixth., pp. 357-385).

Simon, P., & Kolman, L. (2001). DSC study of oxidation induction periods. *Journal of Thermal Analysis and Calorimetry*, *64*, 813-820.

Simon, P., Kolman, L., Niklová, I., & Schmidt, S. (2000). Analysis of the induction period of oxidation of edible oils by differential scanning calorimetry. *Journal of the American Oil Chemists' Society*, *77*, 639-642.

Song, J., Yoshikazu, I., & Miyazawa, T. (1997). Oxidative stability of docosahexaenoic acid-containing oils in the form of phospholipids, tryacylglycerols, and ethyl esters. *Bioscience, Biotechnology, and Biochemistry*, *61*(12), 2085-2088.

Tan, C., & Che Man, Y. (2002). Recent developments in differential scanning calorimetry for assessing oxidative deterioration of vegetable oils. *Trends in Food Science & Technology*, *13*(9-10), 312-318.

Tan, C., Che Man, Y., Selamat, J., & Yusoff, M. (2002). Comparative studies of oxidative stability of edible oils by differential scanning calorimetry and oxidative stability index methods. *Food Chemistry*, *76*(3), 385-389.

Tan, C., Man, Y., Selamat, J., & Yusoff, M. (2001). Application of Arrhenius kinetics to evaluate oxidative stability in vegetable oils by isothermal differential scanning calorimetry. *Journal of the American Oil Chemists Society*, *78*(11), 1133-1138.

Thurgood, J., Ward, R., & Martini, S. (2007). Oxidation kinetics of soybean oil/anhydrous milk fat blends: A differential scanning calorimetry study. *Food Research International*, *40*(8), 1030-1037.

Velasco, J., & Dobarganes, C. (2002). Oxidative stability of virgin olive oil. *European Journal of Lipid Science and Technology*, *104*(1), 661-676.

Vittadini, E., Lee, J., Frega, N., Min, D., & Vodovotz, Y. (2003). DSC determination of thermally oxidized olive oil. *Journal of the American Oil Chemists' Society*, *80*(6), 533-537.

Wassef, N. (1996). Lipids. In Owen R. Fennema (Ed.), *Food Chemistry* (3rd ed., pp. 225-314).

Wijesundera, C., Ceccato, C., Watkins, P., Fagan, P., Fraser, B., Thienthong, N., & Perlmutter, P. (2008). Docosahexaenoic acid is more stable to oxidation when located at the sn-2 position of triacylglycerol compared to sn-1(3). *Journal of the American Oil Chemists' Society*, *85*(6), 543-548.

Zubr, J. (2009). Unique dietary oil from Camelina sativa seed. *AgroFood Industry Hi-Tech*, *20*, 42-46.

PUBLICATIONS AND CONFERENCES

Carolina Garcia-Darras, Christophe Pradere, Jean Toutain, Alain Sommier and Maud Cansell. Validation of a new calorimetric thermal analysis device for the study of fat and oil oxidation. **Journal of Food Engineering**, (Under review).

C. Garcia-Darras, C. Pradere, J. Toutain, A. Sommier and M. Cansell. Validation of differential calorimetry analysis for the evaluation of oil oxidation. **Young Scientist Symposium at IECB**, Pessac (France), 19 mai 2011.

C. Garcia-Darras, C. Pradere, J. Toutain, A. Sommier and M. Cansell. Validation of differential calorimetry analysis for the evaluation of oil oxidation. **2nd International ISEKI-Food Conference**, Milan (Italie), 31 août-2 septembre 2011.

C. Garcia-Darras, C. Pradere, J. Toutain, A. Sommier and M. Cansell. Validation of differential calorimetry analysis for the evaluation of oil oxidation. **9th Euro Fed Lipid Congress**, Rotterdam (Pays-bas), 18-21 septembre 2011.

Abstract

Lipid oxidation results of many reactions generating numerous oxidation products that are worth characterizing in fats and oils. Among the analysis methods available, differential scanning calorimetry, based on the differential measurement of heat flux dissipated during the oxidation reactions, is convenient because it avoids the use of organic solvents. In this context, we have conceived and developed a microcalorimeter that allows the analysis of up to 5 samples simultaneously, in containers of variable sizes (allowing to vary the surface/volume ratio). For the conception of the microcalorimeter, the thermopiles are used in adiabatic configuration. The system is very stable and allowed flux measurement with a high sensitivity. The validation of the method is performed by Joule effect and by comparison of melting points of paraffins with classical differential scanning calorimetry. The modelization of the oxidation reaction is performed to point out the influence of oxygen on the kinetics. For a polyunsaturated oil (cameline oil), the enthalpy values obtained, at the beginning of the oxidation process, under isothermal condition (100°C) are correlated with the diene conjugated hydroperoxide amount. On the whole, the developed device provided an adaptable, sensitive, solvent-free and low cost method for the measurement of lipid oxidation, particularly suitable for the fast screening of a large set of samples.

KEYWORDS: Lipid oxidation, microcalorimetry, differential scanning calorimetry, cameline oil

L'oxydation des lipides est un phénomène complexe qui génère de nombreux produits qu'il est nécessaire de caractériser de manière précise afin de prévenir leur apparition. Parmi les méthodes pour analyser les produits d'oxydation, l'analyse thermique différentielle, basée sur la mesure différentielle du flux de chaleur dissipé au cours des réactions d'oxydation, est intéressante car elle n'utilise pas de solvant organique. De plus, elle peut être corrélée à l'apparition de produits primaires ou secondaires d'oxydation. Dans ce contexte, nous avons conçu et développé un microcalorimètre basé sur le principe de l'analyse thermique différentielle mais plus adaptable dans la mesure où il permet l'analyse de plusieurs échantillons simultanément dans des coupelles d'analyse de dimensions variables (variation du rapport surface/volume en relation avec les phénomène de diffusion de l'oxygène). Pour le développement du microcalorimètre, les thermopiles sont utilisées dans la configuration adiabatique. Le système de mesure des flux est stable et possède une sensibilité élevée. La validation de la méthode est réalisée par effet Joule et par comparaison des points de fusion de paraffines en calorimétrie différentielle classique. La modélisation des réactions d'oxydation est réalisée afin de mettre en évidence l'influence de l'oxygène sur les cinétiques. Pour une huile riche en acides gras polyinsaturés (huile de cameline), l'enthalpie de la réaction d'oxydation (en début de cinétique) obtenue en condition isotherme (100°C) est corrélée avec la mesure des dienes conjugués (produits primaires d'oxydation). Dans l'ensemble, le microcalorimètre développé est suffisamment sensible et fiable pour mesurer les enthalpies de réactions d'oxydation des lipides des huiles alimentaires.

MOTS-CLES: Oxydation des lipides, microcalorimétrie, analyse thermique différentielle, huile de cameline